600/3-80-048

United States
Environmental Protection
Agency

Environmental Research
Laboratory
Duluth MN 55804

EPA-600/3-80-048
May 1980

Research and Development

EPA

Air Pollution Studies Near a Coal-Fired Power Plant

Wisconsin Power Plant Impact Study

NEWARK PUBLIC LIBRARY
AUG 5 1980
U. S. GOVT. PUBS.
DEPOSITORY 376

EP1.23:

RESEARCH REPORTING SERIES

Research reports of the Office of Research and Development, U.S. Environmental Protection Agency, have been grouped into nine series. These nine broad categories were established to facilitate further development and application of environmental technology. Elimination of traditional grouping was consciously planned to foster technology transfer and a maximum interface in related fields. The nine series are:

1. Environmental Health Effects Research
2. Environmental Protection Technology
3. Ecological Research
4. Environmental Monitoring
5. Socioeconomic Environmental Studies
6. Scientific and Technical Assessment Reports (STAR)
7. Interagency Energy-Environment Research and Development
8. "Special" Reports
9. Miscellaneous Reports

This report has been assigned to the ECOLOGICAL RESEARCH series. This series describes research on the effects of pollution on humans, plant and animal species, and materials. Problems are assessed for their long- and short-term influences. Investigations include formation, transport, and pathway studies to determine the fate of pollutants and their effects. This work provides the technical basis for setting standards to minimize undesirable changes in living organisms in the aquatic, terrestrial, and atmospheric environments.

This document is available to the public through the National Technical Information Service, Springfield, Virginia 22161.

EPA-600/3-80-048
May 1980

AIR POLLUTION STUDIES NEAR A COAL-FIRED POWER PLANT

Wisconsin Power Plant Impact Study

by

Kenneth W. Ragland
Bradley D. Goodell
Terry L. Coughlin
Department of Mechanical Engineering
University of Wisconsin-Madison
Madison, Wisconsin 53706

Grant No. 803971

Project Officer

Gary E. Glass
Environmental Research Laboratory-Duluth
Duluth, Minnesota

This study was conducted in cooperation with
Wisconsin Power and Light Company,
Madison Gas and Electric Company,
Wisconsin Public Service Corporation,
Wisconsin Public Service Commission,
and Wisconsin Department of Natural Resources

ENVIRONMENTAL RESEARCH LABORATORY-DULUTH
OFFICE OF RESEARCH AND DEVELOPMENT
U.S. ENVIRONMENTAL PROTECTION AGENCY
DULUTH, MINNESOTA 55804

DISCLAIMER

This report has been reviewed by the Environmental Research Laboratory-Duluth, U.S. Environmental Protection Agency, and approved for publication. Approval does not signify that the contents necessarily reflect the views and policies of the U.S. Environmental Protection Agency, nor does mention of trade names or commercial products constitute endorsement or recommendation for use.

FOREWORD

The U.S. Environmental Protection Agency (EPA) was created because of increasing public and governmental concern about the dangers of pollution to the health and welfare of the American people. Polluted air, water, and land are tragic testimony to the deterioration of our natural environment. The complexity of that environment and the interplay between its components require a concentrated and integrated attack on the problem.

Research and development, the necessary first steps, involve definition of the problem, measurement of its impact, and the search for solutions. The EPA, in addition to its own laboratory and field studies, supports environmental research projects at other insitutions. These projects are designed to assess and predict the effects of pollutants on ecosystems.

One such project, which the EPA is supporting through its Environmental Research Laboratory in Duluth, Minnesota, is the study "The Impacts of Coal-Fired Power Plants on the Environment." This interdisciplinary study, involving investigators and experiments from many academic departments at the University of Wisconsin, is being carried out by the Environmental Monitoring and Data Acquistion Group of the Institute for Environmental Studies at the University of Wisconsin-Madison. Several utilities and state agencies are cooperating in the study: Wisconsin Power and Light Company, Madison Gas and Electric Company, Wisconsin Public Service Corporation, Wisconsin Public Service Commission, and the Wisconsin Department of Natural Resources.

During the next year reports from this study, will be published as a series within the EPA Ecological Research Series. These reports will include topics related to chemical constituents, chemical transport mechanisms, biological effects, social and economic effects, and integration and synthesis.

In this report, a product of the Air Pollution Modeling group of the Columbia project, the authors apply a mathematical model, the Gaussian Plume Model, to the specific conditions at the Columbia site. In order to assess the model's accuracy, they then make detailed comparisons between the model's predictions of sulfur-dioxide emissions and actual measurements of the emissions from the stack.

Norbert A. Jaworski, Ph.D.
Director
Environmental Research Laboratory-Duluth
Duluth, Minnesota

ABSTRACT

Concentrations and dry deposition of sulfur dioxide were investigated near a new 540-MW coal-fired generating station located in a rural area 25 miles north of Madison, Wis. Monitoring data for 2 yr before the start-up in July 1975 and for the year 1976 were used to assess the impact of the plume and to investigate the hourly performance of the Gaussian plume model. The Gaussian plume model was successful in predicting annual average concentrations ($r = 0.95$), but inadequate for simulating hourly averages ($r = 0.36$). The incremental annual average increase in ambient SO_2 concentrations within 15 km of the plant was 1-3 $\mu g/m^3$.

Dry deposition of SO_2 was measured within the plume using the gradient transfer method. An annual SO_2 dry deposition flux of 0.5 kg/hectare-year or less within 10 km of the plant was inferred, which is about 3% of the regional background deposition.

This report was prepared with the cooperation of faculty and graduate students in the department of Mechanical Engineering at the University of Wisconsin-Madison.

Most of the funding for the research reported here was provided by the U.S. Environmental Protection Agency. Funds were also granted by the University of Wisconsin-Madison, Wisconsin Power and Light Company, Madison Gas and Electric Company, Wisconsin Public Service Corporation, and the Wisconsin Public Service Commission. This report was submitted in fulfillment of Grant No. R803971 by the Environmental Monitoring and Data Acquisition Group, Institute for Environmental Studies, University of Wisconsin-Madison, under the partial sponsorship of the U.S. Environmental Protection Agency. The report covers the period of 1 July 1975 to 1 July 1978, and work was completed as of January 1979.

CONTENTS

Foreword iii
Abstract iv
Figures vi
Tables x
Acknowledgment xii

1. Introduction 1
2. Conclusions and Recommendations 3
3. Validation Study of the Gaussian Plume Model 5
   Mathematical development of the model 5
   The data base 14
   The computer program GAUSPLM 25
   Results of the validation study 31
   Average concentrations at the seven monitoring sites 55
   Worst-case or highest sulfur dioxide concentrations 55
   Mobile measurements of air pollutants downwind of the stack 73
   Predicted annual concentrations of sulfur dioxide, nitrogen oxides, and particulate matter 73
4. Dry Deposition of Sulfur Dioxide from the Columbia Plume 78
   Theory of gradient-transfer method 79
   Experimental technique 81
   Data collection and analysis 82
   Results and discussion of deposition measurements 91
5. Calculation of Dry Deposition of Sulfur Dioxide from the Columbia Plume 93

References 94
Appendix

Printout of program GAUSPLM 96

FIGURES

Number		Page
1	Reflection of diffusing cloud by ground level and by inversion lid	8
2	Effective stack height	13
3	Crosswind dispersion coefficients	15
4	Vertical dispersion coefficients	16
5	Location of SO_2 monitoring sites in the vicinity of the Columbia Generating Station	19
6	Stack gas flow, stack temperature, and heat input in relation to gross megawatt load at the Columbia Generating Station	22
7	Frequency distribution of stability class (A-E) occurrences based on the Hino stability typing scheme	26
8	Frequency distribution of wind speed and wind direction at the Messer site, 1 January-31 December 1976	27
9	Sector angle as a function of plume width	29
10	Frequency distributions of calculated and observed SO_2 concentrations for all occurrences	32
11	Scatter plot of hourly data points of calculated and observed SO_2 concentrations for all occurrences	33
12	Frequency distributions of calculated and observed SO_2 concentrations for nighttime occurrences	35
13	Scatter plot of hourly data point of calculated and observed SO_2 concentrations for nighttime occurrences	36
14	Frequency distributions of calculated and observed SO_2 concentrations for class A stability occurrences	37
15	Scatter plot of hourly data points of calculated and observed SO_2 concentrations for class A stability occurrences	38

16 Frequency distributions of calculated and observed SO_2 concentrations for class AB stability occurrences 39

17 Scatter plot of hourly data points of calculated and observed SO_2 concentrations for class AB stability occurrences 40

18 Frequency distributions of calculated and observed SO_2 concentrations for class B stability occurrences 41

19 Scatter plot of hourly data points of calculated and observed SO_2 concentrations for class B stability occurrences 42

20 Frequency distributions of calculated and observed SO_2 concentrations for class BC stability occurrences 43

21 Scatter plot of hourly data points of calculated and observed SO_2 concentrations for class BC stability occurrences 44

22 Frequency distributions of calculated and observed SO_2 concentrations for class C stability occurrences 45

23 Scatter plot of hourly data points of calculated and observed SO_2 concentrations for class C stability occurrences 46

24 Frequency distributions of calculated and observed SO_2 concentrations for class CD stability occurrences 47

25 Scatter plot of hourly data points of calculated and observed SO_2 concentrations for class CD stability occurrences 48

26 Frequency distributions of calculated and observed SO_2 concentrations for class D stability occurrences 49

27 Scatter plot of hourly data points of calculated and observed SO_2 concentrations for class D stability occurrences 50

28 Frequency distributions of calculated and observed SO_2 concentrations for class E stability occurrences 51

29 Scatter plot of hourly data points of calculated and observed SO_2 concentrations for class E stability occurrences 52

30 Frequency distributions of calculated and observed SO_2 concentrations for occurrences at the Portage cemetery site (site 002) 56

31 Scatter plot of hourly data points of calculated and observed SO_2 concentrations for occurrences at the Portage cemetery site (site 002) 57

32 Frequency distributions of calculated and observed SO_2 concentrations for occurrences at the Lake George site (site 003) 58

33 Scatter plot of hourly data points of calculated and observed SO_2 concentrations for occurrences at the Lake George site (site 003) 59

34 Frequency distributions of calculated and observed SO_2 concentrations for occurrences at the Dekorra site (site 004) 60

35 Scatter plot of hourly data points of calculated and observed SO_2 concentrations for occurrences at the Dekorra site (site 004) 61

36 Frequency distributions of calculated and observed SO_2 concentrations for occurrences at the Messer site (site 005) 62

37 Scatter plot of hourly data points of calculated and observed SO_2 concentrations for occurrences at the Messer site (site 005) 63

38 Frequency distributions of calculated and observed SO_2 concentrations for occurrences at the Genrich site (site 008) 64

39 Scatter plot of hourly data points of calculated and observed SO_2 concentrations for occurrences at the Genrich site (site 008) 65

40 Frequency distributions of calculated and observed SO_2 concentrations for occurrences at the Bernander site (site 009) 66

41 Scatter plot of hourly data points of calculated and observed SO_2 concentrations for occurrences at the Bernander site (site 009) 67

42 Frequency distributions of calculated and observed SO_2 concentrations for occurrences at the Russell site (site 010) 68

43 Scatter plot of hourly data points of calculated and observed SO_2 concentrations for occurrences at the Russell site (site 010) 69

44 Annual averages of calculated and observed SO_2 concentrations for all seven sites 71

45 Calculated 1976 average concentrations of SO_2 ($\mu g/m^3$) near the Columbia Generating Station 74

46 Calculated 1976 average concentrations of NO_x ($\mu g/m^3$) near the Columbia Generating Station 75

47 Calculated 1976 average concentrations of particulate matter ($\mu g/m^3$) near the Columbia Generating Station 76

TABLES

Number		Page
1	Definition of Pasquill Stability Classes	11
2	Pasquill Stability Classes as a Function of ΔT (AEC Typing Scheme)	11
3	The Pasquill Stability Classes (A-F) Modified by the Meteorological Agency of Japan (Hino Typing Scheme)	12
4	Fitted Constants for the Pasquill Diffusion Parameters	17
5	Information on SO_2 Monitoring Sites in the Vicinity of the Columbia Generating Station	18
6	Distribution of Hourly Ambient SO_2 Concentrations at all Monitoring Sites Before and After Operation of the Columbia Generating Station	20
7	Maximum SO_2 Concentrations ($\mu g/m^3$) for Various Averaging Times Before (Pre-Op) and After (1976) Operation of the Columbia Generating Station	21
8	Federal Ambient Air Standards for SO_2	23
9	Average Load, Coal Rate, and Emissions for The Columbia Generating Station--1976	24
10	Meteorological Data Collected at the Messer Site	24
11	Sector Angle θ (Ave.) as a Function of Stability	30
12	Analysis of Calculated and Observed SO_2 Concentrations According to Classes of Atmospheric Stability	53
13	Analysis of Calculated and Observed SO_2 Concentrations at Each Monitoring Site	70
14	Calculated and Observed Average SO_2 Concentrations ($\mu g/m^3$) at the Seven SO_2 Monitoring Sites Arranged in Order of Decreasing Value	72

15 Worst-Case or Highest SO_2 Concentrations ($\mu g/m^3$) at the Columbia Generating Station--1976 72

16 Summary of SO_2 Mobile Monitoring Data Near the Columbia Generating Station 77

17 Data from Eight Field Tests in which SO_2 Deposition was Measured Near the Columbia Generating Station 83

18 Summary of SO_2 Deposition Measurements--Reduced Data 92

19 Summary of Total-Deposition-Resistance, Aerodynamic-Resistance and Surface-Resistance Data for Sulfur Dioxide 92

20 Deposition of SO_2 from the Plume at the Monitoring Sites 93

ACKNOWLEDGMENT

Meteorological data were supplied by Prof. C.R. Stearns and B. Bowen. Monitoring data and emissions were supplied by the Wisconsin Power and Light Company. The cooperation of Keith Parker and Ben Ziesmer of the Wisconsin Power and Light Company is greatly appreciated. The encouragement of Dan Willard and the administrative help of Jim Jondrow in the project office in the Institute for Environmental Studies bear special mention.

SECTION 1

INTRODUCTION

Gaseous and particulate air pollutants emitted into the ambient air by a large coal-fired electric power generating station are transported and diffused by the wind and are removed from ambient air by dry deposition, precipitation scavenging, and chemical transformation. Environmental impact is caused by excessive ambient air concentrations of various trace gases, fly ash, and aerosol and by deposition of these components to the ground. Sulfur dioxide and nitrogen oxides are the most voluminous of the gaseous pollutants emitted; sulfate aerosol and fly-ash particulate matter are the most significant liquid and solid pollutants emitted. This study focused on sulfur dioxide because more sulfur dioxide is emitted from the stack than any other pollutant and because extensive SO_2 monitoring equipment and monitoring data were available.

The object of this study was to investigate the ambient air concentrations and dry deposition near the Columbia Generating Station. The approach was to validate a plume model by using sulfur dioxide monitoring data, and then use this model to infer the concentrations of nitrogen oxides and fly ash. The Gaussian plume model was used since it is in widespread use today, but has never been completely validated. The dry deposition of SO_2 from the plume to the ground near the generating station was also investigated with a series of field measurements and computer calculations.

This work is part of a larger study entitled "The Impacts of Coal-Fired Power Plants on the Environment," which is sponsored by the Environmental Protection Agency-Duluth. The Columbia Generating Station is a new power plant 25 miles north of Madison, Wis. Unit I (527 MW) came on line in the summer of 1975. The station burns coal from Colstrip, Mont., which averages 0.8% sulfur. An electrostatic precipitator is used. There is no other flue-gas control equipment. The stack is 500 ft high. The utility is owned primarily by the Wisconsin Power and Light Company, and their cooperation is greatly appreciated.

Except for the city of Madison, which is 25 miles south of the station, there are no other major sources of air pollution within a 75-mile radius of the site. The town of Portage (population 7,800), 4 miles north of the stack, has no major emission sources. The terrain in the vicinity of the site is very flat except for the west-southwestern sector where the eastern edge of the Baraboo Bluffs range approaches to within 4 miles of the stack. The Baraboo range consists of wooded, rolling hills which rise to 600 ft above the

base of the stack. The rest of the land is farmland with occasional woodlots and extensive wetlands.

After summarizing the conclusions and recommendations, the validation study of the Gaussian plume model is presented. Then the measurements of sulfur dioxide dry deposition in the plume and the calculations of deposition flux are presented.

SECTION 2

CONCLUSIONS AND RECOMMENDATIONS

The overall results of this validation study, as shown in Figures 10 and 44, reveal that the Gaussian plume model is quite satisfactory for the prediction of annual average concentrations of sulfur dioxide near a coal-fired generating station. There were 492 h during 1976 when the generating station plume registered more than 10 $\mu g/m^3$ of SO_2 above the background levels at one of the seven monitoring sites. The correlation coefficient based on the average calculated and average observed concentrations at each of the seven sites when the plume was present was 0.954. Hence the Gaussian plume model can be expected to yield accurate results for annual average calculations of nonreactive air pollutants.

Even though the model predicts well on the average, much more work should be done to improve the model's ability to predict accurately the various stability classes. The model tends to slightly underpredict for stability classes A, AB, B, and BC; overpredict for classes C and CD; and underpredict for classes D and E. Since the model is most sensitive to changes in the dispersion parameters σ_y and σ_z, more research is necessary to find values of σ_y and σ_z which pertain strictly to emissions from tall stacks.

The model tends to underpredict during hours of light winds or near calms. During these periods it is extremely difficult to model the plume because of isolated wind puffs that affect the dispersing cloud in many different ways.

Another tendency of the Gaussian plume model is to slightly underpredict for the monitoring sites farthest away from the stack and to overpredict for the sites nearest the stack.

On an hour-by-hour basis for each of the 492 h when the plume was present at a monitoring site, the correlation coefficient between measured concentrations (with the background removed) and the model output was only 0.36. The highest observed hourly concentration during 1976 (with the background removed) was 247 $\mu g/m^3$, and the highest model output was 157 $\mu g/m^3$ for the sector-averaged value, which corresponds to a plume centerline concentration of 245 $\mu g/m^3$. The highest observed and calculated values did not occur at the same time, however.

Improvements of the hour-by-hour correlation coefficient seem to hinge on better knowledge of the input data. The sector-averaged concentration proved more appropriate for the validation study. The plume centerline concentration

best represents the worst-case 1-h concentration. The utility of the Gaussian plume model to predict hour-by-hour concentrations over a year is doubtful.

Mobile monitoring data confirmed the general range of levels predicted by the Gaussian plume model.

The model does an accurate job of predicting annual average concentrations from 5 to 15 km from the stack. This conclusion is further borne out by the fact that annual average concentration due to the generating station over the 5,929 h of the year for which the data were complete was 1-3 $\mu g/m^3$ within 15 km of the stack. This annual incremental increase is roughly the same as that noted in Table 7 between 1976 and the pre-operation monitoring data. However, the fine tuning of the Gaussian model to predict concentrations more accurately in each stability category needs further work.

Dry deposition measurements of SO_2 at the plume-surface interface by using the gradient-transfer method showed no evidence that a transient plume resulted in higher deposition velocities than would be expected due to slowly changing background concentrations. Sulfur dioxide deposition velocities were 0.3 cm/sec in pasture land, 0.75 cm/sec in marsh land, 1.8 cm/sec in a tall prairie, 0.21 m/sec in a dry prairie, and 0.55 m/sec on snow. The tests were difficult to conduct because of the highly transient nature of the plume; continuation of this approach does not appear feasible.

Calculation of the SO_2 dry deposition from the plume, by using the ambient air monitoring data and the deposition velocities showed that flux was 0.5 kg/hectare-year or less within 10 km of the generating station, which is only 3% of the regional background depositon flux.

The data base of hourly emissions, monitoring data, and meteorological data provides an excellent opportunity to validate other atmospheric plume models. We recommend that a grid model with deposition and chemical transformation be run, compared to the monitoring data, and extended to a larger region to investigate regional effects of the generating station.

SECTION 3

VALIDATION STUDY OF THE GAUSSIAN PLUME MODEL

In this section the mathematical background of the Gaussian plume model is developed; the data base for the validation study is presented; the computer program GAUSPLM is described; and the results of the validation study are presented in detail.

MATHEMATICAL DEVELOPMENT OF THE MODEL

Ambient air concentrations of sulfur dioxide and other pollutants that are emitted by an elevated point source such as a power plant are often calculated by using a so-called Gaussian plume model. The Gaussian plume model is widely used for this type of application, and although there are numerous names for the model they are all basically the same. In spite of the widespread utilization of the model for environmental impact assessment, field validation of the model is relatively sparse. This report presents the results of a validation study of the Gaussian plume model and the associated empirical constants.

Sulfur dioxide (SO_2) is the primary pollutant used in this validation study for two reasons: (1) More SO_2 is emitted from the stack than any other pollutant, and (2) ambient levels of SO_2 are recorded continuously at seven monitoring sites throughout the study region. Hourly meteorological data and hourly generating station data were used in conjunction with the hourly SO_2 data to validate the model. Theoretical average concentrations were calculated for those hours when the plume was determined to be at a monitoring site. During the study year 1976 an annual average calculated value and an annual average observed value for each of the seven SO_2 recording stations were determined. The hourly data that form the annual averages were examined by means of frequency distributions and scatter plots. The results were divided into stability classes to show model tendencies to overpredict and underpredict for the various classes.

The variables in atmospheric diffusion are so complex that no completely rigorous mathematical solution has yet been developed, but a statistical representation of the problem is often satisfactory. Therefore, one widely used approach is based on the idea that the concentration distribution of a dispersing plume or cloud is Gaussian. To understand this representation a review of the major points of the Gaussian diffusion theory developed by Sutton (1953) is useful.

The Gaussian Model

Since the diffusion of pollutants in the atmosphere is really a mass transfer problem, mass transfer theory serves as a basis for the Gaussian diffusion theory. From Fick's law of diffusion the rate of diffusion, N_x, of a gaseous species in the x direction at some cross-sectional area, A, is given by the expression

$$N_x = -K_x \, \partial C/\partial x, \tag{1}$$

where N_x is the mass transfer per unit time per unit area; K_x is the mass diffusivity in the x direction; and C is the mass concentration per unit volume. Fick's law of diffusion applies to laminar flow and is assumed to hold for turbulent flow as well.

Gaussian theory applies this general equation to the diffusion of a gas carried downwind (x direction) with wind speed, u, which originates from a continuous source, through a differential volume in space. The horizontal and vertical velocity components, v and w, are assumed zero. Therefore, from the continuity equation u does not vary in the x direction, making the flow field uniform. For flow in the x direction only, the species continuity equation takes on the following form:

$$\frac{\partial C}{\partial t} = -u \frac{\partial C}{\partial x} + \frac{\partial}{\partial x}\left(K_x \frac{\partial C}{\partial x}\right) + \frac{\partial}{\partial y}\left(K_y \frac{\partial C}{\partial y}\right) + \frac{\partial}{\partial z}\left(K_z \frac{\partial C}{\partial z}\right) . \tag{2}$$

Equation (2) can be simplified to a more reasonable form with the following assumptions:

(1) Mass transfer in the x direction is due mainly to the motion of the wind; therefore, the diffusion term in the x direction, $\frac{\partial}{\partial x}\left(K_x \frac{\partial C}{\partial x}\right)$ may be negligible;

(2) only steady state solutions are considered, hence $\partial C/\partial t = 0$; and

(3) the mass diffusivities K_y and K_z are assumed constant.

After these three simplifying assumptions, Eq. (2) reduces to

$$u \cdot \partial C/\partial x = K_y \, \partial^2 C/\partial y^2 + K_z \, \partial^2 C/\partial z^2 . \tag{3}$$

If a further assumption is made (4), namely, that the wind speed u is constant, then the general solution to this second-order partial differential equation is:

$$C = K x^{-1} \exp\left\{-\left[\frac{y^2}{K_y} + \frac{z^2}{K_z}\right] \frac{u}{4x}\right\} , \tag{4}$$

where K is a constant whose value is dependent on the choice of boundary conditions. One boundary condition that must be satisfied is that in any y-z plane downwind from the point source the mass transfer rate must be constant

and equal to the pollution emission rate Q; that is, all pollutant transport downwind must be accounted for. For this to be true, two more assumptions must be made:

(5) No chemical reactions occur in the plume; and

(6) the ground acts as a perfect reflector, that is, no deposition to the ground is considered.

If a second boundary condition is satisfied, namely, that the point source is located at some distance above ground, and an assumption (7), that the terrain is uniform, is made, it can be shown that

$$K = Q/4\pi(K_y K_z)^{1/2}. \tag{5}$$

After defining $\sigma_y^2 = 2K_y \frac{x}{u}$, where σ_y = crosswind dispersion coefficient, and

$\sigma_z^2 = 2K_z \frac{x}{u}$, where σ_z = vertical dispersion coefficient, Eq. (4), after

substitution of Eq. (5), may be written in the following form:

$$C = \frac{Q}{2\pi u \sigma_y \sigma_z} \exp\left[-\frac{1}{2}\left(\frac{y^2}{\sigma_y^2} + \frac{z^2}{\sigma_z^2}\right)\right]. \tag{6}$$

Equation (6) is a double Gaussian distribution in the two coordinate directions y and z, but this solution to the general diffusion equation given in Eq. (2) takes on the Gaussian distribution form only after the application of the seven simplifying assumptions. The real distribution of atmospheric pollutants at any instant may or may not be Gaussian; however, it may be assumed so as a first approximation, so that equations such as Eq. (6) may be used to represent the average concentration distribution over a short time interval.

In the modeling of air pollution it is often necessary to take into consideration the height to which pollutants may rise. At this height (often referred to as the mixing height) a usually thin atmospheric layer exists in which there is little fluid motion. This layer, which is formed by the stabilizing effect of gravity, acts as a diffusion lid or ceiling; such an inversion ceiling stops the upward dispersion of effluents.

In light of the previous discussion on the Gaussian distribution of air pollutant concentrations, the mixing height, along with the ground, serves to reflect the plume as shown in Figure 1.

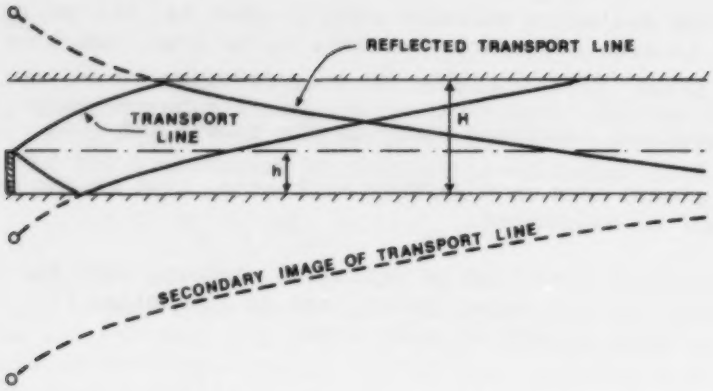

Figure 1. Reflection of diffusing cloud by ground level and by inversion lid.

When either of the reflected lines reaches the other boundary level, it is reflected, and so on. Mathematically, each reflection may be represented by an image source. The result is an infinite series of exponential terms. For a point source of emission strength Q at height h above the ground, and for a mixing height of H, the ground level concentration field in a uniform wind u is given by the equation

$$C = \frac{Q}{2\pi\sigma_y\sigma_z} \exp\left(\frac{-y^2}{2\sigma_y^2}\right) \sum_{n=-\infty}^{+\infty} \exp\left(\frac{-(h-2nH)^2}{2\sigma_z^2}\right) . \qquad (7)$$

Equation (7) (Casanady 1973) is the basic equation used in this validation study of the Gaussian plume model.

Before Eq. (7) can be implemented for use by the computer, the infinite series must be rewritten in a more usable form. This can be done as follows:

$$\sum_{n=-\infty}^{+\infty} \exp\left(\frac{-(h-2hH)^2}{2\sigma_z^2}\right) = \sum_{n=-\infty}^{\infty} \exp\left(\frac{-h^2}{2\sigma_z^2} + \frac{2hnH}{\sigma_z^2} - \frac{2n^2H^2}{\sigma_z^2}\right)$$

$$= \sum_{n=-\infty}^{\infty} \exp\left(\frac{-h^2}{2\sigma_z^2}\right) \exp\left(\frac{2nhH}{\sigma_z^2} - \frac{2n^2H^2}{\sigma_z^2}\right) .$$

Since $\frac{-h^2}{2\sigma_z^2}$ is independent of n, it is a constant and may be placed in front of the summation:

$$\sum_{n=-\infty}^{\infty} \exp\left(\frac{-(h-2nH)^2}{2\sigma_z^2}\right) = \exp\left(\frac{-h^2}{2\sigma_z^2}\right) \sum_{n=-\infty} \exp\left(\frac{2nhH}{\sigma_z^2} - \frac{2n^2H^2}{\sigma_z^2}\right) .$$

Now let us do the first few terms of the summation:

$$\sum_{n=-\infty}^{\infty} \exp\left(\frac{-(h-2nH)^2}{2\sigma_z^2}\right) = \exp\left(\frac{-h^2}{2\sigma_z^2}\right) \left[1 + \exp\left(\frac{2(1)hH}{\sigma_z^2} - \frac{2(1)^2H^2}{\sigma_z^2}\right)\right.$$

$$+ \exp\left(\frac{2(-1)hH}{\sigma_z^2} - \frac{2(-1)^2H^2}{\sigma_z^2}\right) + \exp\left(\frac{2(2)hH}{\sigma_z^2} - \frac{2(2)^2H^2}{\sigma_z^2}\right) \qquad (7f)$$

$$\left. + \exp\left(\frac{2(-2)hH}{\sigma_z^2} - \frac{2(-2)^2H^2}{\sigma_z^2}\right) + \text{----------}\right] . \qquad (7g)$$

After inspection, it can be seen that the exponential terms repeat in the form:

$$\exp\left(\frac{2nhH}{\sigma_z^2} - \frac{2n^2H^2}{\sigma_z^2}\right) + \exp\left(\frac{-2nhH}{\sigma_z^2} - \frac{2h^2H^2}{\sigma_z^2}\right)$$

as n ranges from 1 to ∞. Therefore the infinite series may be be rewritten:

$$\sum_{n=-\infty}^{\infty} \exp\left(-\frac{(h-2nH)^2}{2\sigma_z^2}\right) = \exp\left(\frac{-h^2}{2\sigma_z^2}\right) \left\{1 + \sum_{n=1}^{\infty} \left[\exp\left(\frac{2nhH-2h^2H^2}{\sigma_z^2}\right)\right.\right.$$

$$\left.\left. + \exp\left(\frac{-2nhH-2n^2H^2}{\sigma_z^2}\right)\right]\right\}.$$

Equation (7) then takes on the form

$$C = \frac{Q}{2\pi\sigma_y\sigma_z u} \exp\left(\frac{-y^2}{2\sigma_y^2}\right) \exp\left(\frac{-h^2}{2\sigma_y^2}\right) \left\{1 + \sum_{n=1}^{\infty} \left[\exp\left(\frac{2nhH-2h^2H^2}{\sigma_z^2}\right)\right.\right.$$

$$\left.\left. + \exp\left(\frac{-2nhH-2n^2H^2}{\sigma_z^2}\right)\right]\right\}.$$

Since the exponential terms in the summation are of the form e^{-x^2}, the upper bound of the summation may be replaced by some integer N such that for any $n \geq N$, the exponential terms are approximately zero. Because of the nature of the constants, a value of 10 for N is sufficient to represent the problem.

The Gaussian plume model has come into widespread use since its first appearance in the late 1940's. Recently, it has become the most frequently used air-quality simulation model (Sauter 1975). Studies involving the Gaussian diffusion equation have been made by Klug (1975), Lee et al. (1975), Mills and Record (1975), Mills and Stern (1975), and Bowers and Cramer (1976). Both the U.S. Environmental Protection Agency and the Wisconsin Department of Natural Resources use Gaussian-type diffusion models.

As is the case with any model, the Gaussian model has some limitations. One limitation is the assumption that the wind field is constant and uniform. In practice its use is therefore limited to time periods of several hours and distances less than 30 km. Further, the Gaussian model is not applicable on calm or nearly calm days. The omission of atmospheric chemical reactions and pollutant deposition may become important as one moves farther away from the point source. However, within 10-20 km of the stack the above factors are expected to have little effect on the observed concentrations. Finally, the model is not accurate in situations with complex topography.

The advantages of the Gaussian model far outweigh the disadvantages. Its relative prediction accuracy is the most important factor. Klug (1975) has shown a ratio of calculated to observed annual concentration of 1.25. Lee et al. (1975) showed that the second highest hourly SO_2 concentration could be calculated within a factor of 2 at two-thirds of the sampling sites, and the ratio of predicted to measured second-highest 24-h concentration ranged from 0.2 to 2.7 at 90% of the sites.

Atmospheric Turbulence, Stability, and Turbulent Diffusion Typing Schemes

The dispersion of pollutants is accomplished by wind advection and atmospheric turbulence. For most air pollution problems turbulence includes wind-flow fluctuations with a frequency greater than 2 cycles/h. The most important fluctuations are in the range of 1-0.01 cps. Atmospheric turbulence is the result of atmospheric heating or cooling caused by a temperature difference between the air and the ground, and mechanical turbulence produced by wind-shear effects.

Since the dispersion of pollutants is dependent on the state of the atmospheric turbulence, it is useful to describe the boundary-layer turbulence in terms of the meteorological quantities that most affect it, namely, the vertical temperature gradient and the horizontal wind speed. Theoretical relations between these quantities and vertical diffusion are known, but the lateral spread is not well understood. Therefore, turbulence typing schemes that are empirically based have been developed to handle practical atmospheric dispersion problems.

Probably the most widely used typing system is based on the scheme proposed by Pasquill (1974) of the British Meteorological Office. Pasquill created seven stability classes based on varying amounts of turbulence (Table 1). Since stability near the ground is primarily dependent on net radiation and wind speed, Pasquill's typing scheme relates various combinations of these two variables to his stability classifications.

TABLE 1. DEFINITION OF PASQUILL STABILITY CLASSES

Class	Definition
A	Extremely unstable (extreme turbulence)
B	Unstable
C	Slightly unstable
D	Neutral
E	Slightly stable
F	Stable
G	Extremely stable (no turbulence)

The U.S. Atomic Energy Commission (AEC) (1972) developed a turbulence typing scheme that relates the vertical temperature gradient to the Pasquill categories (Table 2). Another typing scheme, developed by Hino (1968) of the Meteorological Agency of Japan, relates solar radiation and wind speed to the Pasquill stability classes (Table 3).

TABLE 2. PASQUILL STABILITY CLASSES AS A FUNCTION OF ΔT (AEC TYPING SCHEME)

Class	Temperature change with height ($^{o}C/100m$)
A	<-1.9
B	-1.9 to -1.7
C	-1.7 to -1.5
D	-1.5 to -0.5
E	-0.5 to 1.5
F	1.5 to 4.0
G	>4.0

Of course the three typing systems listed above were designed to yield the same result. The choice of which typing scheme to use depends on the meteorological information available. In this validation study both the AEC

TABLE 3. THE PASQUILL STABILITY CLASSES (A-F) MODIFIED BY THE METEOROLOGICAL AGENCY OF JAPAN (HINO TYPING SCHEME)

Surface wind speed (m/sec)	Insolation ($cal/cm^2/h$)			Overcast (10-8)[a]	Night	
	>50	30-25	<25	(Day and night)	High cloud (10-5)[a] Middle or low cloud (7-5)[a]	Cloud amount (4-0)[a]
<2	A	A-B	B	D	---	---
2-3	A-B	B	C	D	E	F
3-4	B	B-C	C	D	D	E
4-6	C	C-D	D	D	D	D
>7	C	D	D	D	D	D

[a]Represents cloud cover in tenths.

and the Hino method were tried. The Hino method turned out to be more realistic. The reasons for this choice will be discussed later in light of the meteorological data.

The consideration of turbulence, stability, turbulent diffusion typing schemes, and their relation to atmospheric dispersion gives rise to one question: What effects do turbulence and stability have on the Gaussian-type equation developed above? These aspects of the problem will be explained in detail in the following sections on plume rise and dispersion coefficients.

Plume Rise

To simplify the treatment of dispersion, it is convenient to assume that plume diffusion begins from a fictitious height above the actual source instead of rising and diffusing as it actually does. This fictitious height is called the "effective stack height" or the height of the point source [variable h in Eq. (7)]. It is equal to the sum of the actual stack height (h_s) and the rise of the plume after emission (Δh) (Figure 2). Plume rise (Δh) is a result of two separate effects: The momentum of the gas leaving the stack and the buoyancy effect that occurs because the stack-gas exit temperature is higher than the ambient air temperature. Plume rise continues until the gas loses its momentum and until the gas sufficiently mixes with the atmosphere to lose the effects of buoyancy.

The extent of the plume rise is closely related to the amount of turbulence present in the atmosphere. A literature search yielded literally scores of equations giving plume rise as a function of various stack parameters, wind speed, and atmospheric turbulence. Briggs (1971, 1972) has done extensive work on plume-rise calculation; he has found mathematical relationships that show plume rise as a function of stack heat flux, wind

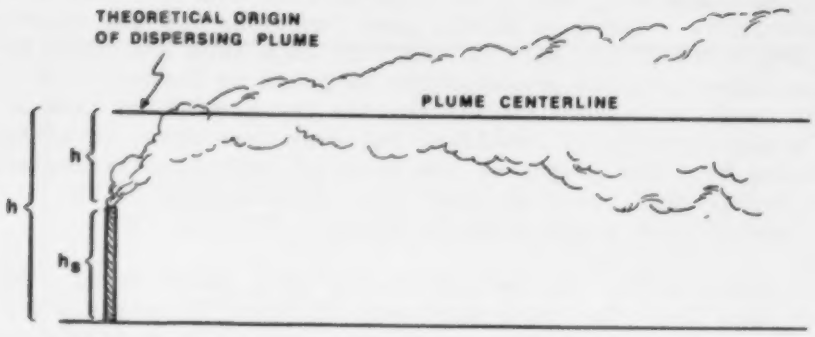

Figure 2. Effective stack height.

velocity, stack height, and stability. The following equations developed by Briggs are used in this validation study: For unstable and neutral conditions

$$\Delta h = 2.47 \frac{(Q_H)^{1/3} (h_s)^{2/3}}{u} ;$$

for stable conditions

$$\Delta h = 2.45 \left(\frac{Q_H}{0.00\epsilon 4u} \right)^{1/3} ,$$

where Q_H = stack gas heat flux (kcal/sec), h_s = stack height (m), and u = wind speed at stack height (m/sec).

Actual measurements of plume rise (Bacci et al. 1974, Bowers and Cramer 1976) show that Briggs' equations give the best agreement. A study of a West Virginia power plant shows a ratio of calculated plume rise to observed plume rise of 1.08 (Bowers and Cramer 1976). Briggs' equations are in widespread use (Klug 1975, Mills and Record 1975, Mills and Stern 1975, Bowers and Cramer 1976).

Dispersion Coefficients σ_y and σ_z

Application of the Gaussian diffusion equation [Eq. (7)] requires knowledge of the vertical and horizontal growth of the plume. This growth is usually expressed in terms of the standard deviation of the concentrations in the crosswind and vertical directions, σ_y and σ_z respectively. It is primarily in terms of these two parameters that the use of the Gaussian form in Eq. (7) maintains flexibility, because different methods of obtaining σ_y and σ_z can be used without changing the whole computation system.

Many empirical functions have been proposed by investigators to represent the dispersion parameters σ_y and σ_z as functions of downwind distance (x) and atmospheric stability. The most widely used functions for the dispersion coefficients are based on the work of Pasquill in a form presented by Gifford (1976). A convenient graphic presentation is given by Turner (1970), who indicates that these values are representative for a sampling time of minutes to hours and apply strictly to low-level releases over open, level terrain (Figure 3, Figure 4). The graphs of the Pasquill diffusion parameters have been approximated in this study by power law relationships of the form $\sigma = bx^q$, where b and q are given in Table 4 (Gifford 1976).

Studies of power plants (Barber and Martin 1973, Bacci et al. 1974) have shown that the empirical functions developed by Pasquill consistently underpredict the actual values of plume height and width as measured by laser techniques. The main reason for this discrepancy is that the Pasquill diffusion parameters apply to low-level releases and not to the high-level (large stacks) releases from power plants. Since no consistent set of data for high-level releases has been developed, however, the Pasquill dispersion coefficients are widely used.

THE DATA BASE

The previous section was devoted to a discussion of the Gaussian plume model and the parameters associated with it. These parameters were shown to be fundamental to the accurate prediction of air pollution concentrations downwind from a point source. Because these variables are dependent on the condition of the atmosphere at any given time, sufficient meteorological data are required to determine values for them. Also, ambient air data characterizing the background concentration levels in the adjoining region and emissions data from the source are essential. All three types of data were obtained on an hourly basis for this validation study. In this section the ambient SO_2 data, the station generating data, and the meteorological data will be discussed in detail.

Ambient Sulfur Dioxide Data

The SO_2 monitoring network surrounding the Columbia Generating Station is quite complete. Monitoring installations at seven sites (Table 5, Figure 5) were in operation during the study year 1976. Four of the SO_2 monitoring stations were in operation 2 yr before the generating station opened on 15 July 1975. For this reason the SO_2 background in the area near Portage, Wis., is well known.

Phillips Model PW9700 continuous SO_2 analyzers housed in temperature-controlled buildings were used at all sites. The intake ports were 1.8 m above the ground. The limit of detection of these instruments was 10 $\mu g/m^3$. The instruments were fully calibrated once every 3 months and were internally calibrated every 24 h. Data reduction to hourly average values was

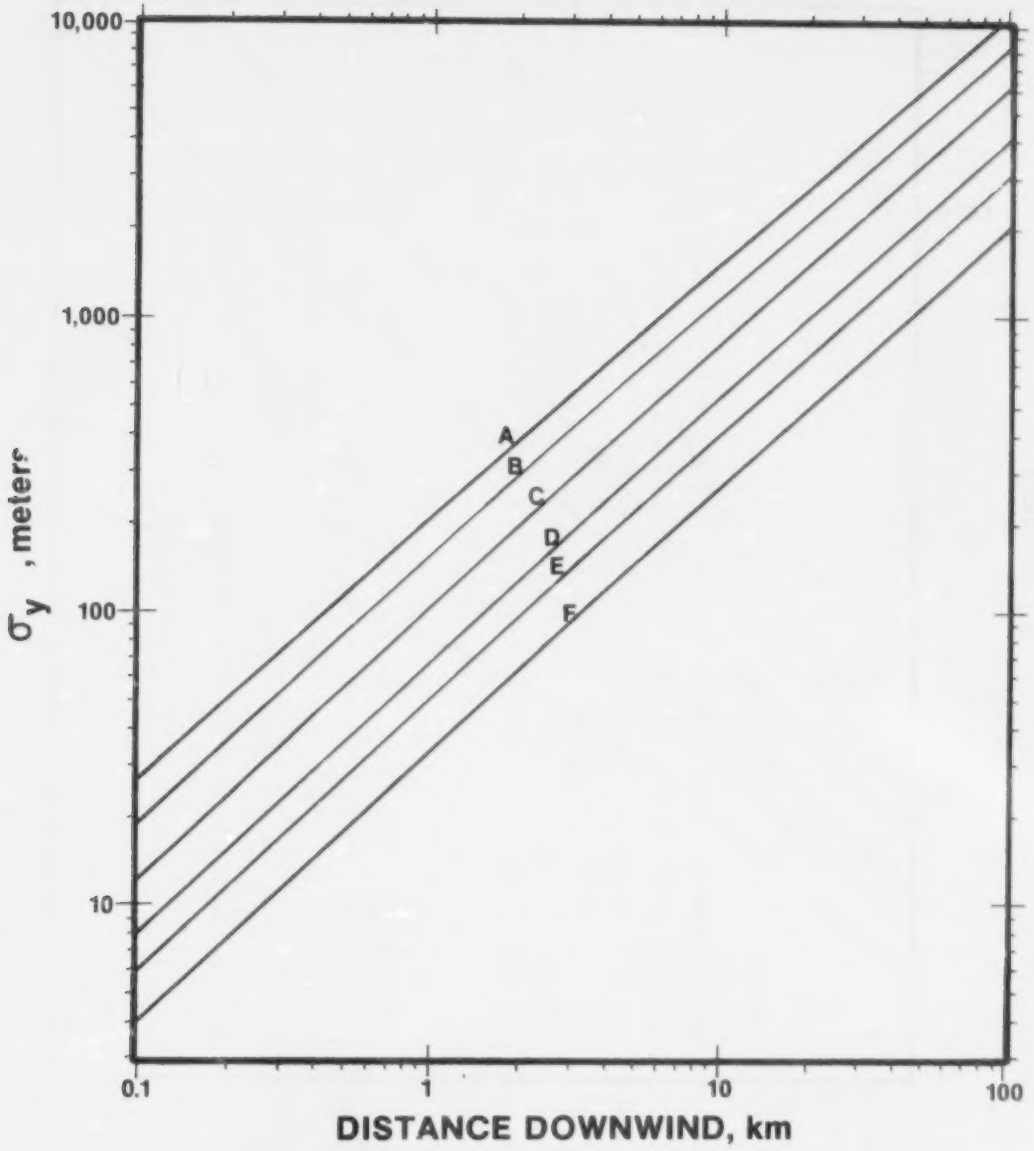

Figure 3. Crosswind dispersion coefficients.

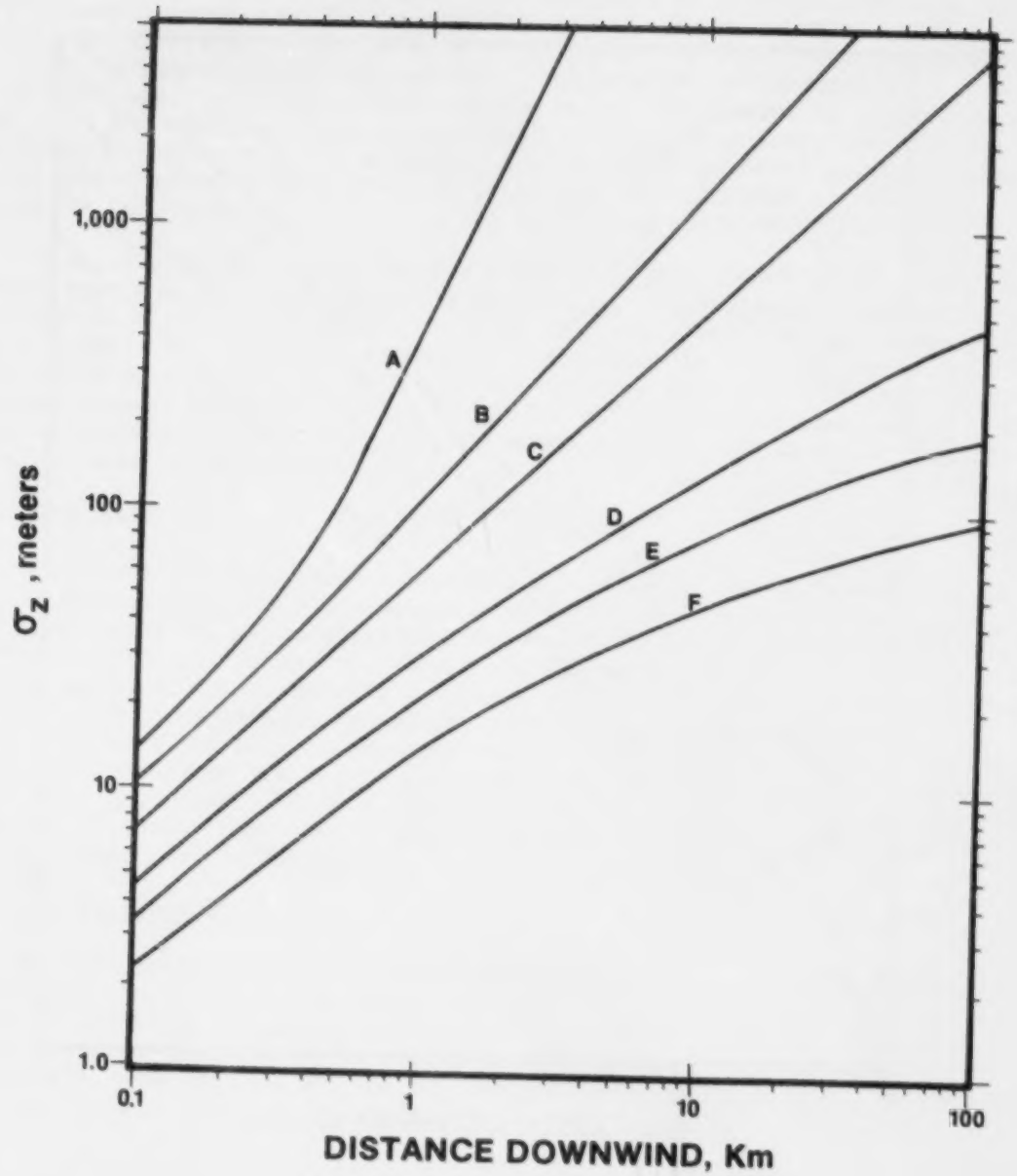

Figure 4. Vertical dispersion coefficients.

TABLE 4. FITTED CONSTANTS FOR THE PASQUILL DIFFUSION PARAMETERS

Stability class	Crosswind constant[a]	Constants for vertical diffusion parameter σ_z[b]							
		$X \leq X_1$		X_1	$X_1 \leq X \leq X_2$		X_2	$X_2 \leq X$	
	a	b	q	(m)	b	q	(m)	b	q
A	0.4	0.125	1.03	250	0.00883	1.51	500	0.000226	2.1
B	0.295	0.119	0.986	1,000	0.0579	1.09	10,000	0.0579	1.09
C	0.20	0.111	0.911	1,000	0.111	0.911	10,000	0.111	0.911
D	0.13	0.105	0.827	1,000	0.392	0.636	10,000	0.948	0.540
E	0.098	0.100	0.778	1,000	0.373	0.587	10,000	2.85	

[a] $\sigma_y = ax^{0.903}$, where x is downwind distance from source; σ_y and x are in meters.

[b] $\sigma_z = bx^q$; σ_z and x are in meters.

TABLE 5. INFORMATION ON SO_2 MONITORING SITES IN THE VICINITY OF THE COLUMBIA GENERATING STATION[a]

Site number	Site name	Distance from station (km)	Direction from station		Start of SO_2 monitoring
			Direction	In degrees	
002	Portage Cemetery	9.9	NNW	332	March 1973
003	Lake George	5.9	ENE	69	March 1973
004	Dekorra	4.4	SW	227	July 1973
005	Messer	7.3	W	267	March 1973
008	Genrich	8.3	N	7	May 1976
009	Bernander	14.6	E	97	May 1976
010	Russell	15.5	NE	37	May 1976

[a]Generating station began operation on 15 July 1975.

done manually and keypunched. A zero drift up to 25 $\mu g/m^3$ could occur, but this factor was corrected for in the data-reduction procedure.[1]

A frequency distribution of hourly SO_2 concentrations averaged over all the sites for 2 yr before operation of the generating station and for the operating year 1976 is given in Table 6. The maximum SO_2 concentrations on a 1-h, 3-h, daily, monthly, and annual basis were generally lower for the pre-operation period than for 1976 (Table 7). The monthly and annual average concentrations are somewhat low because hourly concentrations less than 10 $\mu g/m^3$, which could not be measured, were set equal to zero. In general the SO_2 concentrations increased as a result of the operation of the generating station. The data are examined further to separate the background levels from the contribution of the station later in the report. The observed concentrations are far below the federal ambient air standards (Table 8).

[1]The SO_2 data collection was the responsibility of the Wisconsin Power and Light Company. Data reduction was done by the University of Wisconsin before March 1976 and by the Dames and Moore Company after March 1976.

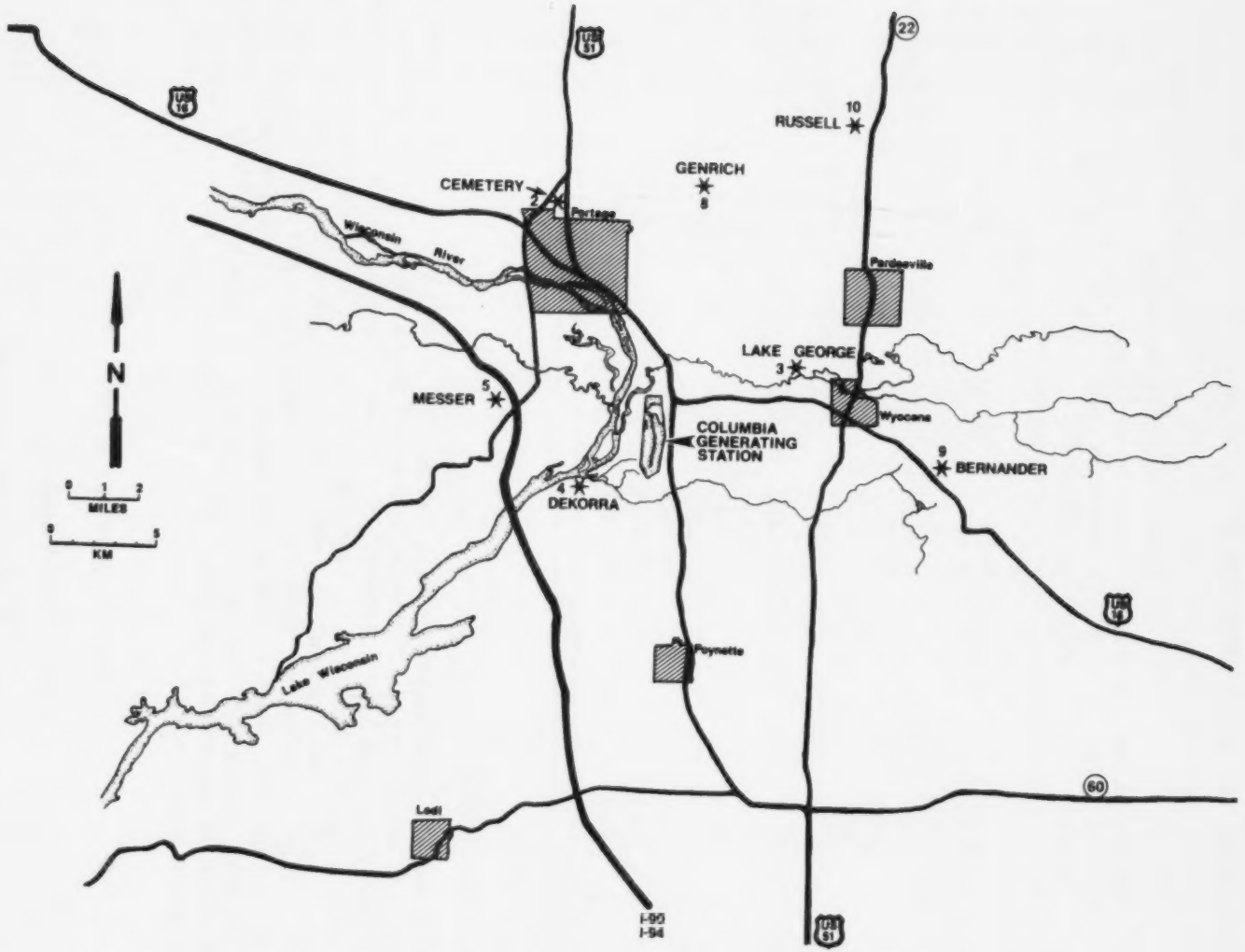

Figure 5. Location of SO_2 monitoring sites (starred) in the vicinity of the the Columbia Generating Station.

TABLE 6. DISTRIBUTION OF HOURLY AMBIENT SO_2 CONCENTRATIONS AT ALL MONITORING SITES BEFORE AND AFTER OPERATION OF THE COLUMBIA GENERATING STATION

Concentration greater than: ($\mu g/m^3$)	Percentage time exceeded	
	Before Columbia operation (1973-75)	After Columbia operation (1976)
10	12.9	15.0
20	6.75	9.17
40	2.03	3.75
60	0.701	1.72
80	0.340	0.856
100	0.166	0.501
120	0.0908	0.306
140	0.0545	0.176
160	0.0333	0.113
180	0.0227	0.0692
200	0.0136	0.0422
220	0.0121	0.0270
240	0.0076	0.0220
260	0.0045	0.0135
280	0.0015	0.0084
300	0.0000	0.0068

Station Generating Data

The plume rise and emissions data needed for input to the plume model were obtained from stack tests and hourly records of gross megawatt load provided by Wisconsin Power and Light Company. The plume rise depends on the heat flux up the stack, Q_H. In general, Q_H is a function of the stack gas volume flow rate and the stack gas temperature, which are functions of the gross generation load in megawatts. The functions that relate gas flow rate, gas temperature, and heat input to the gross megawatt load will differ with each boiler design. Tests were run in 1976 by the WPL to determine these relations for the Columbia Generating Station. The test results are shown in Figure 6 and are given numerically:

$$CMS = 1.7GMW(IH) + 103.9,$$

$$TSK = 0.064GMW(IH) + 370.8,$$

$$QH = 84.88CMS(TSK-TAK)/TSK,$$

where CMS = stack gas flow rate (m^3/sec), GMW(IH) = gross megawatt load at hour IH, TSK = stack gas temperature (^oK), TAK = ambient temperature (^oK)

TABLE 7. MAXIMUM SO_2 CONCENTRATIONS ($\mu g/m^3$ FOR VARIOUS AVERAGING TIMES BEFORE (PRE-OP) AND AFTER (1976) OPERATION OF THE COLUMBIA GENERATING STATION

Site	Averaging time				
	1 h	3 h	24 h	Month	Year
002					
Pre-op	296 (10 am, 9/14/73)	220 (1-4 am, 5/2/75)	65 (11/9/74)	8 (12/73, 2/74)	3.7
1976	210 (11 am, 3/11/76)	172 (10-1 am, 3/11/76)	56 (1/11/76)	14 (3/76)	5.4
003					
Pre-op	227 (8 am, 7/16/73)	163 (10-1 am, 8/7/73)	62 (8/7/73)	9 (9/73, 1/75)	3.1
1976	254 (11 am, 5/19/76)	201 (10-1 am, 3/19/76)	135 (3/6/76)	22 (3/76)	6.4
004					
Pre-op	154 (11 pm, 4/16/74)	102 (1-4 pm, 9/8/73)	51 (12/5/74)	11 (2/75)	4.7
1976	386 (4 pm, 5/7/76)	279 (2-5 pm, 5/7/76)	66 (5/6/76)	24 (5/76)	5.5
005					
Pre-op	244 (11 am, 10/28/74)	95 (10-1 pm, 11/9/74)	46 (1/6/75)	8 (1/75)	2.0
1976	335 (7 am, 5/26/76)	153 (6-9 am, 5/26/76)	60 (5/29/76)	22 (5/76)	5.0
008					
Pre-op					
1976	353 (9 am, 7/13/76)	224 (7-10 pm, 7/19/76)	70 (7/19/76)	13 (7/76)	
009					
Pre-op					
1976	133 (9 am, 9/8/76)	127 (7-10 am, 9/8/76)	33 (5/13/76)	10 (5/76)	
010					
Pre-op					
1976	142 (1 pm, 7/22/76)	128 (12-3 pm, 7/22/76)	56 (6/16/76)	13 (5/76)	

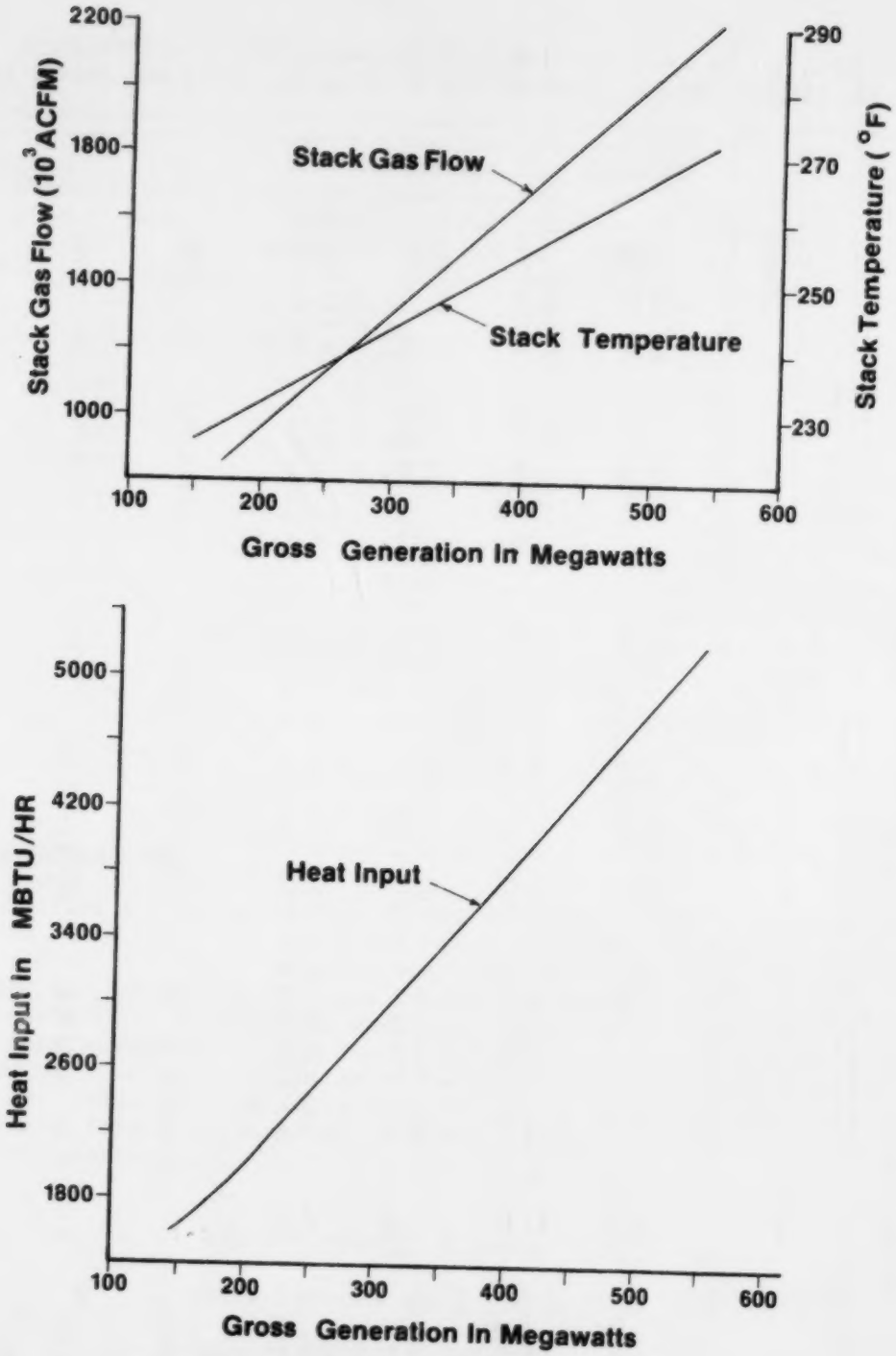

Figure 6. Stack gas flow, stack temperature, and heat imput in relation to gross megawatt load at the Columbia Generating Station.

TABLE 8. FEDERAL AMBIENT AIR STANDARDS FOR SO_2

Time of average (h)	Primary standard[a]	Secondary standard[a]
3	---	1,300 $\mu g/m^3$ (0.5 ppm)[b]
24	365 $\mu g/m^3$ (0.14 ppm)[b]	260 $\mu g/m^3$ (0.10 ppm)[b]
Annual	80 $\mu g/m^3$ (0.03 ppm)	60 $\mu g/m^3$ (0.02 ppm)

[a]Corrected to 25°C and 760 mm Hg.
[b]Concentration not to be exceeded more than once per year; ppm on volume basis.

(from hourly meteorological data), and QH = heat flux from the stack (Kcal/sec).

The average SO_2 emission rate measured in the stack tests was 1.74 lb/10^6 BTU. Knowing that the average higher heating value of the coal is 8,662 BTU/lb, the emissions were 30.14 lb SO_2/ton coal, and thus the emission rate used in the modeling was

$$QSO_2 = 3.8TCH \text{ (g/sec)}, \tag{8}$$

where TCH = coal flow in tons/h.

The TCH was determined as a function of GMW:

If GMW > 400, then TCH = 0.5426GMW + 1.15;

if 175 < GMW < 400, then TCH = 0.5137GMW + 12.4;

if GMW < 175, then TCH = 0.3394GMW + 42.74.

Knowing TCH as a function of GMW, the emission rate of SO_2 in grams per second (QSO_2) can be calculated from Eq. (8).

In a similar fashion the emission rates of nitrogen oxides (NO_x) and particulate matter (PM) can be determined. Based on stack test results the equations are as follows.

$$QNO_x = 1.03TCH \text{ (g/sec)} \tag{9}$$

and

$$QPM = (0.46 \text{ to } 2.94)TCH \text{ (g/sec)}. \tag{10}$$

Operating problems have been experienced with the electrostatic precipitator at the generating station. Consequently, the emission rate of particulate matter can vary greatly at this time, as shown in the preceding equation.

The average load, coal rate, and emissions were calculated for the Columbia Generating Station by using the preceding equations for the study year 1976 (Table 9). For PM a coefficient of 1.31 was used. This corresponds

to Unit I of the generating station meeting the federal standard for PM, which is 0.61 lb/10^6 BTU. The averages are summarized in Table 9.

TABLE 9. AVERAGE LOAD, COAL RATE, AND EMISSIONS FOR THE COLUMBIA GENERATING STATION--1976

GMW load	Coal input (tons/h)	Emmission rate (metric tons/day)		
		SO_2	NO_x	PM
407.6	223.5	73.4	19.9	25.3

Meteorological Data

Windspeed, solar radiation, and temperature were measured at four sites. The stations were located at the first four SO_2 monitoring sites (Table 5, Figure 5). The meteorological data used in this validation study come from the Messer site (Table 10).

TABLE 10. METEOROLOGICAL DATA COLLECTED AT THE MESSER SITE

Item	Units
Solar radiation	cal/cm^2/min.
Air temperature	^oC
32-m wind direction	degrees
32-m mean wind speed	m/sec
2-m mean wind speed	m/sec

The solar radiation and the 2-m wind speed are used in conjunction with the Hino method for determining stability. The Hino stability typing scheme described in Table 3 uses wind speed at 10 m. However, a review of the actual data showed that the 2-m wind speed at Messer was equivalent to the 10-m wind speed measured at the other sites because of the higher elevation. The solar radiation and wind speed should be measured at the same location to insure proper use of the typing system.

The difference in air temperature at the Messer site between the 2-m and 32-m level was at one time used to determine the stability (AEC turbulent typing scheme, Table 2). When these data were used, however, discrepancies were noted. The temperature gradient gave some stability of class A during January. Physically, this result is not expected since turbulence due to atmospheric heating is much smaller in January than in July when the sun is

near its summer solstice. The temperatures did not shift to a neutral case during high winds as would be expected from turbulent diffusion theory. Because of the discrepancies the method was discarded, and the Hino method was used for the entire study year. A frequency distribution of stability class occurrences based on this stability typing scheme is given in Figure 7.

One of the simplifying assumptions made in developing the Gaussian equation was that the wind speed is uniform between ground level and mixing layer; in reality this is untrue. However, in holding to the assumption, the question arises as to which wind speed to use, one at 10 m, stack height, mixing height, or somewhere in between. The wind speed most widely used according to reports in the literature is that measured at stack height. The 32-m tower at the Messer site was designed to be at the same height above sea level as the top of the 500-ft stack of the generating station. Therefore, the Messer 32-m wind speed is a fair representation of the wind speed at stack height, and this velocity is used in the program.

Wind direction is measured twice at each of the four monitoring sites giving a total of eight possible wind directions. The Messer wind directions are measured at 32 m, whereas the other six are measured at 9 m. In agreement with wind-shear theory the directions measured at 32 m are significantly different from those measured at lower levels. The question again arises: Which one should be used? Weidner (1976) showed that the wind directions measured at Wyocena best represent the flow in the region near the generating station. Unfortunately, for the study year 1976 the Wyocena wind-direction data were not complete. In the computer model wind direction is not considered exact, but is used as a reference position only. Therefore, since the Messer wind direction is a good representation of the flow at stack height, and because the Messer wind-direction data set is quite complete (Figure 8), the wind direction is used in the validation study.

THE COMPUTER PROGRAM GAUSPLM

In previous sections we have developed the Gaussian diffusion equation, discussed the dispersion parameters, and examined the data base. These three quantities are united by the computer program GAUSPLM, from which the validation study proceeds. How the program functions and how its output is validated will be discussed in this section.

The Model

The program GAUSPLM is based on the Gaussian diffusion equation for the dispersion of effluents from an elevated point source and uses the data base discussed in the previous section. A printout of GAUSPLM is given in the appendix. This model is slightly different from most models in that the calculations of average SO_2 concentrations are based on an angle of plume spread that varies with stability. These concentrations are determined only when a monitoring site is in the plume. If a site is in the plume, then an SO_2 background level is predicted, subtracted from the monitoring-site reading, and the theoretical average is compared to this calculated observed value with the background removed. In this manner the Gaussian diffusion equation may be validated.

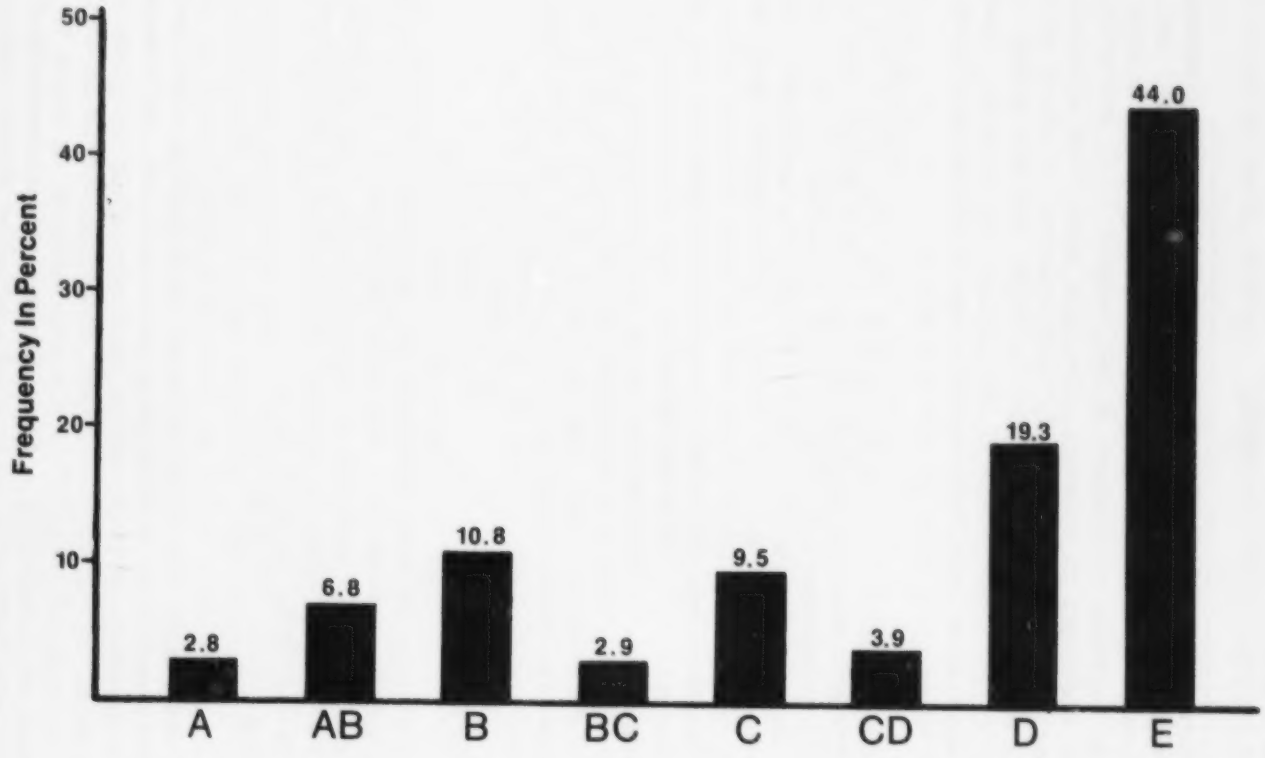

Figure 7. Frequency distribution of stability class (A-E) occurrences based on the Hino stability typing scheme.

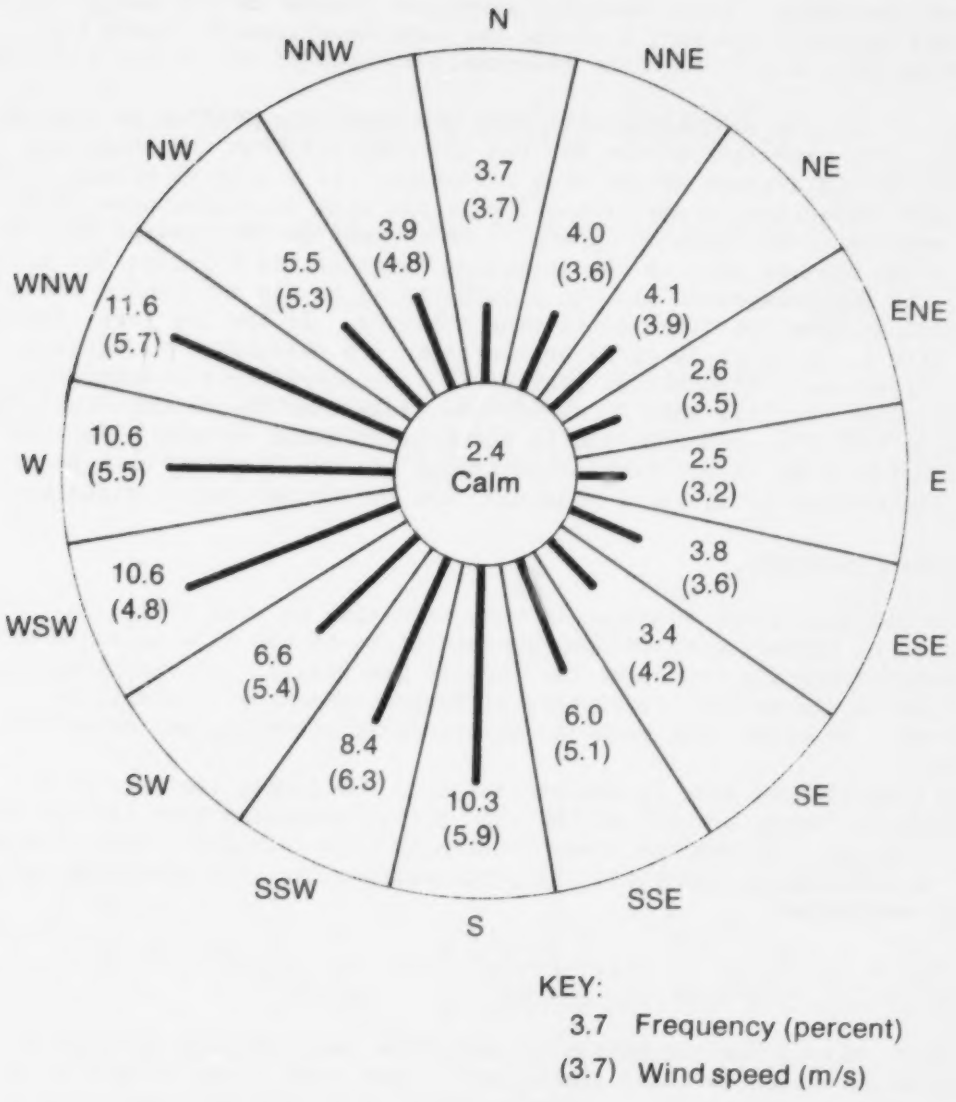

Figure 8. Frequency distribution of wind speed and wind direction at the Messer site, 1 January - 31 December 1976.

Method for Determining Sulfur Dioxide Background Level

Background levels of SO_2 are often of the same order of magnitude as the SO_2 from the stack. This condition makes the removal of the background very difficult indeed. However, a scheme has been developed to remove the background SO_2, and it has been reasonably successful.

All of the SO_2 monitoring-site data are read into GAUSPLM in 1-month periods. For each hour of the day the SO_2 readings from the sites are compared to the average Messer wind direction. If a site is within 22.5° of the plume centerline (plume centerline is the wind direction plus 180°) and has a reading of at least 10 $\mu g/m^3$, it is assumed in the plume. The value 10 $\mu g/m^3$ is used as this is the detection limit of the Phillips SO_2 Monitor PW 9700. The SO_2 background is then considered to be the arithmetic average of the readings from the other monitoring stations. If the SO_2 level for the plume site is at least 10 $\mu g/m^3$ greater than the calculated background, the model calculates a theoretical average SO_2 concentration for that site. If the difference is less than 10 $\mu g/m^3$, the background SO_2 becomes the average of all of the site readings, and no model calculation is made. For the cases in which the plume is not near a monitoring station, the SO_2 background is again the average of all site readings, and no further calculations are made.

Averaging Procedure

The Gaussian plume equation is very sensitive to wind direction. The wind direction at Messer, even though representative of the flow at stack height, does not necessarily represent the flow in the valley. If the direction is off by as little as 10°, completely different concentrations will be predicted. To avoid this problem, an averaging procedure was developed.

If a monitoring site is assumed to be in the plume, then the wind direction is "swung around" so that the plume centerline goes through the receptor point. An average concentration is then calculated over a sector, whose angle changes with stability. Mathematically, this averaging procedure is expressed thus:

$$\theta x \overline{C} = \frac{Q}{2\pi \sigma_y \sigma_z u} \int_{-\infty}^{\infty} \exp\left[-\left(\frac{y^2}{\sigma_y^2}\right)\right] dy \sum_{n=-\infty}^{\infty} \exp\left(-\frac{(h-2nH)^2}{2\sigma_z^2}\right) . \quad (11)$$

In effect, all of the concentration under the Gaussian distribution in the crosswind direction is being summed up and put into an arc length of size θx. At this downwind distance x, over an angle of θ, the SO_2 concentration is made constant.

In carrying out the integration, we note that

$$\int_{-\infty}^{\infty} e^{-a^2x^2} dx = \frac{\sqrt{\pi}}{a} \quad (12)$$

If we apply this to Eq. (11),

$$\theta x\bar{C} = \frac{Q}{2\pi\sigma_y\sigma_z u}\sqrt{2\pi\sigma_y}\sum_{-\infty}^{\infty}\exp\left(-\frac{(h-2nH)^2}{2\sigma_z^2}\right). \tag{13}$$

The concentration at the plume centerline (y=0) is given by

$$C(x,o) = \frac{Q}{2\pi\sigma_y\sigma_z u}\sum_{-\infty}^{\infty}\exp\left(-\frac{(h-2nH)^2}{2\sigma_z^2}\right). \tag{14}$$

Equation (11) may now be solved for the average concentration, $\bar{C}$:

$$\bar{C} = \frac{\sqrt{2\pi\ \sigma_y}\ C(x,o)}{x\theta}. \tag{15}$$

The average concentration C is now compared to the observed SO_2 reading at the site in question. The averaging procedure was done in an attempt to desensitize the Gaussian plume equation to wind direction. The sector angle θ is a function of the plume width (W) and the downwind distance x (Figure 9).

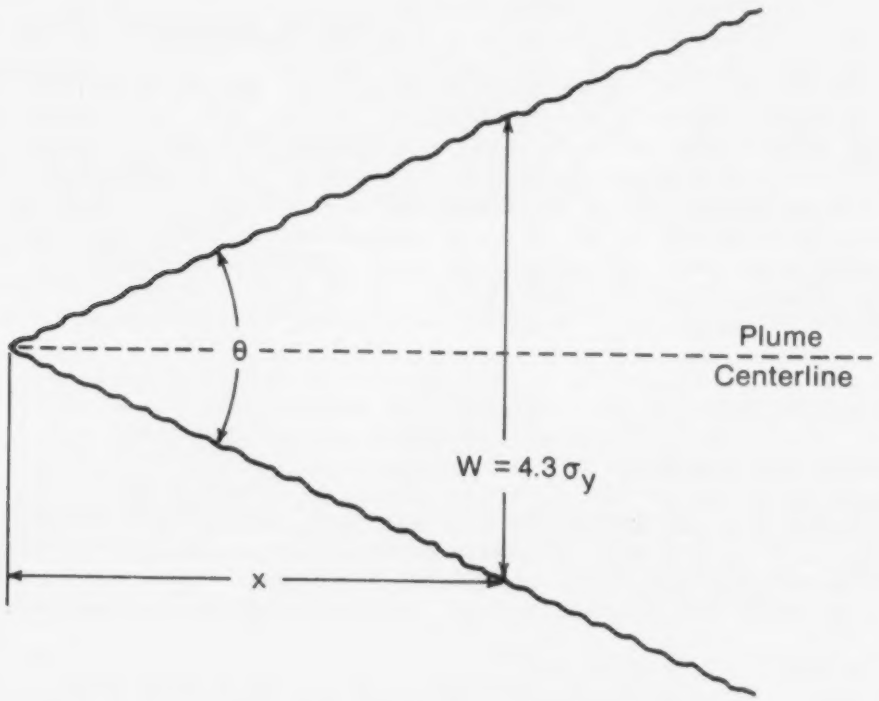

Figure 9. Sector angle as a function of plume width.

The plume width is defined as that distance in the crosswind direction at which the concentration falls to one-tenth of the centerline value. Relating the plume width to σ_y, it can be shown that

$$W = 4.3\sigma_y .$$

If we use the empirical expression for σ_y given in Table 4,

$$\sigma_y = ax^{0.903},$$

where a is a constant varying with stability classification. The sector angle (θ) may be written as

$$\theta = 2 \tan^{-1} (2.15\ ax^{-0.097}) .$$

From the above equation it can be seen that (θ) is a function of stability (a) and downwind distance x. Since θ varies with x for a given stability, a (Ave.) was determined by numerical integration. Values for x are the downwind positions of the seven monitoring sites. Table 11 gives θ (Ave.) as a function of stability.

TABLE 11. SECTOR ANGLE θ (AVE.) AS A FUNCTION OF STABILITY

Stability class	Constant a	θ(Ave.) (degrees)
A	0.4	39.3
A-B	0.3475	34.4
B	0.295	29.5
B-C	0.2475	24.9
C	0.2	20.2
C-D	0.165	16.7
D	0.13	13.2
E	0.098	10.0

Model Output and its Use

The computer model GAUSPLM is run for the data year 1976. From this year's worth of hourly data, the validation study was made. The output from the program GAUSPLM contains the following information:

(1) Year
(2) Month
(3) Day
(4) Hour
(5) Monitoring site number
(6) Stability class
(7) Average Messer wind direction
(8) Average wind speed at stack height

(9) Average background SO_2 value
(10) Maximum SO_2 reading from the sites not in the plume (gives an idea of background variance)
(11) SO_2 reading of the site in the plume
(12) Calculated theoretical centerline concentration
(13) Calculated average SO_2 concentration
(14) Value of observed SO_2 readings

The most important pieces of information are the predicted average and the "calculated" observed concentrations of SO_2. These two numbers are used in the validation procedure of the Gaussian plume model.

The concentrations are compared on an hour-by-hour basis in scatter plots for the following conditions: (1) The year's data lumped together; (2) the year's data broken down into stability classifications; and (3) the values at each monitoring site. The data are then compared by using frequency distributions. Scatter plots show the correlation of the predicted to observed concentrations on an hour-by-hour basis. The frequency plots compare the values on an overall distribution level. An annual average is predicted and compared to the annual observed value for all sites. Annual averages are also predicted for each individual site and compared to the observed averages at the sites.

RESULTS OF THE VALIDATION STUDY

The model GAUSPLM was run for the study year 1976. For the 5,929 operational hours (i.e., those hours in which all data were available) the plume was present at the sites for 492 h, or 8.3% of the time, based on the criteria that the site in the plume was 10 $\mu g/m^3$ above the background. The average calculated value of SO_2 when the plume was present based on all 492 occurrences was 43.5 $\mu g/m^3$. The average observed value during these hours was 44.2 $\mu g/m^3$. The ratio of the calculated average to the observed average is 0.9846, which is extremely close to 1. Given this information alone, we might conclude that the Gaussian diffusion equation is very accurate in predicting an annual average.

When the frequency distributions of the calculated SO_2 concentrations and the observed SO_2 concentrations are compared, the results are indeed reasonable (Figure 10). Both curves are of the same general shape, and their peaks are within a factor of 1.43 of one another. The median value for the observed concentrations is 28 $\mu g/m^3$, that for the calculated concentrations is 40 $\mu g/m^3$. In general, the Gaussian model tends to underpredict for concentrations less than 30 $\mu g/m^3$ and greater than 80 $\mu g/m^3$ and overpredicts for concentrations between these values. On the average, the model predicts quite well.

The hourly data from which the frequency distributions were derived do not correlate well. The 492 data points are shown collectively in the scatter plot given in Figure 11. A correlation coefficient of 0.36 was calculated based on these points. The 45-deg line going through the origin represents the ideal case where the model correlates exactly with the observed. The two other lines represent the initial error bounds which put the calculated values

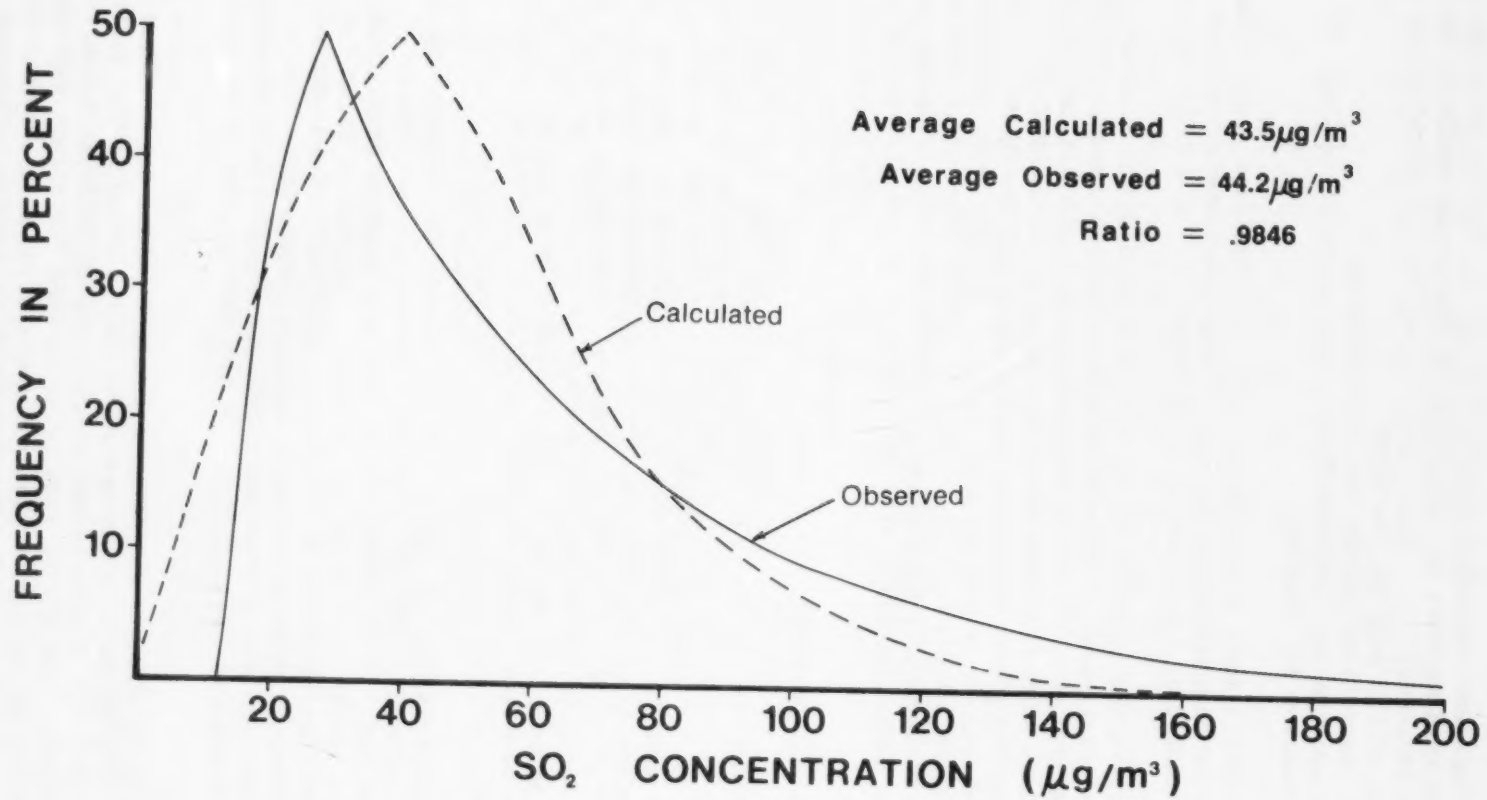

Figure 10. Frequency distributions of calculated and observed SO_2 concentrations for all occurrences.

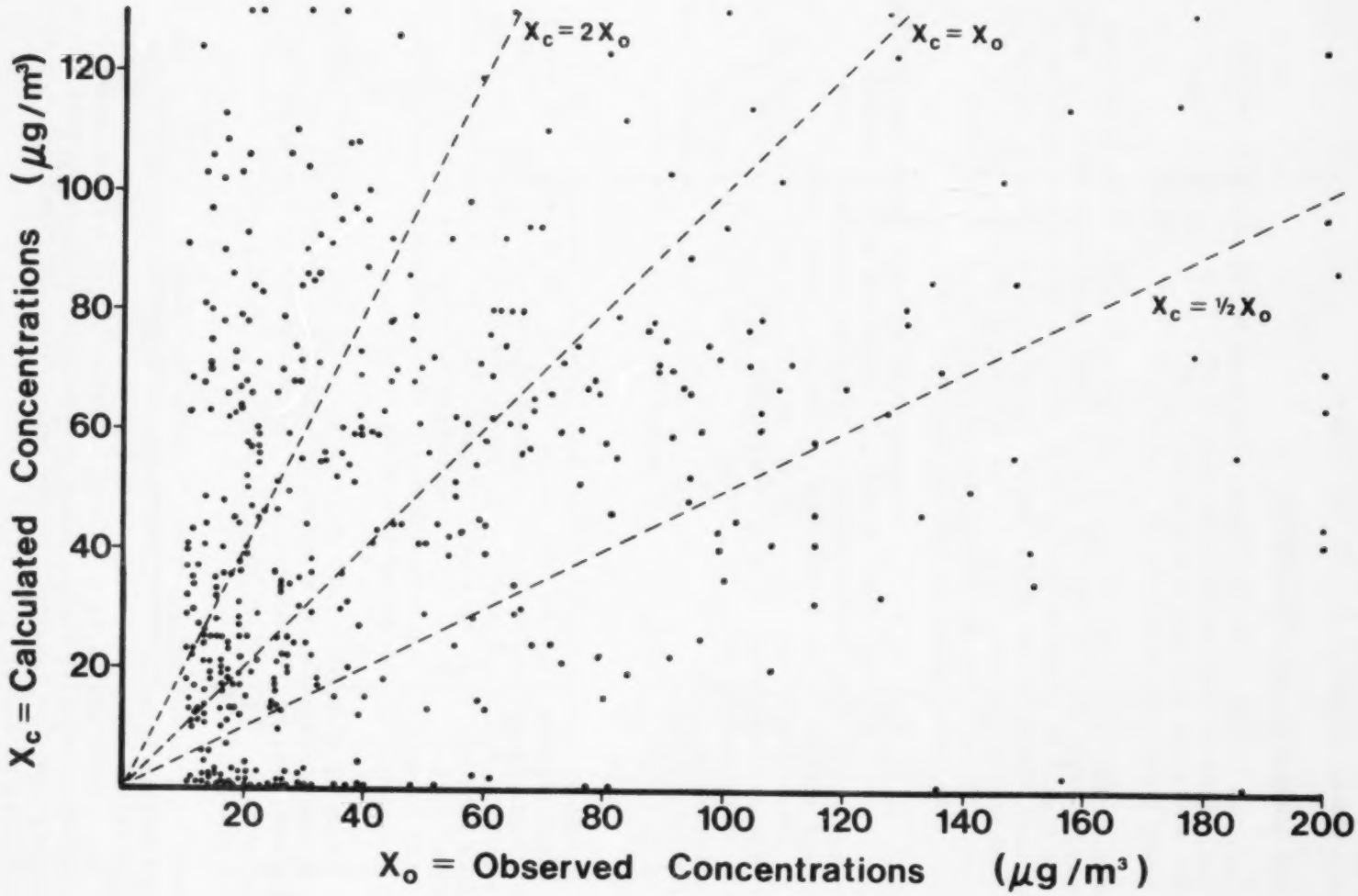

Figure 11. Scatter plot of hourly data points of calculated and observed SO_2 concentrations for all occurrences.

within a factor of 2 of the observed values. Forty-eight percent of the data points fall within a factor of 2 of one another.

Diurnal and Stability-Class Variations

Although the scatter plot in Figure 11 appears to be somewhat randomly distributed, there is more orderliness than first meets the eye. A look at the diurnal variation and the points broken down into stability classes reveals model tendencies that are not apparent at first glance.

Figures 12 and 13 are the frequency and scatter plots of the nighttime occurrences. Ninety-four of the 492 points (19%) occurred between the hours of 5 pm and 7 am. Of these 94 points only 17 (18%) fell within a factor of 2 of one another. Both of the plots reveal the model's tendency to underpredict the observed concentrations. The average calculated value of 4.7 $\mu g/m^3$ is roughly one-fifth as large as the average observed value of 21.9 $\mu g/m^3$. Reasons for this underprediction will be discussed later.

The most useful information is obtained when the data points are divided into stability classes; the model prediction tendencies at the various stability categories then become apparent. Figures 14 through 29 are frequency and scatter plots of the eight stability classes, and Table 12 is a summary of these 16 figures. In Table 12, with the exception of class AB, the observed averages are ranked in descending order from class A through class E. This order is reasonable since the highest SO_2 concentrations are found in the most unstable situations. However, the Gaussian plume model does not completely follow this ranking. This model has the highest average at class C instead of A, and the averages do not descend nicely as do the observed averages.

The frequency distributions of the calculated and observed values for class A stability are close to one another (Figure 14); however, the model tends to grossly underpredict for SO_2 concentrations greater than 100 $\mu g/m^3$. The scatter plot reveals a majority of the points within a factor of 2 and many points with very good agreement (Figure 15). The tendency of the points to be skewed to the right for high concentrations shows the model's incapability to predict high concentrations of this stability class. This could be the result of the sector-averaging technique.

The frequency plot for occurrences in class AB stability shows remarkable overall agreement between the observed and calculated values for SO_2 concentrations (Figure 16), although the calculated values are slight underpredictions. The scatter plot shows 57% of the data points within the set error bounds (Figure 17).

Although the concentration ratio is close for class B, and 67% of the points are within a factor of 2, the frequency distribution curve of the calculated values has a different shape from that of the observed values (Figure 18). This, again, is a general tendency of the Gaussian model for this particular stability class. This same general tendency is observed in the frequency plot for class BC (Figure 20). The model tends to overpredict

(Text continues on p. 54)

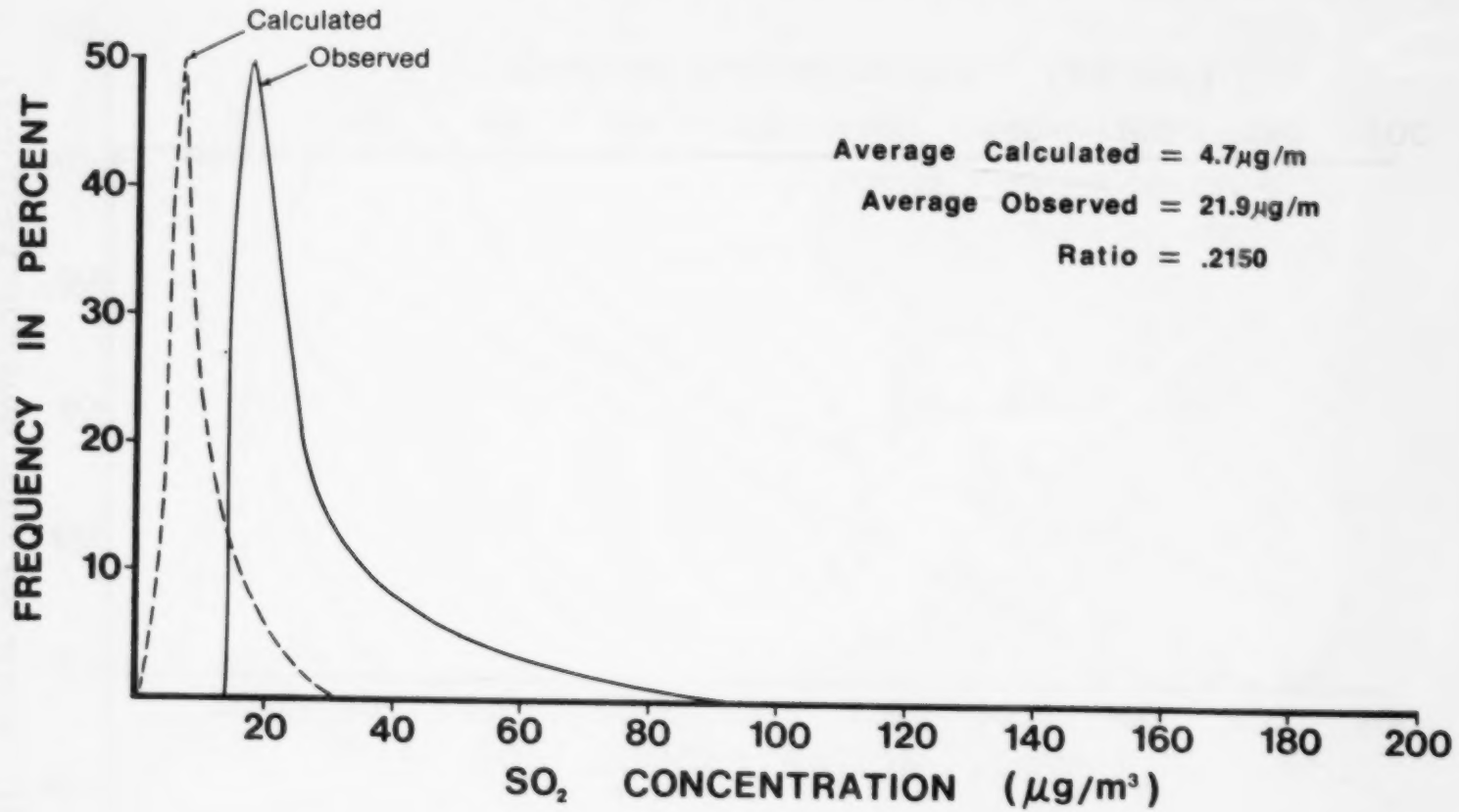

Figure 12. Frequency distributions of calculated and observed SO_2 concentrations for nighttime occurences.

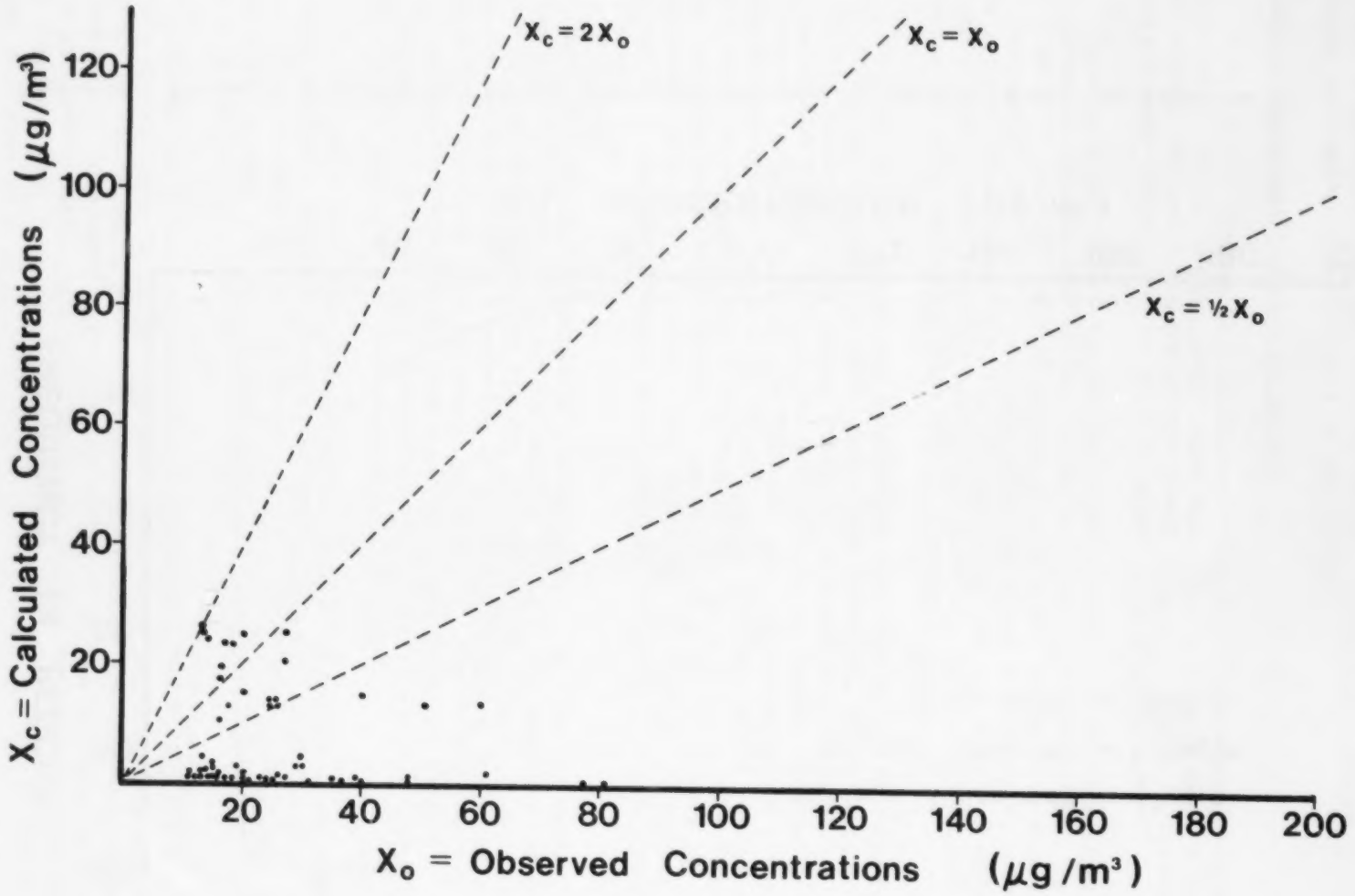

Figure 13. Scatter plot of hourly data points of calculated and observed SO_2 concentrations for nighttime occurrences.

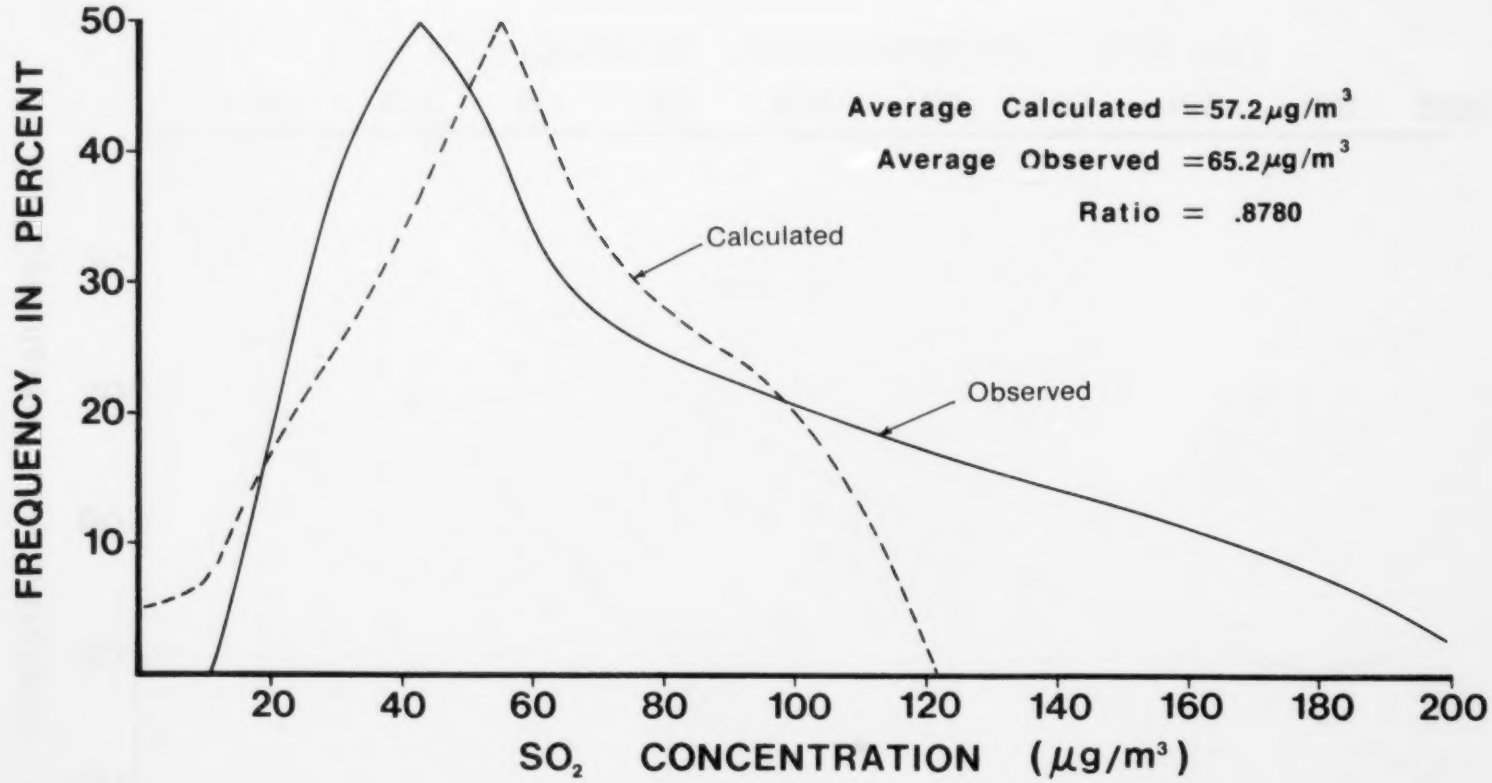

Figure 14. Frequency distributions of calculated and observed SO_2 concentrations for class A stability occurrences.

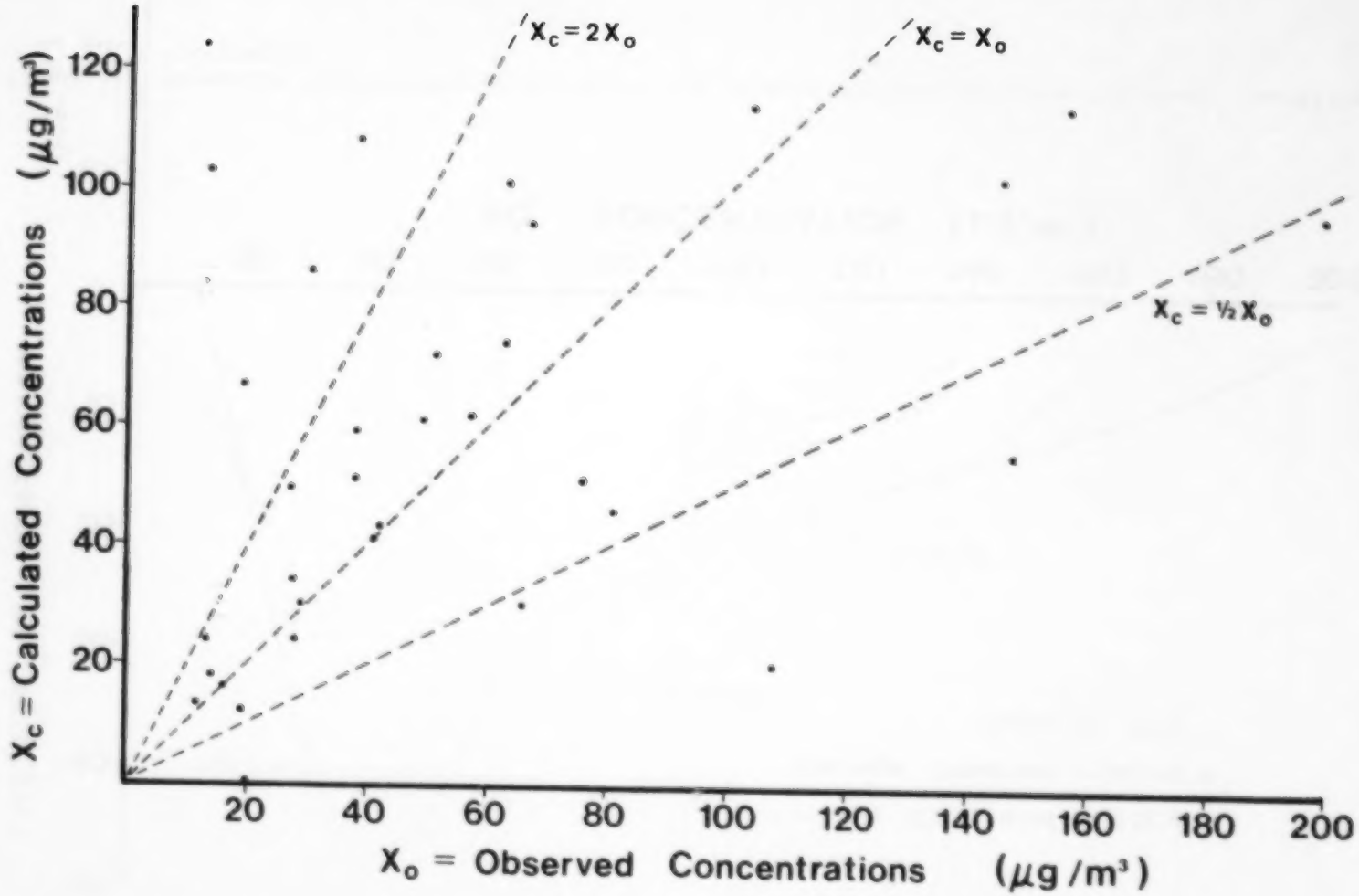

Figure 15. Scatter plot of hourly data points of calculated and observed SO_2 concentrations for class A stability occurrences.

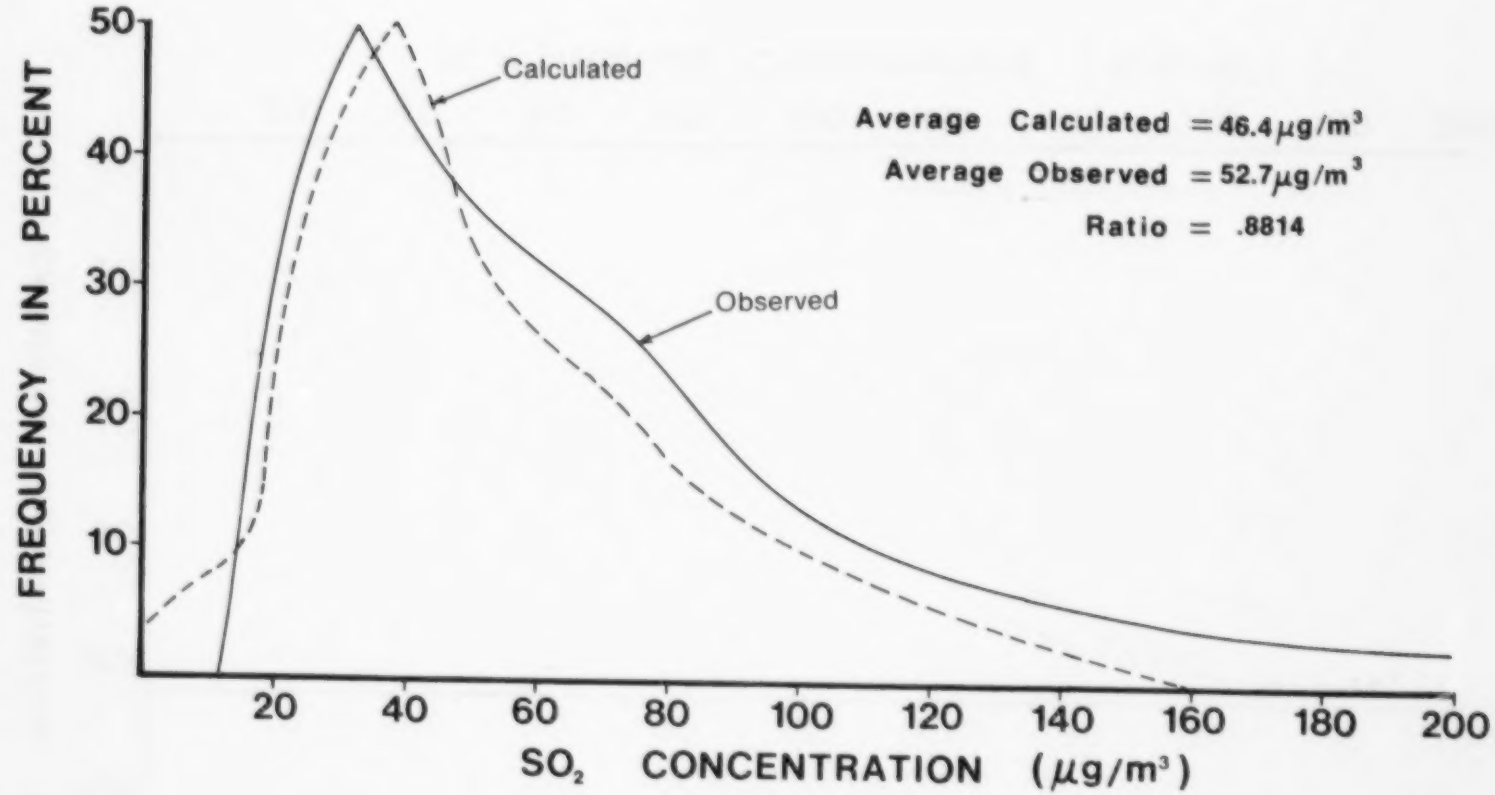

Figure 16. Frequency distributions of calculated and observed SO_2 concentrations for class AB stability occurrences.

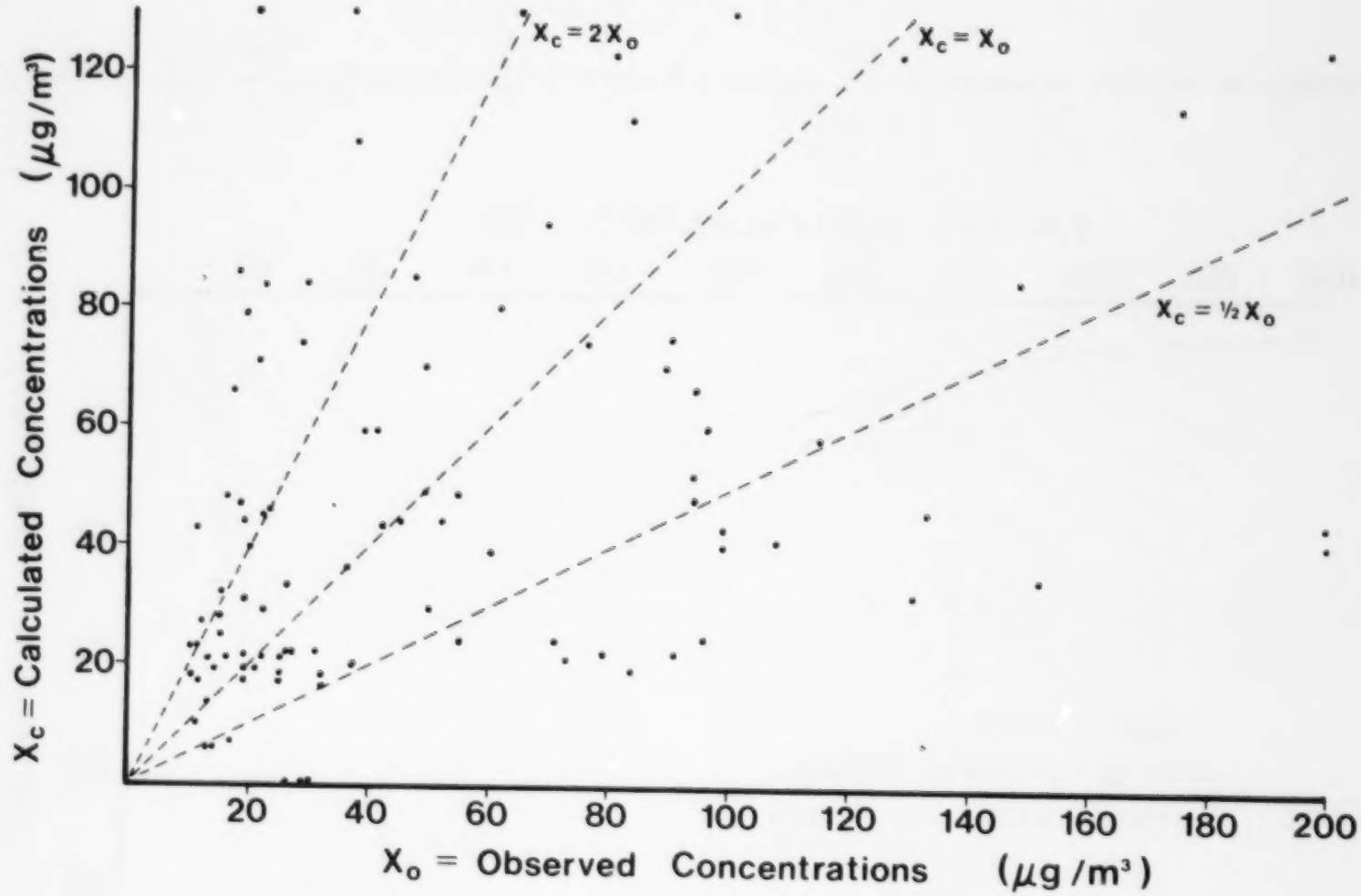

Figure 17. Scatter plot of hourly data points of calculated and observed SO_2 concentrations for class AB stability occurrences.

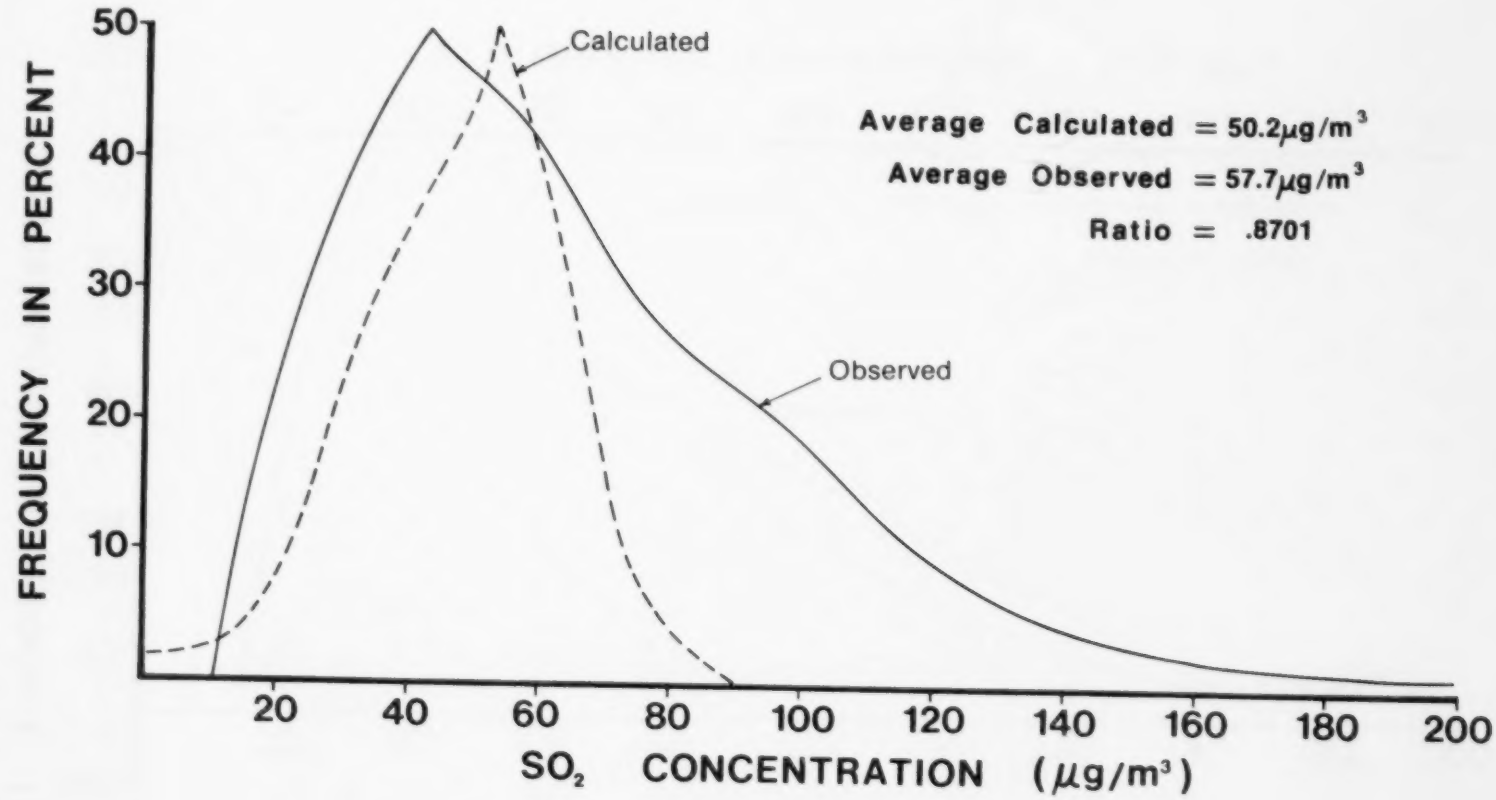

Figure 18. Frequency distributions of calculated and observed SO_2 concentrations for class B stability occurrences.

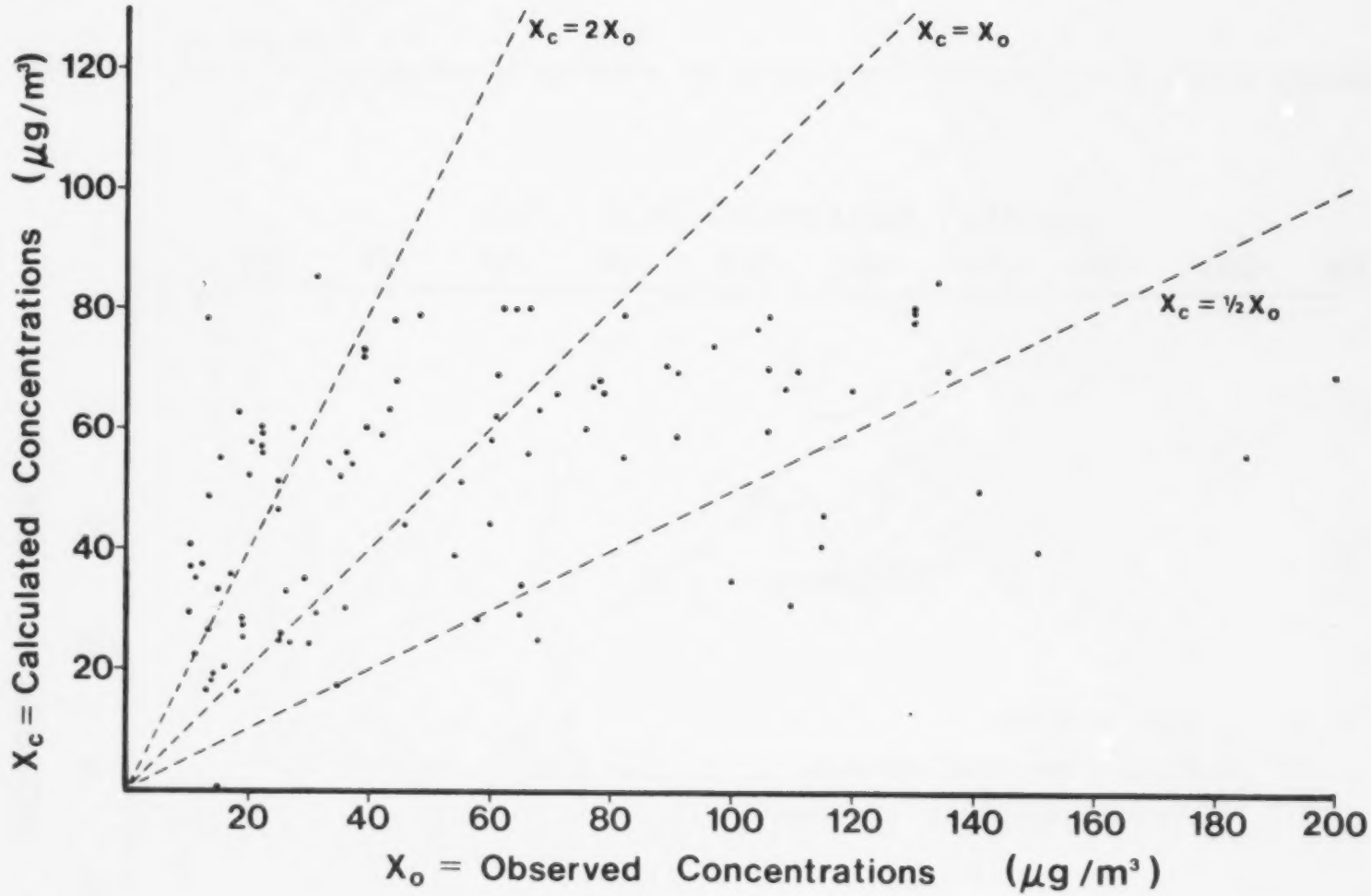

Figure 19. Scatter plot of hourly data points of calculated and observed SO_2 concentrations for class B stability occurrences.

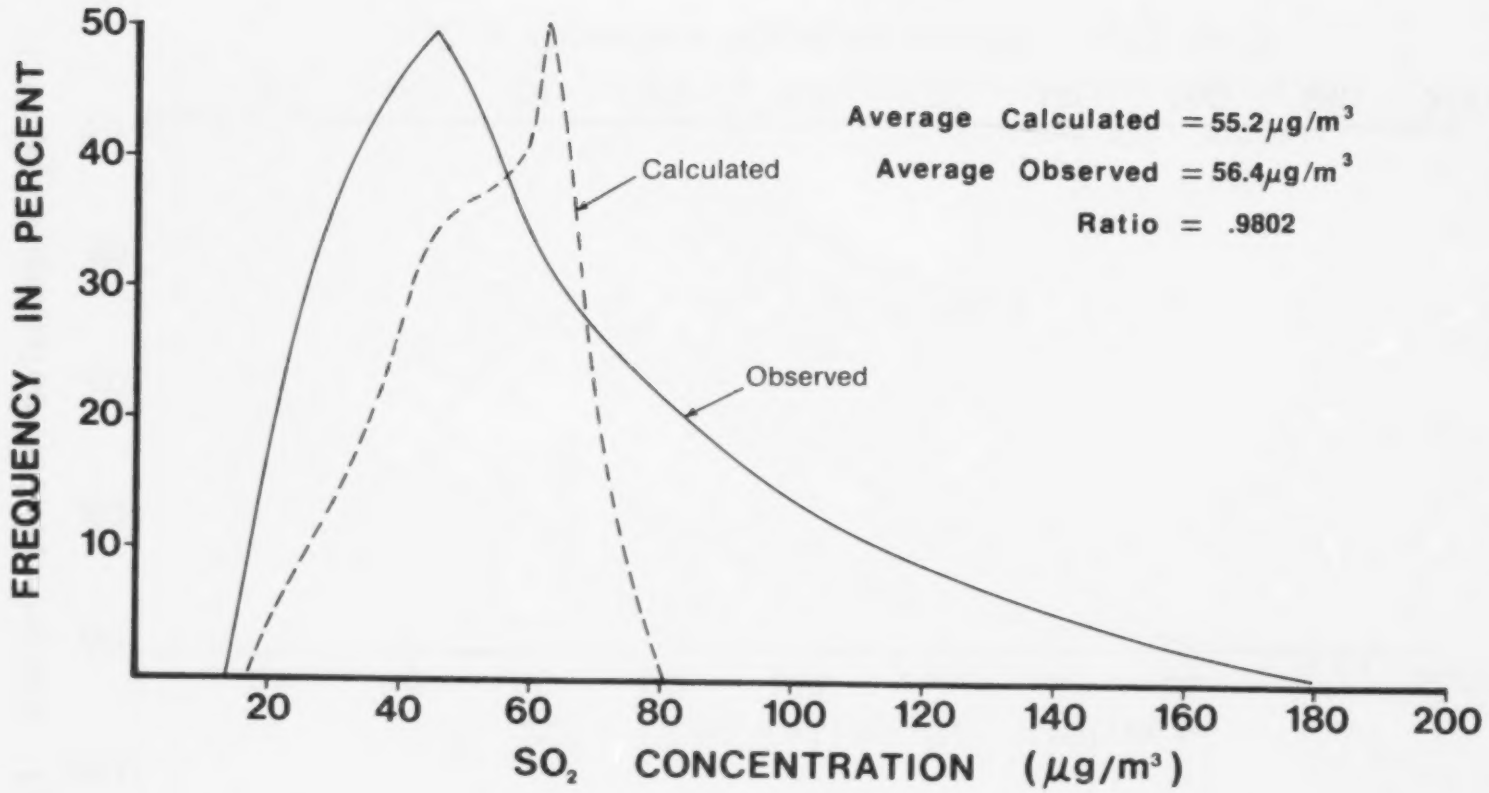

Figure 20. Frequency distributions of calculated and observed SO_2 concentrations for class BC stability occurrences.

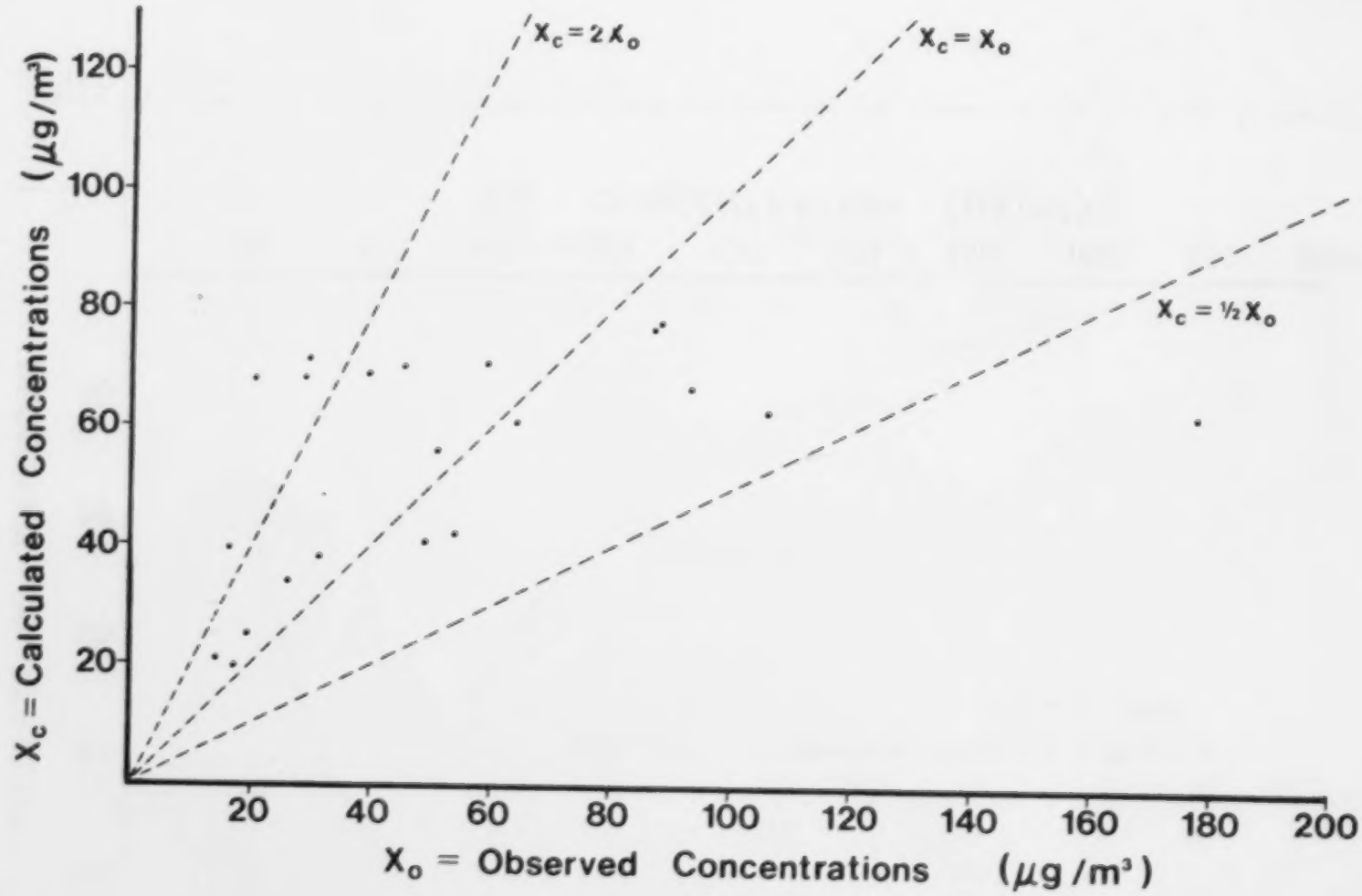

Figure 21. Scatter plot of hourly data points of calculated and observed SO_2 concentrations for class BC stability occurrences.

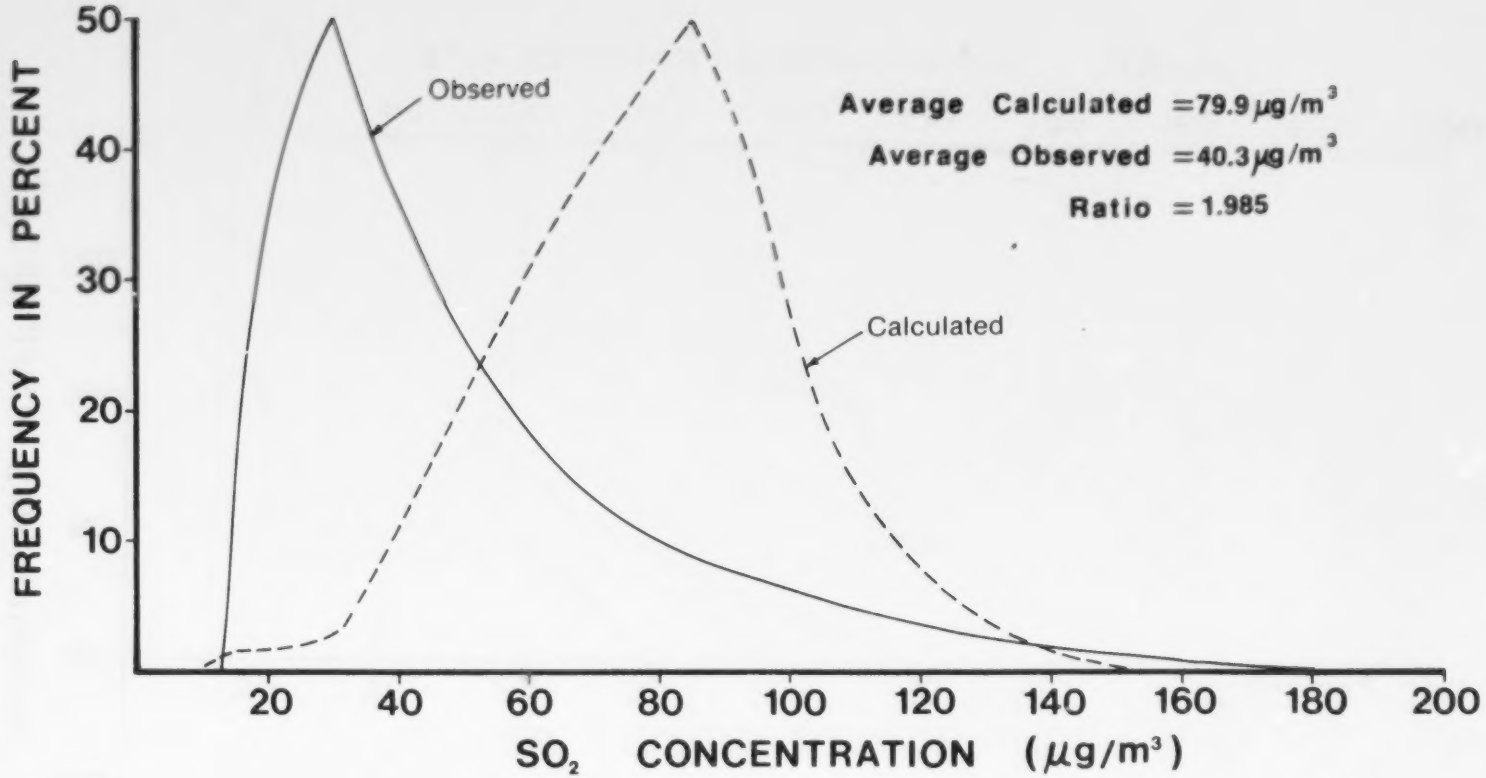

Figure 22. Frequency distributions of calculated and observed SO_2 concentrations for class C stability occurrences.

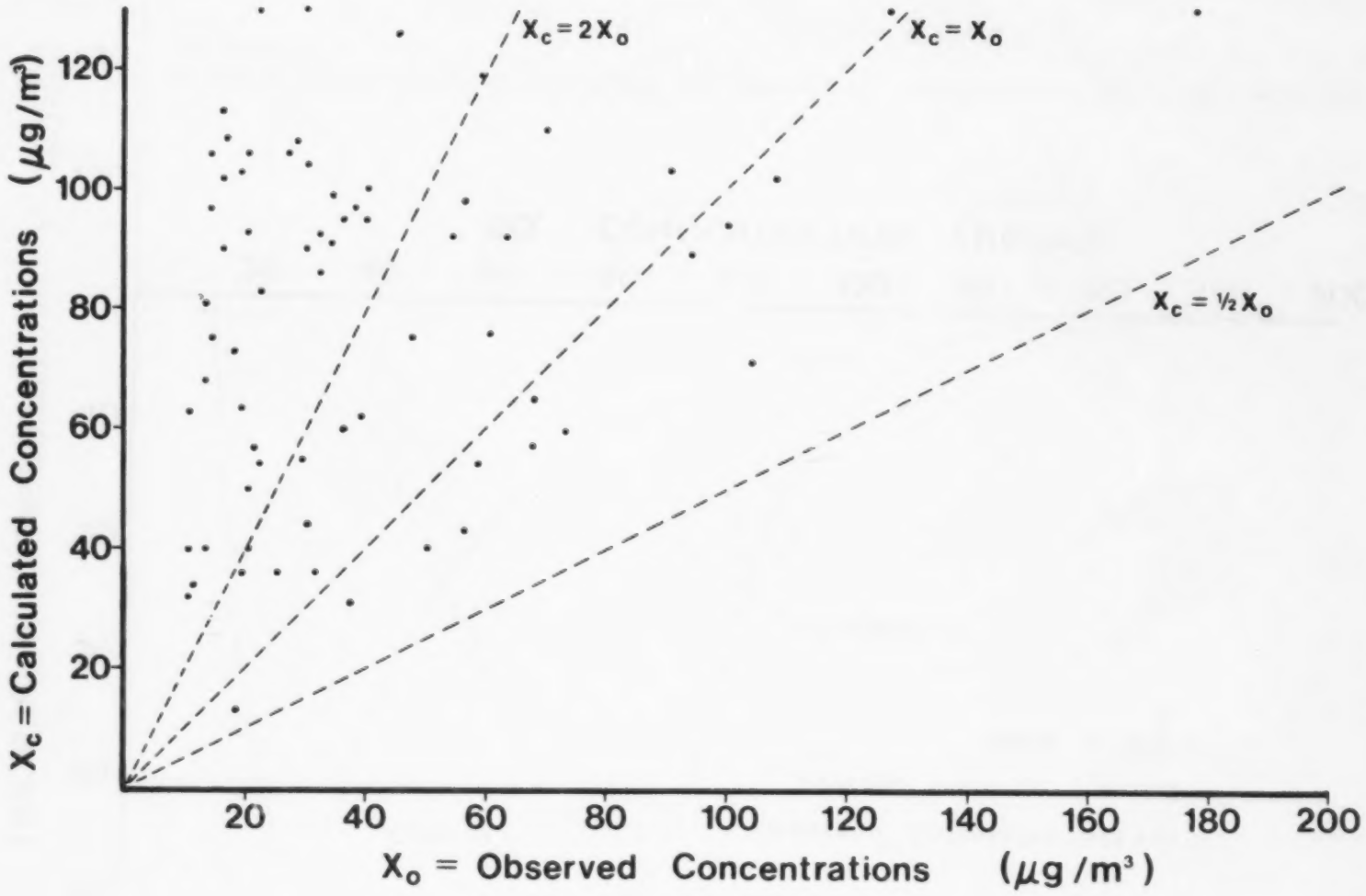

Figure 23. Scatter plot of hourly data points of calculated and observed SO_2 concentrations for class C stability occurrences.

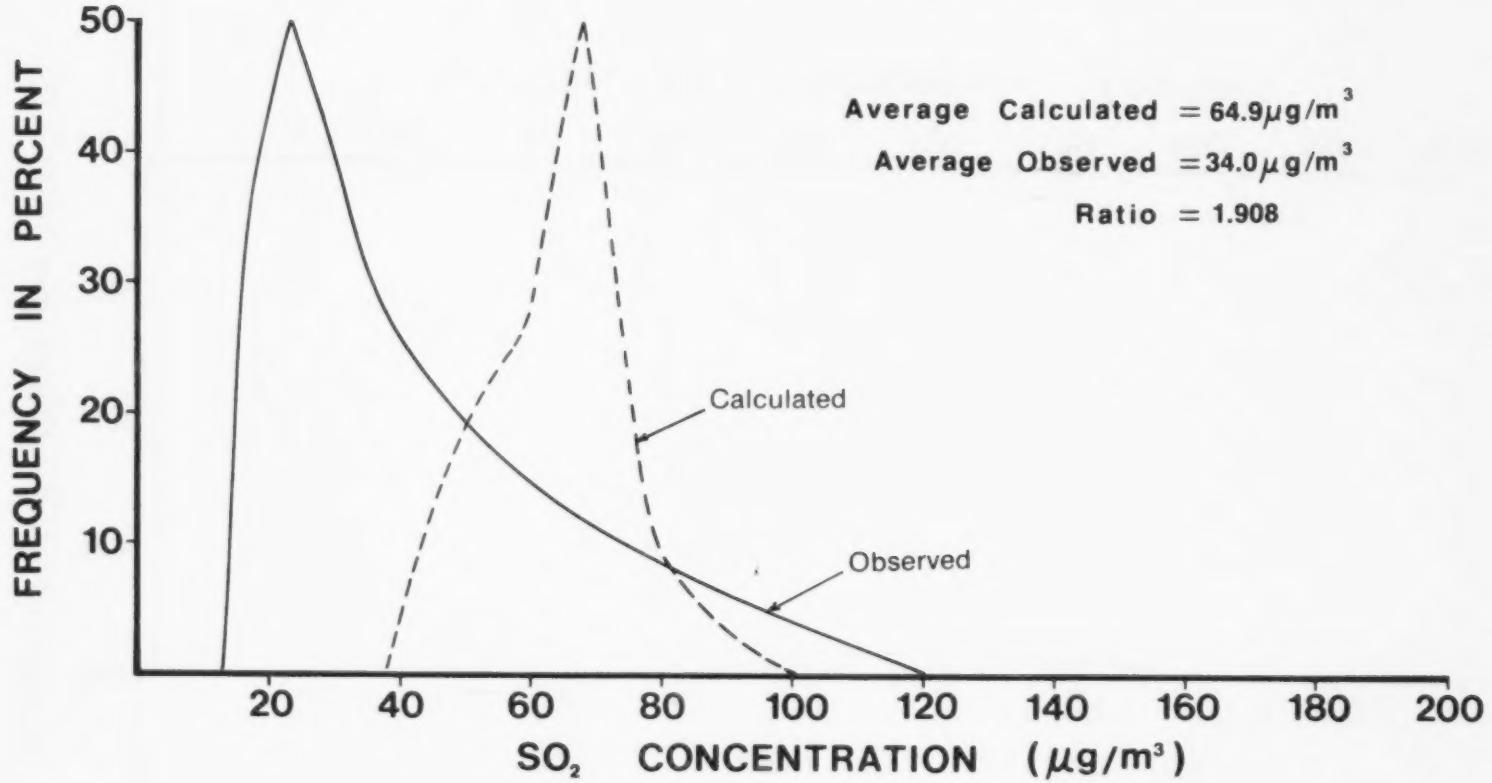

Figure 24. Frequency distributions of calculated and observed SO_2 concentrations for class CD stability occurrences.

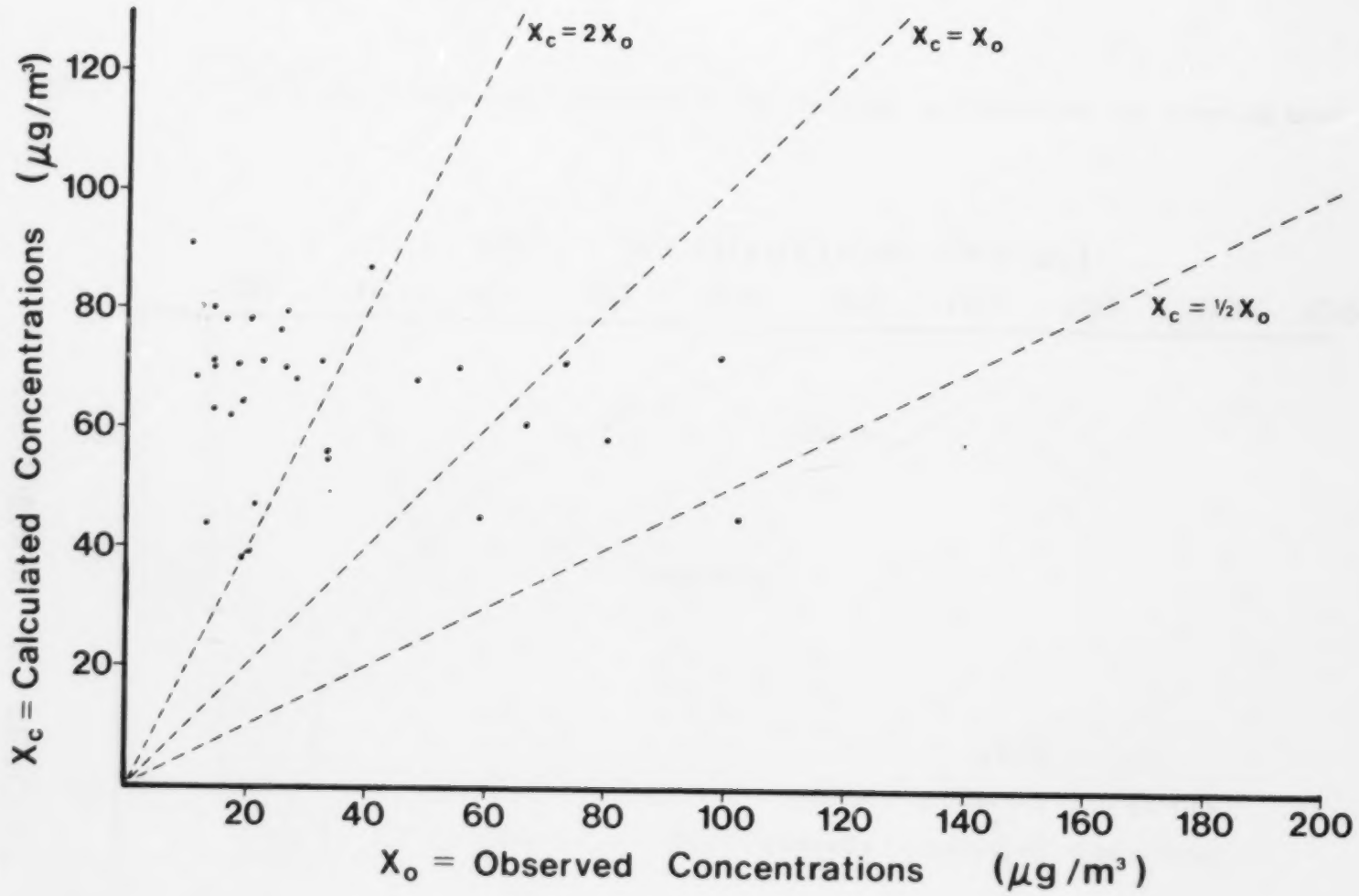

Figure 25. Scatter plot of hourly data points of calculated and observed SO_2 concentrations for class CD stability occurrences.

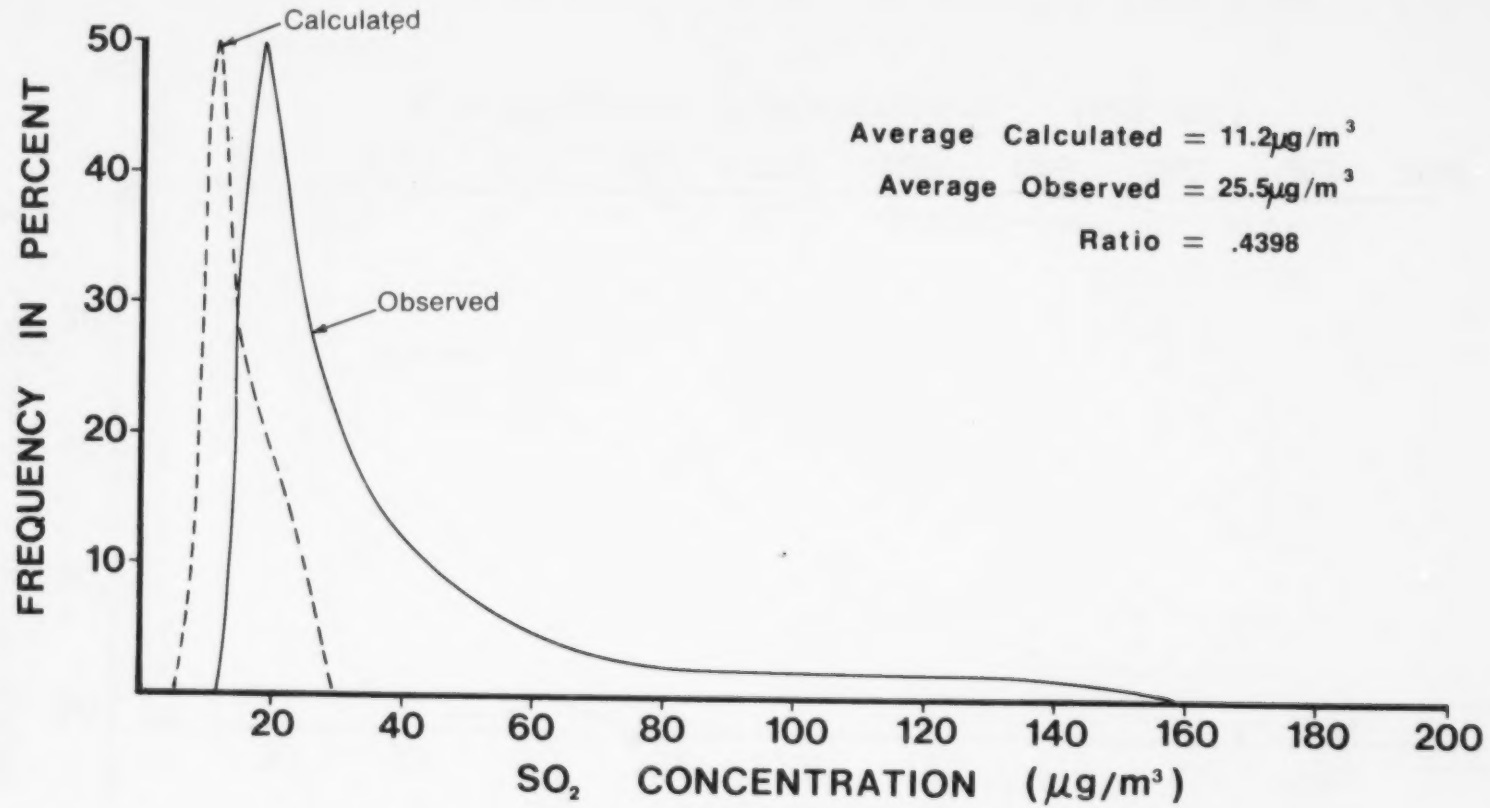

Figure 26. Frequency distributions of calculated and observed SO_2 concentrations for class D stability occurrences.

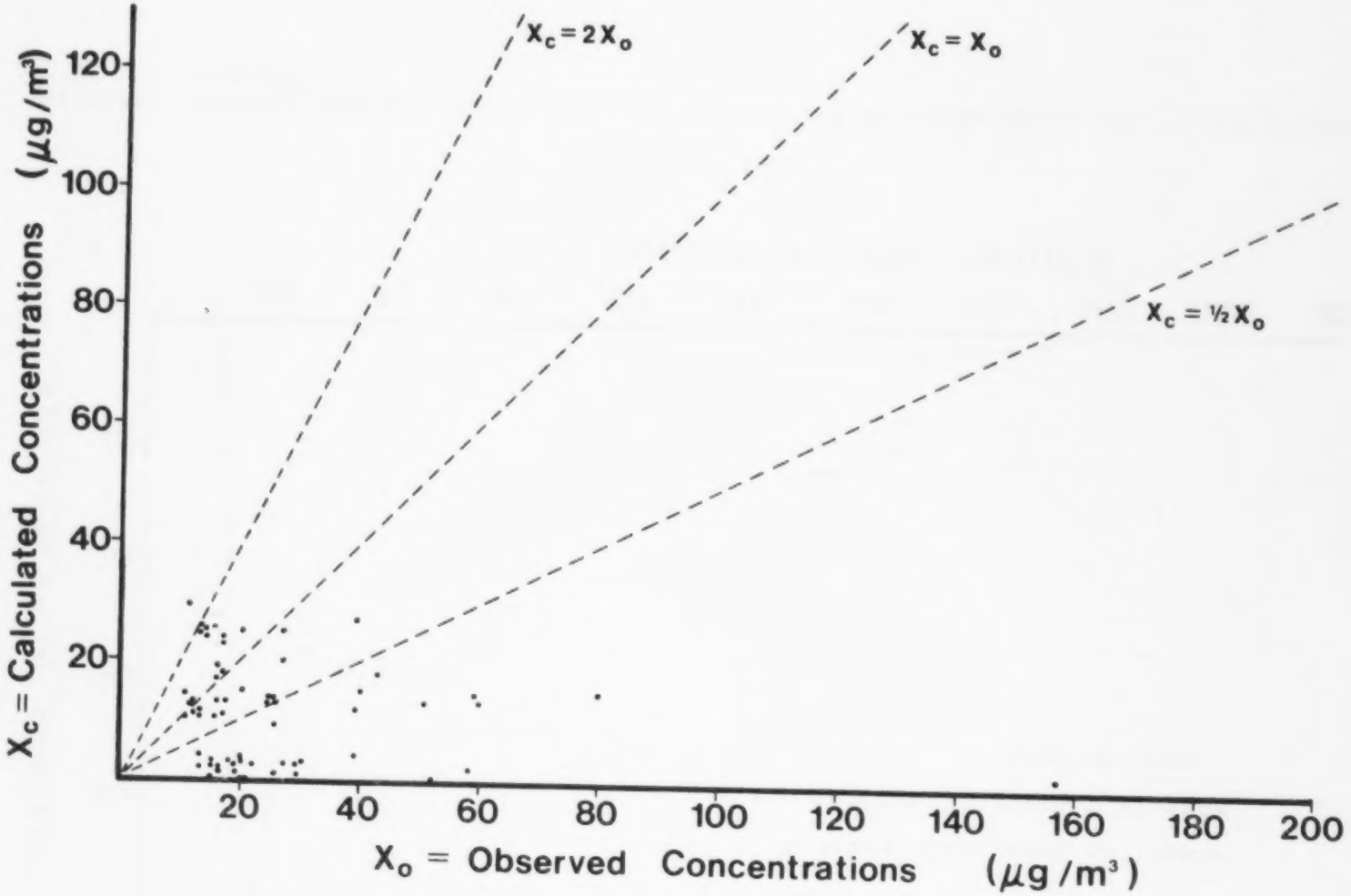

Figure 27. Scatter plot of hourly data points of calculated and observed SO_2 concentrations for class D stability occurrences.

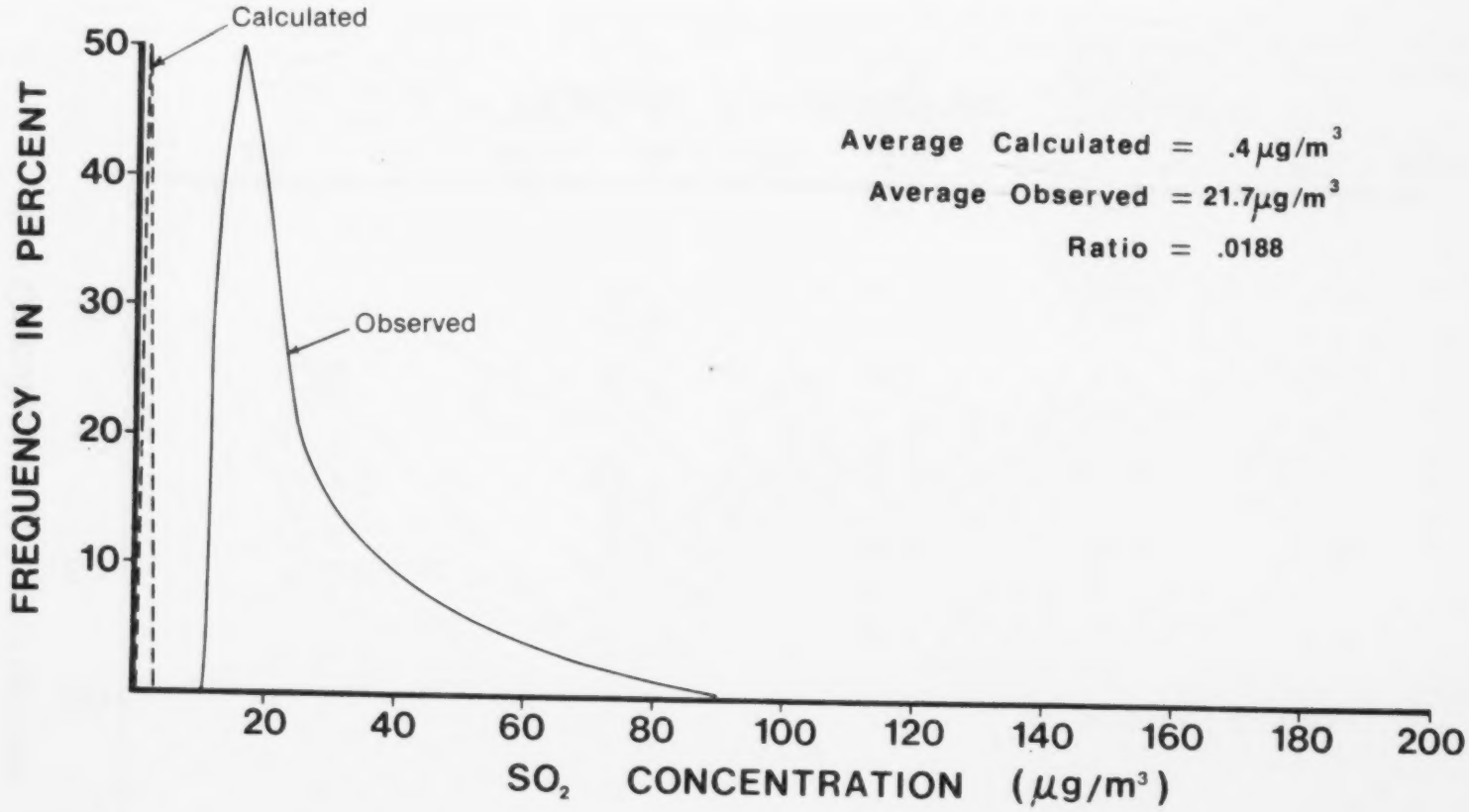

Figure 28. Frequency distributions of calculated and observed SO_2 concentrations for class E stability occurrences.

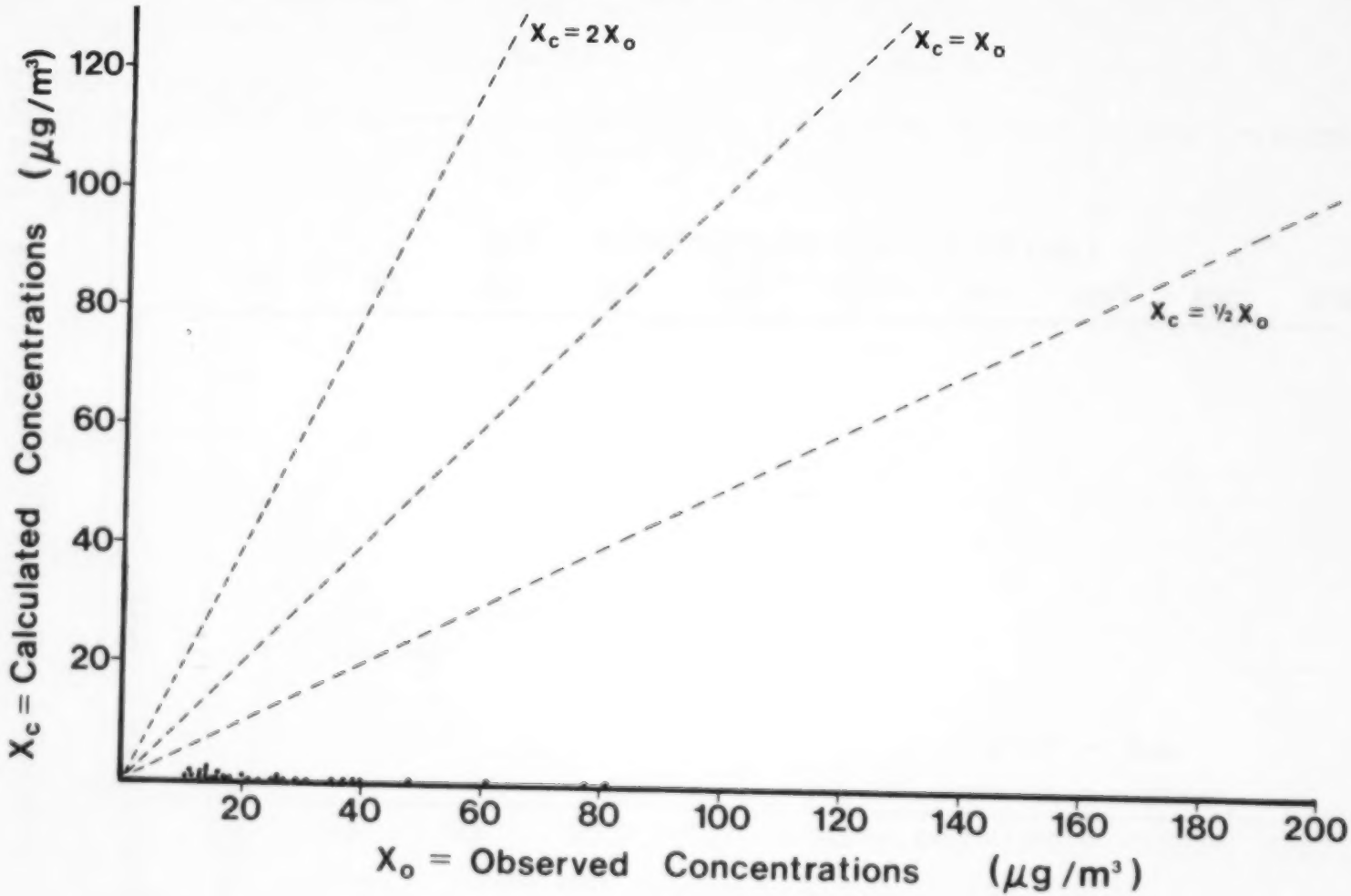

Figure 29. Scatter plot of hourly data points of calculated and observed SO_2 concentrations for class E stability occurrences.

TABLE 12. ANALYSIS OF CALCULATED AND OBSERVED SO_2 CONCENTRATIONS ACCORDING TO CLASSES OF ATMOSPHERIC STABILITY

Stability class	Number and percentage of occurrences out of 492	Number and percentage within a factor of 2	Average calculated SO_2 concentration ($\mu g/m^3$)	Average observed SO_2 concentration ($\mu g/m^3$)	Concentration ratio (calculated to observed)
A	36 (7.3)[a]	24 (66.7)	57.2	65.2	0.878
AB	101 (20.5)	58 (66.7)	46.7	52.7	0.881
B	102 (20.7)	68 (66.7)	50.2	57.4	0.870
BC	22 (4.5)	17 (77.3)	55.2	56.7	0.980
C	68 (13.8)	28 (41.2)	79.9	40.3	0.98
CD	32 (6.5)	10 (31.3)	64.9	34.0	1.91
D	68 (13.8)	31 (45.6)	11.2	25.5	0.440
E	63 (12.9)	0 (0.0)	0.4	21.7	0.019
Overall	492 (100.0)	263 (48.0)	43.5	44.2	0.985

[a]Percentages in parentheses.

up to a certain concentration level and then underpredicts the highest concentrations.

For stability classes C and CD the model shows an inclination to grossly overpredict. The frequency distributions of these stability classes are skewed to the right with respect to the observed values (Figure 22, Figure 24) The scatter plots of classes C and CD show 41% and 31% of the points within a factor of 2 (Figure 23, Figure 25). A majority of the points lie within the upper 22.5-deg sector, which illustrates the model's overprediction for these two stability categories.

The last two categories, D and E, are grossly underpredicted by the Gaussian plume model (Figures 26-29). Class E is by far the worst with a concentration ratio of only 0.0188. However, only those hours that registered more than 10 $\mu g/m^3$ at the monitoring site were selected.

Discussion of the model by stability classes raises many questions. The most sensitive parameters in the Gaussian model are the dispersion coefficients, which are functions of downwind distance x and the atmospheric stability. The largest variance comes from the different stability classifications. In other words, the most sensitive of all parameters associated with the Gaussian plume model is the selection of stability.

In reviewing the scatter plot of all the data points (Figure 11), it was questioned whether or not the scatter was truly random. A portion of the scatter was attributable to nighttime occurrences, with the model underpredicting the observed values by a factor of 5. Nighttime atmospheric stability is either neutral or stable; it can never be unstable because no atmospheric heating due to solar radiation occurs at night. Therefore, the underprediction at night is attributable to the model's tendency to undercalculate for stability classes D and E (neutral and stable). The underprediction of classes D and E is also not random; the scatter plots show definite clusters of points (Figure 27, Figure 29). In the cases where the model overpredicted, namely classes C and CD, it did so consistently, as shown in the scatter plots for these classes (Figure 23, Figure 25).

The four stability classifications A, AB, B, and BC had an average concentration ratio (ratio of calculated value to observed value) of 0.885 and had an average 64% of the data points within a factor of 2. This percentage is much higher than the 48% calculated for all of the classes combined. Some of the scatter in these four cases is possibly due to incorrect stability-class designation.

Calms and Periods of Rainfall

Another pronounced flaw of the Gaussian model is its inability to predict accurately during periods of low wind velocity. As the wind approaches a calm (a wind speed < 1 m/sec was the cutoff for a calm), the effective stack height may be greater than the assumed mixing height of 1,500 m, in which case the calculated ground-level concentration is zero. When wind speeds are low but not calm, plume rise will nevertheless be large, making the predicted ground-level concentration lower than possibly would be observed. This was

the case for several of the observed data points in Figure 11. As a general rule, the model's incapability of accurately calculating high concentrations during low wind speeds caused the model to underpredict.

Some of the scatter in the plots was thought to be caused by periods of rainfall. During rainfall some of the SO_2 is washed out of the air. Rainfall was recorded during 13 of the 492 h when the plume was there. During rainfall the average calculated value of SO_2 was 30 $\mu g/m^3$, and the average observed value was 40 $\mu g/m^3$. Apparently some of the SO_2 in the air is washed out by the action of the rain.

AVERAGE CONCENTRATIONS AT THE SEVEN MONITORING SITES

The annual average concentrations at each of the seven SO_2 monitoring sites were examined. Figures 30 through 43 are frequency distributions and scatter plots of the data observed at the seven monitoring sites; Table 13 is a summary of the results. All of the concentration ratios are close to 1, and the model is therefore consistent in predicting relatively accurate annual average values. A correlation coefficient of 0.954 was calculated based on the annual averages for the seven SO_2 monitoring stations. The annual averages are shown as a scatter plot in Figure 44.

The sites were ranked in order of highest to lowest SO_2 concentration, and the concentrations were compared with the distance from the stack (Table 14). The highest average observed concentrations as well as the highest average calculated concentrations occurred at the sites nearest the stack, and the lowest concentrations occurred at the sites farthest away from the stack.

The highest concentration ratio, 1.24, was observed at the Messer site. The Messer site is the only one of the seven that is located in uneven terrain, namely, the Baraboo Bluffs. The increased turbulence caused by the hills could very well explain the highest concentration ratio. The two lowest concentration ratios, 0.741 and 0.788, were calculated for the Bernander and Russell sites, respectively. These two sites are farthest from the generating station. Higher concentrations would be expected at these stations during periods of neutral or slightly stable atmospheric conditions. Neutral or slightly stable conditions prevailed 73.9% of the time at Bernander and 63.2% of the time at Russell. The highest percentage of occurrences for stability classes D and E, coupled with the model's tendency to underpredict at these stabilities, explains the two lowest concentration ratios.

WORST-CASE OR HIGHEST SO_2 CONCENTRATIONS

The worst-case or highest observed hourly SO_2 concentration due to the generating station during 1976 (with the background removed) was 247 $\mu g/m^3$, and the highest model output was 157 $\mu g/m^3$ for the sector-averaged value, which corresponds to a plume centerline of 245 $\mu g/m^3$. The highest observed and calculated values did not occur at the same time, however. The high concentrations occurred with A and AB stability conditions. The highest observed concentrations were not associated with inversion-breakup or fumigation-type conditions in this study. (Text continues on p.72).

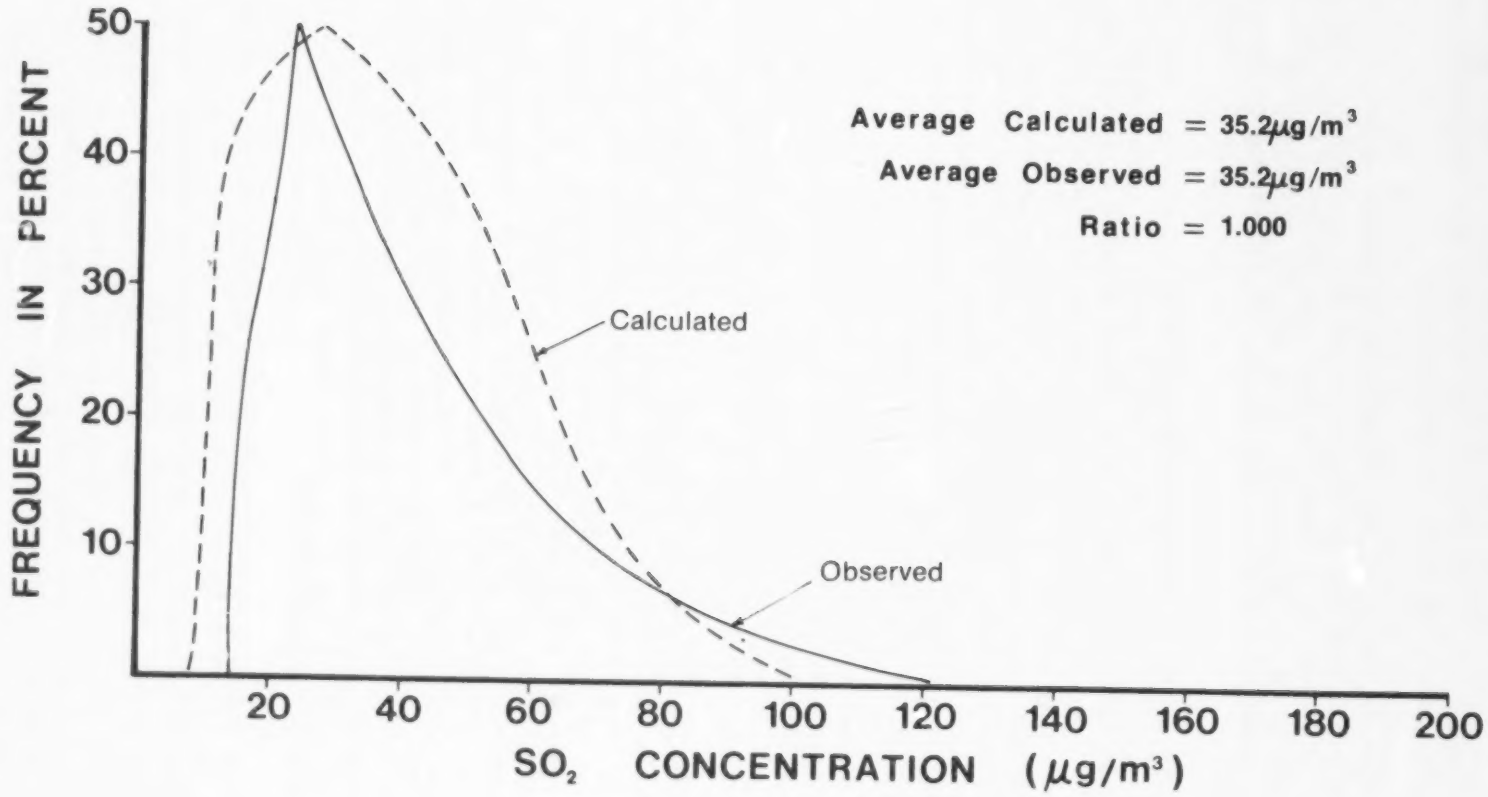

Figure 30. Frequency distributions of calculated and observed SO_2 concentrations for occurrences at the Portage cemetery site (site 002).

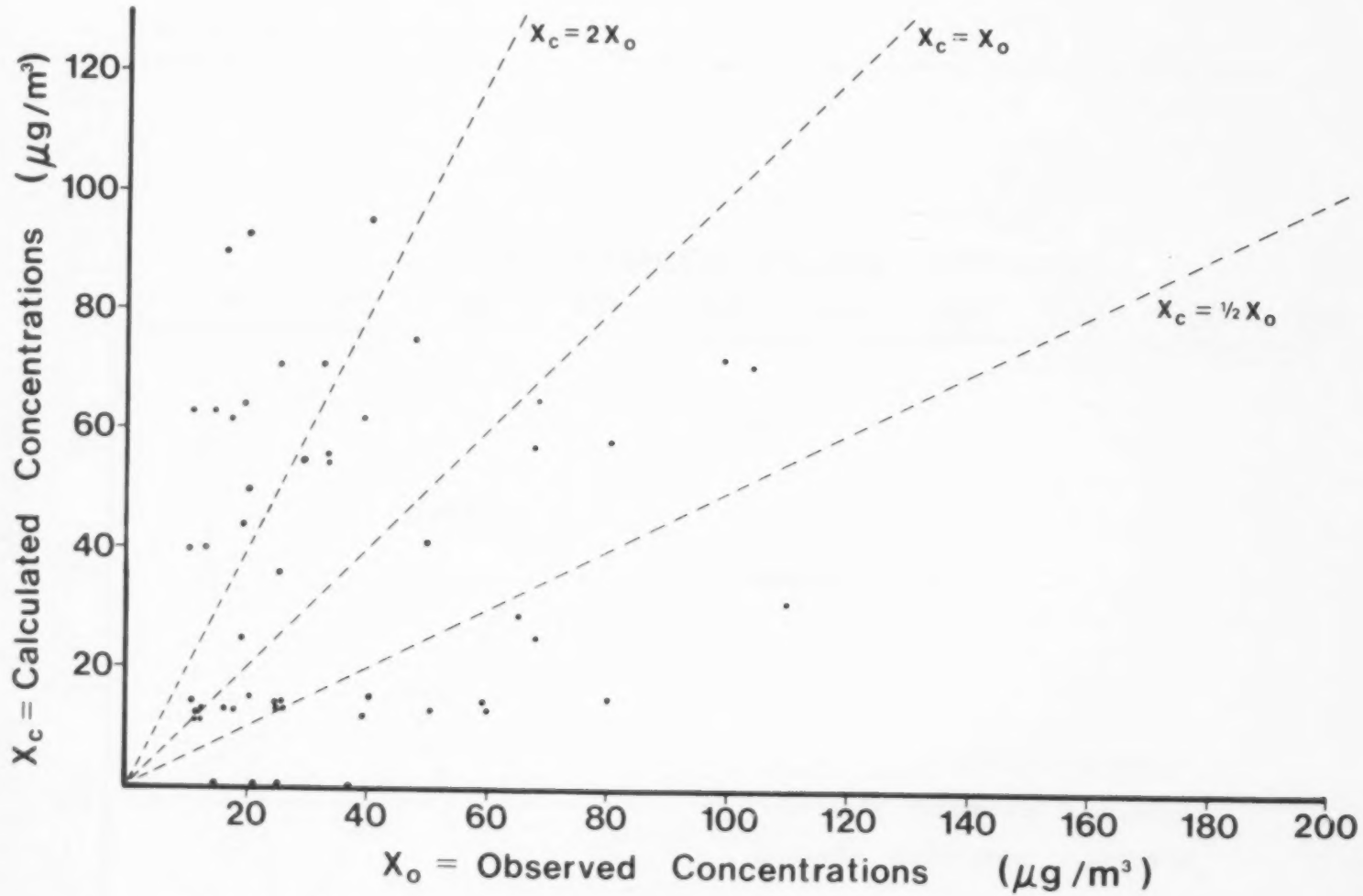

Figure 31. Scatter plot of hourly data points of calculated and observed SO_2 concentrations for occurrences at the Portage cemetery site (site 002).

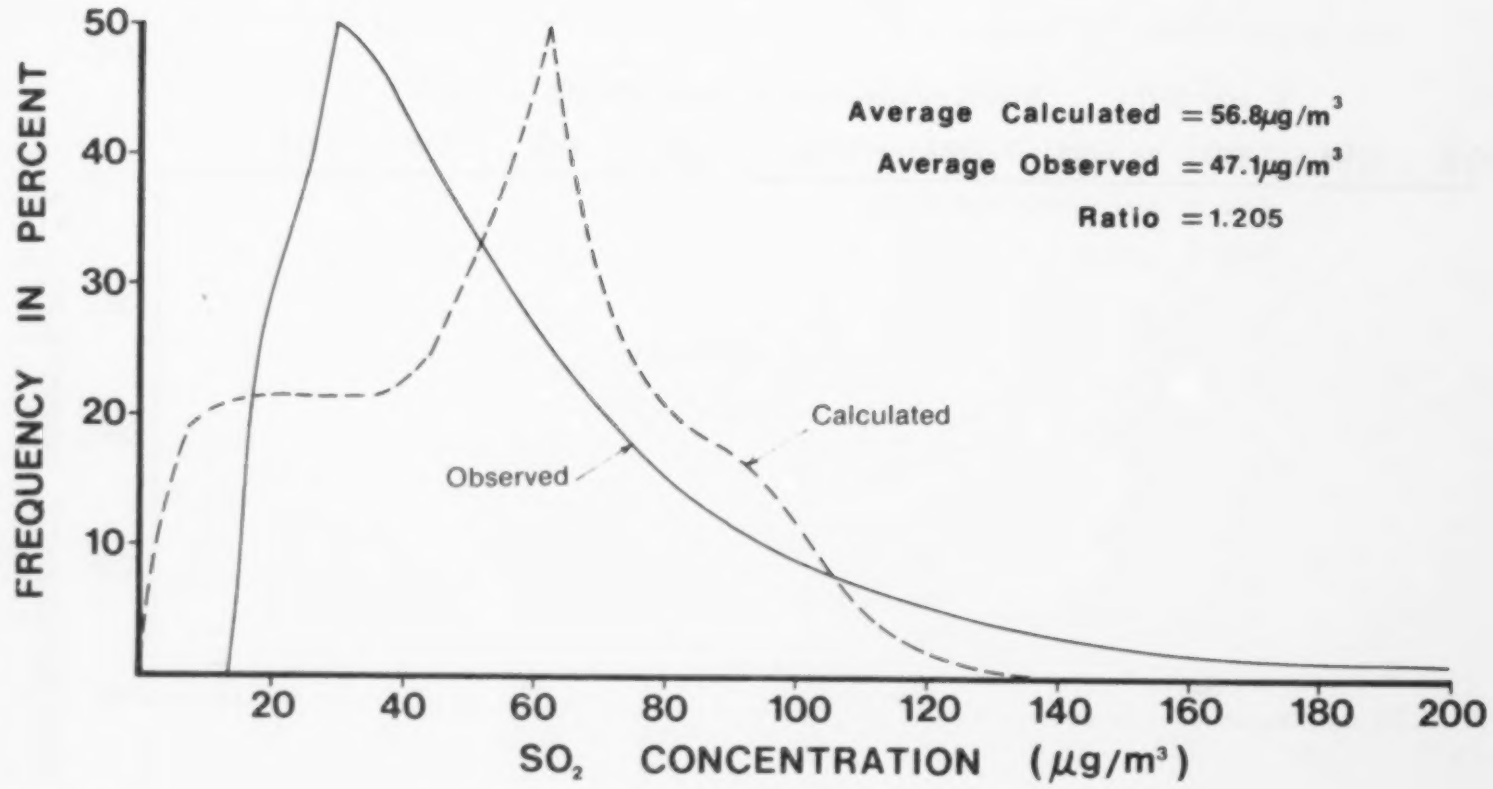

Figure 32. Frequency distributions of calculated and observed SO_2 concentrations for occurrences at the Lake George site (site 003).

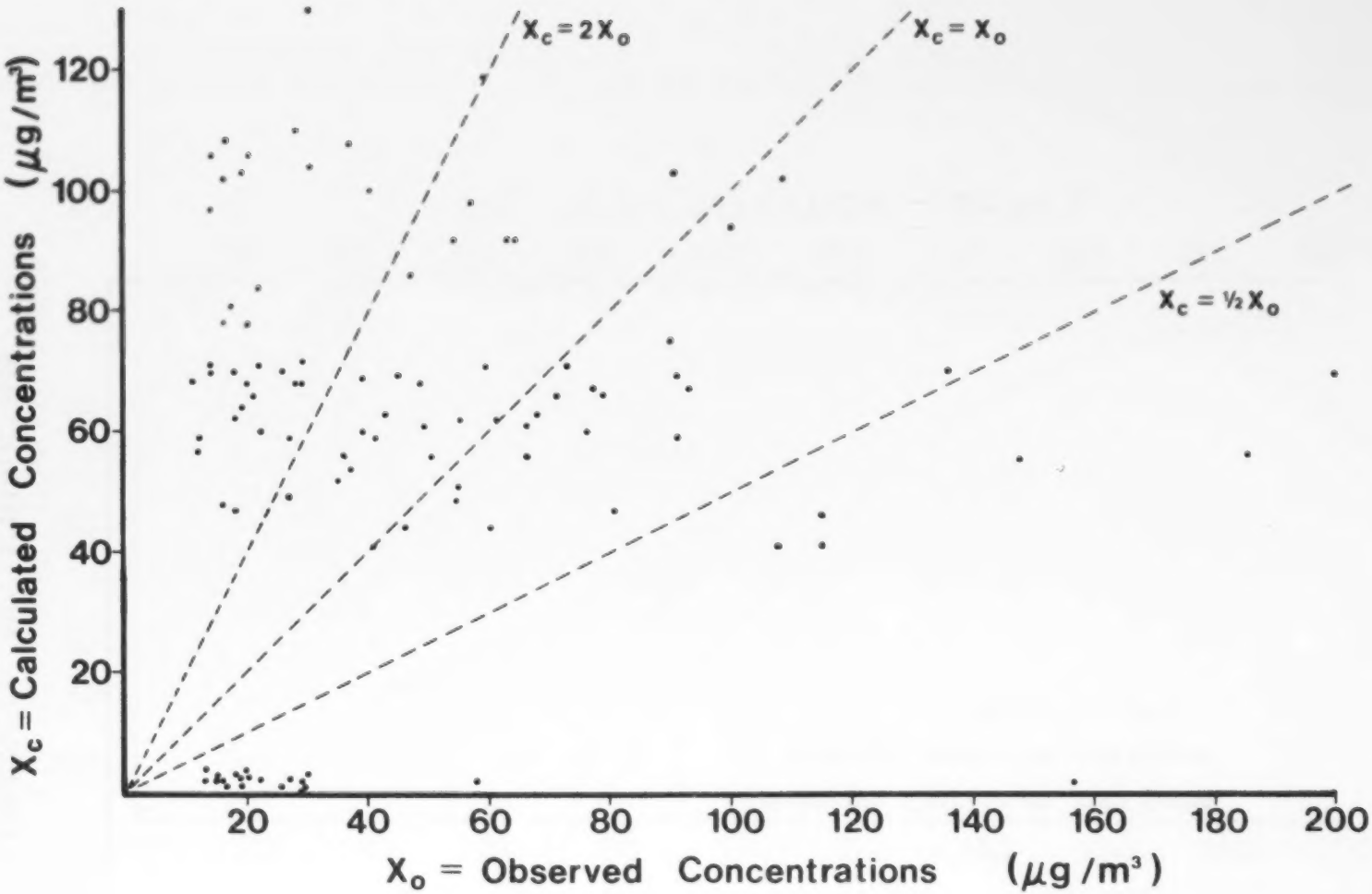

Figure 33. Scatter plot of hourly data points of calculated and observed SO_2 concentrations for occurrences at the Lake George site (site 003).

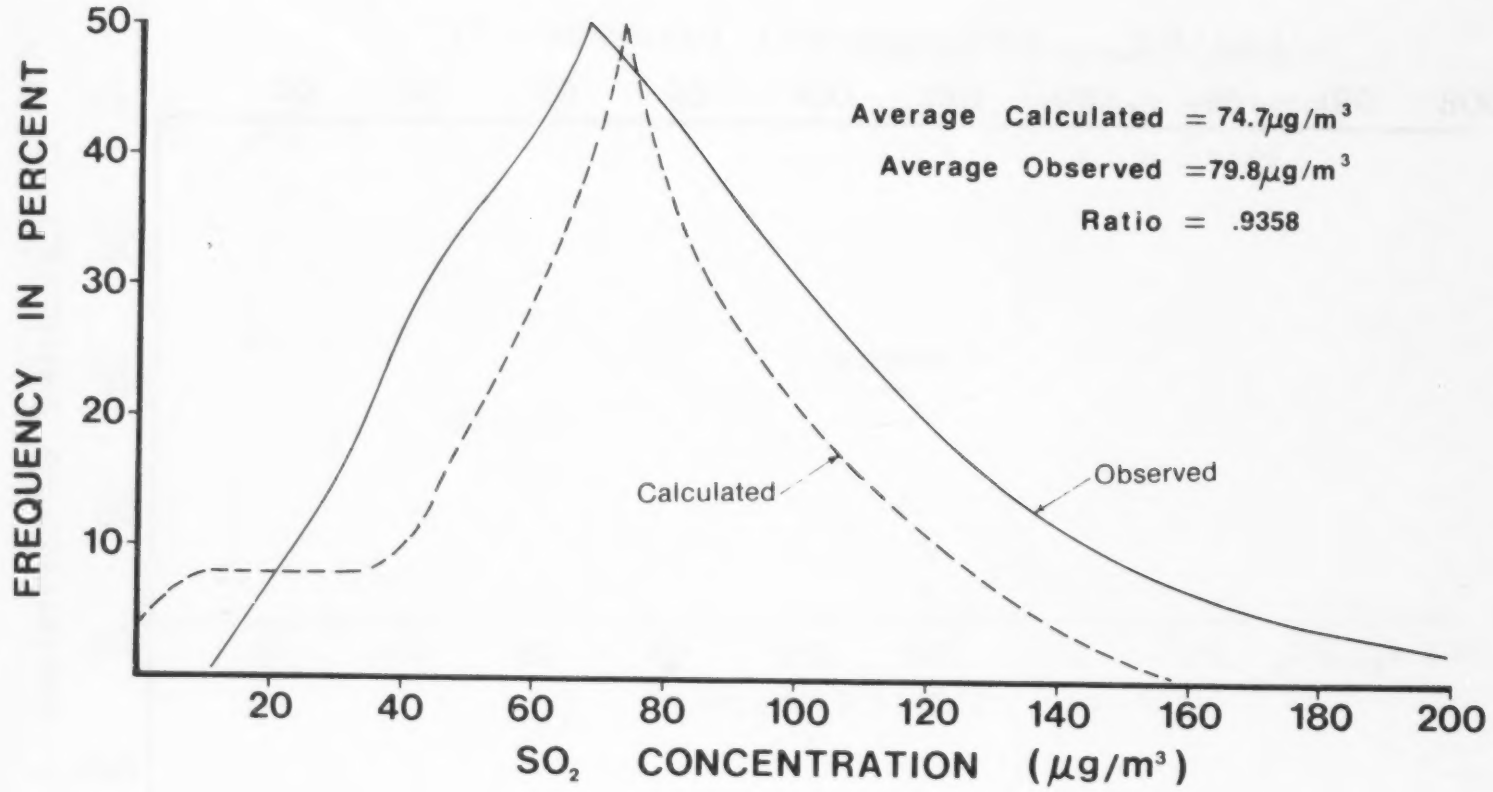

Figure 34. Frequency distributions of calculated and observed SO_2 concentrations for occurrences at the Dekorra site (site 004).

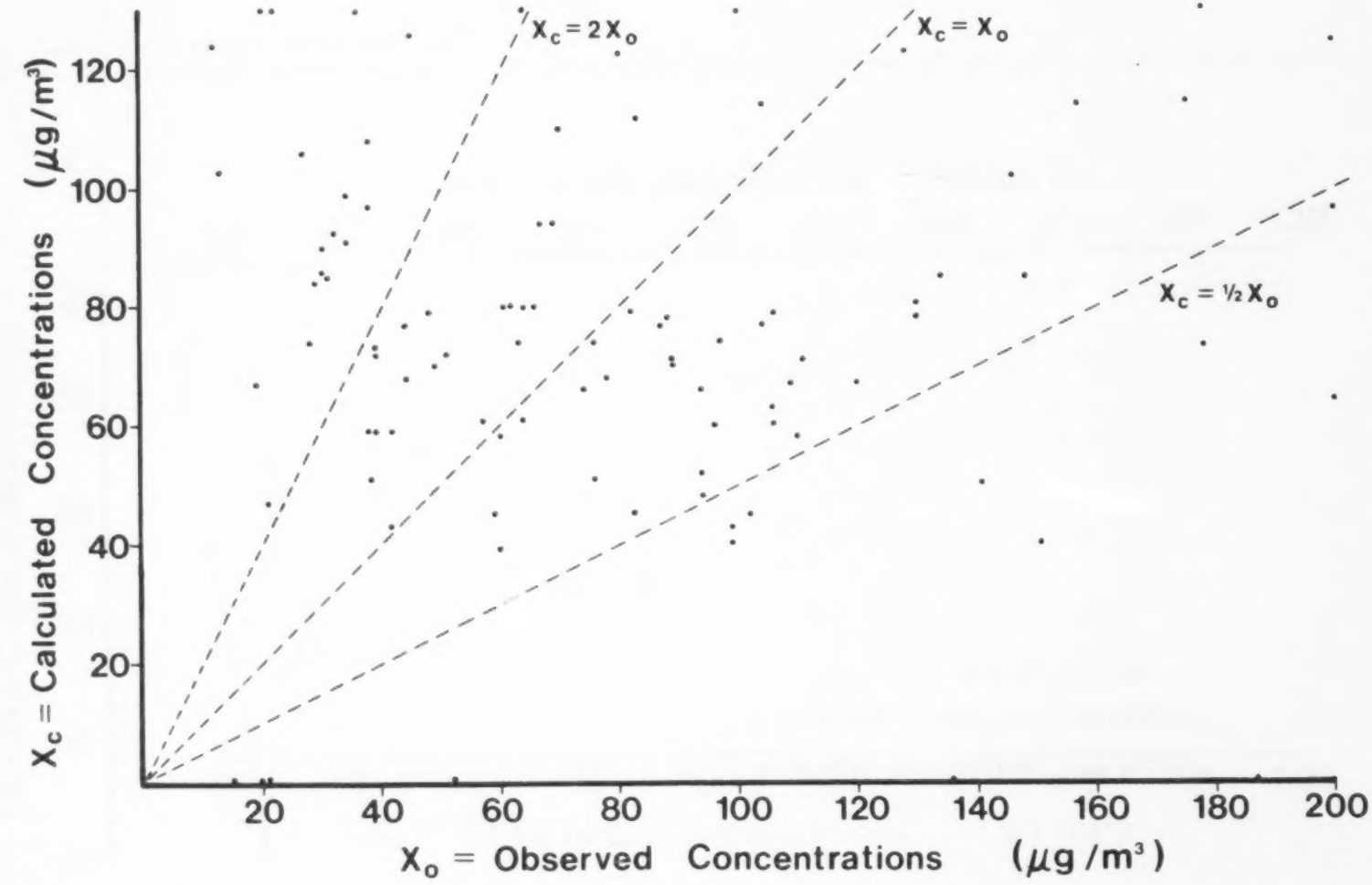

Figure 35. Scatter plot of hourly data points of calculated and observed SO_2 concentrations for occurrences at the Dekorra site (site 004).

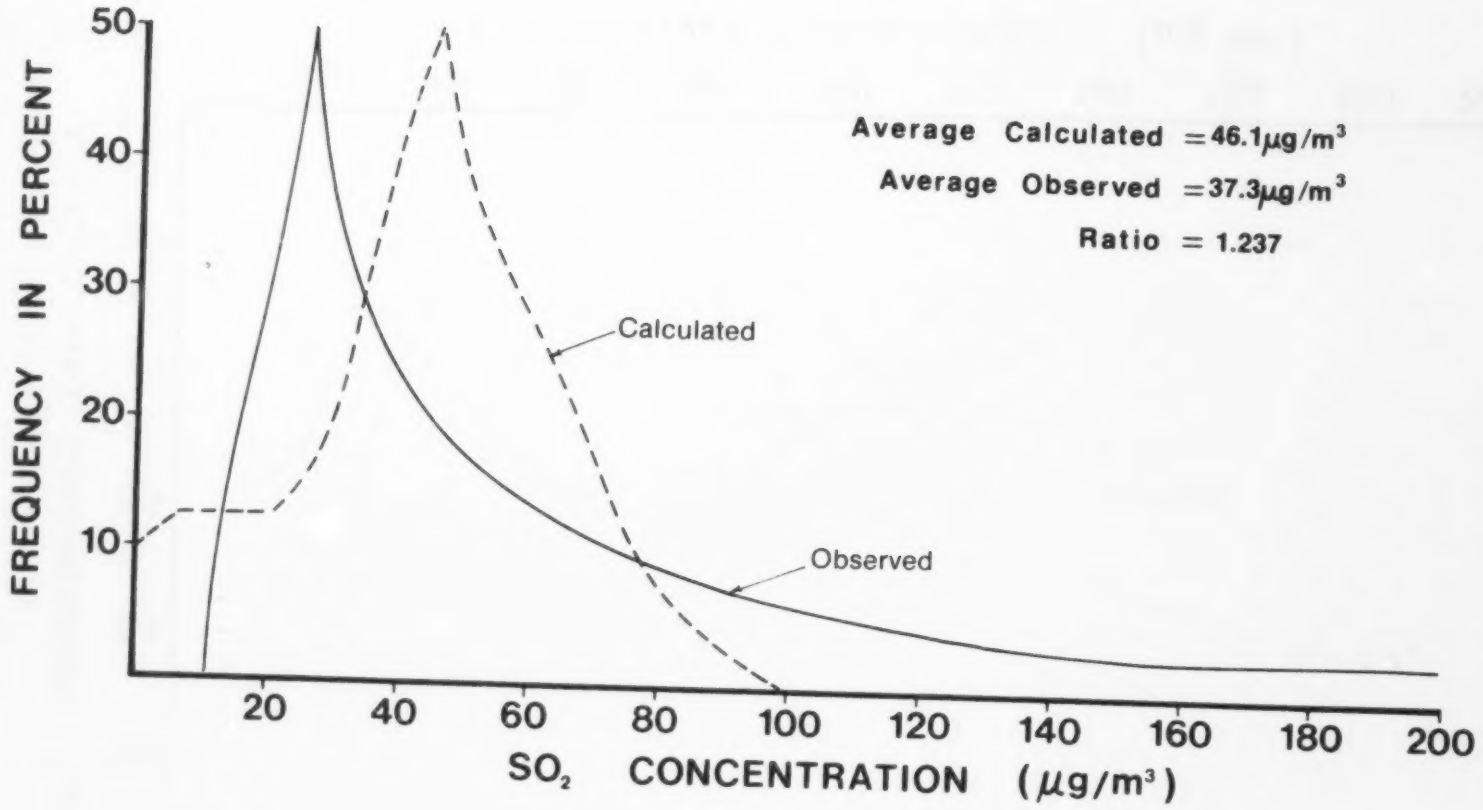

Figure 36. Frequency distributions of calculated and observed SO_2 concentrations for occurrences at the Messer site (site 005).

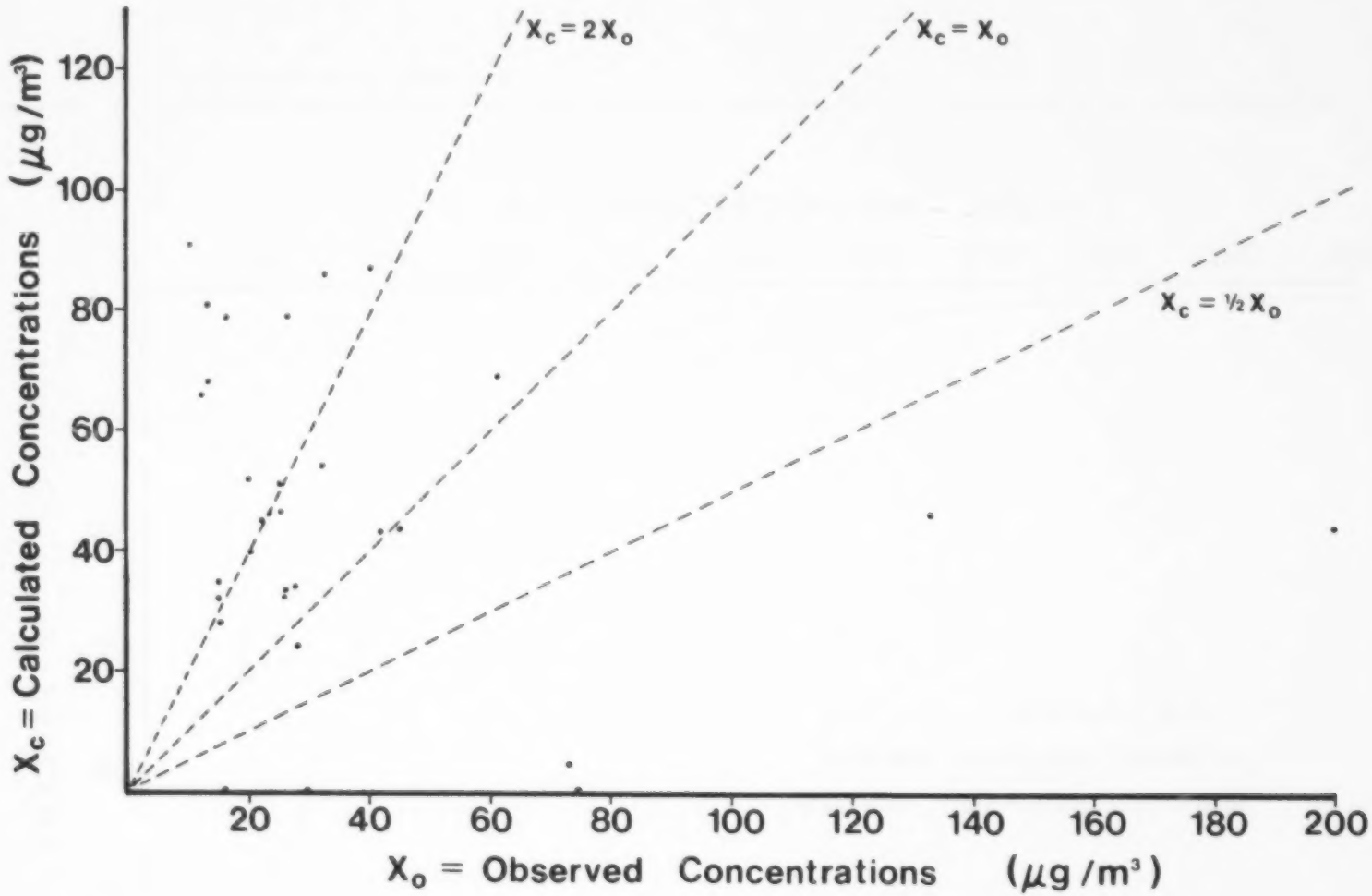

Figure 37. Scatter plot of hourly data points of calculated and observed SO_2 concentrations for occurrences at the Messer site (site 005).

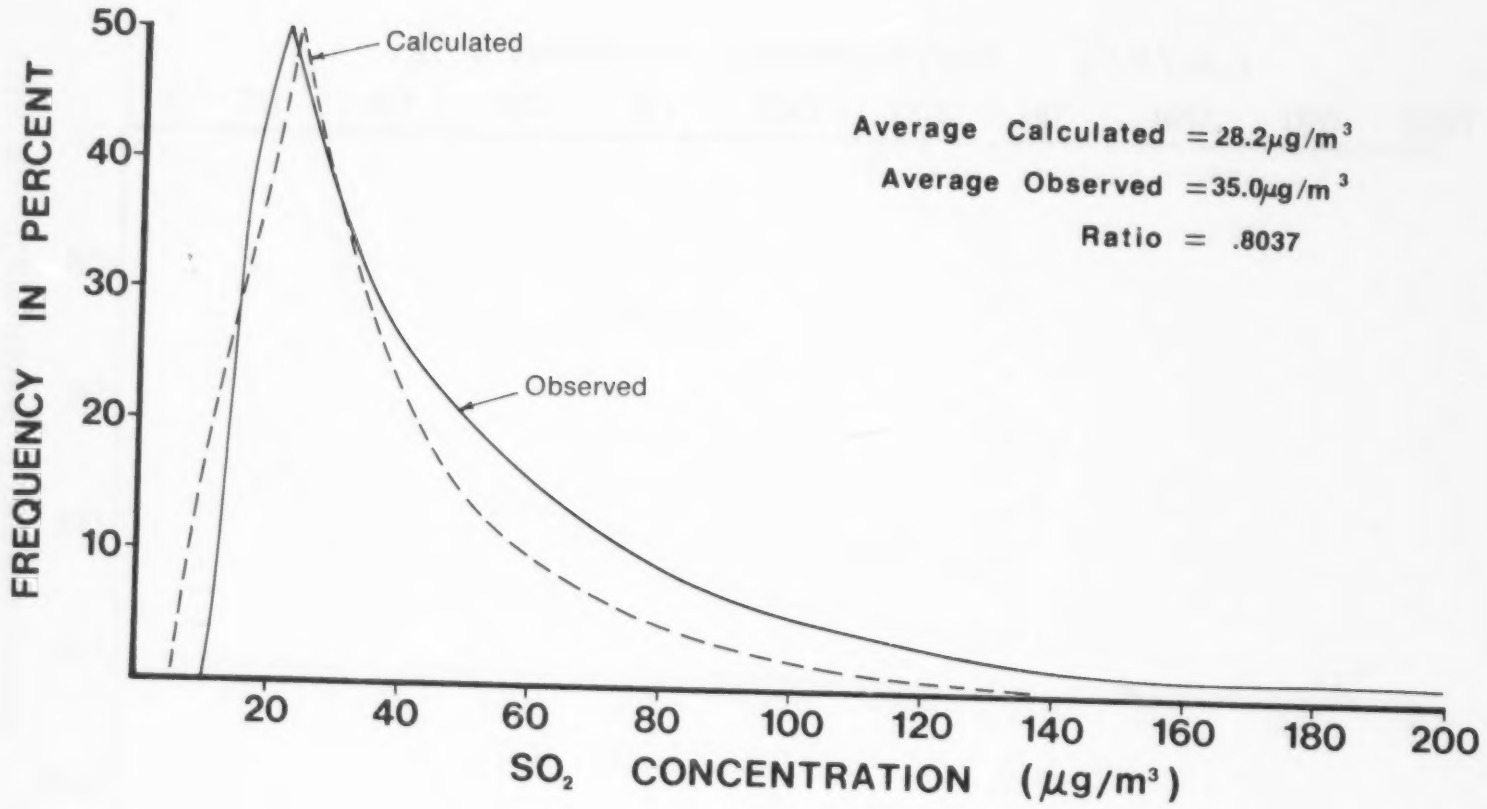

Figure 38. Frequency distributions of calculated and observed SO_2 concentrations for occurrences at the Genrich site (site 008).

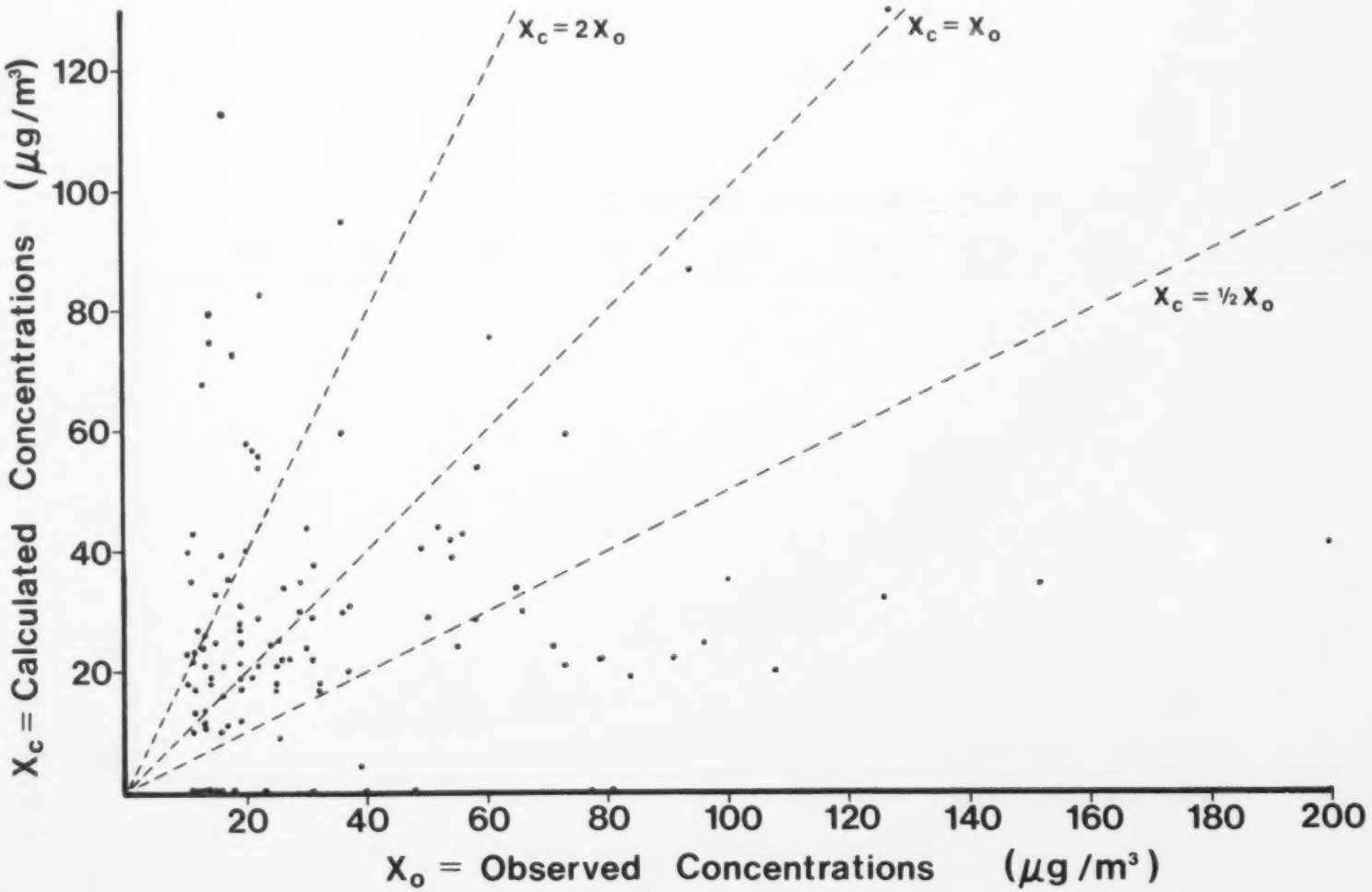

Figure 39. Scatter plot of hourly data points of calculated and observed SO_2 concentrations for occurrences at the Genrich site (site 008).

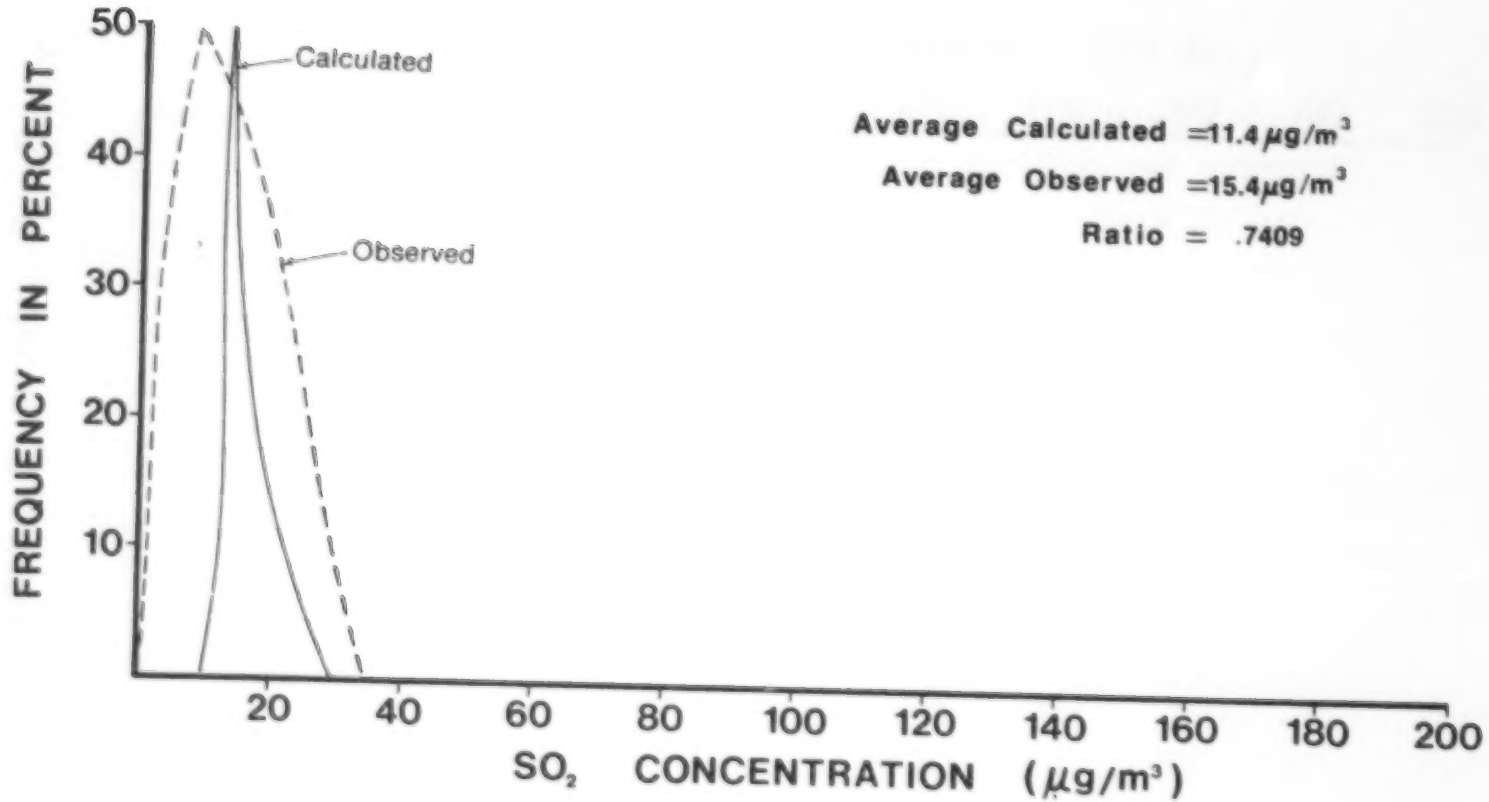

Figure 40. Frequency distributions of calculated and observed SO_2 concentrations for occurrences at the Bernander site (site 009).

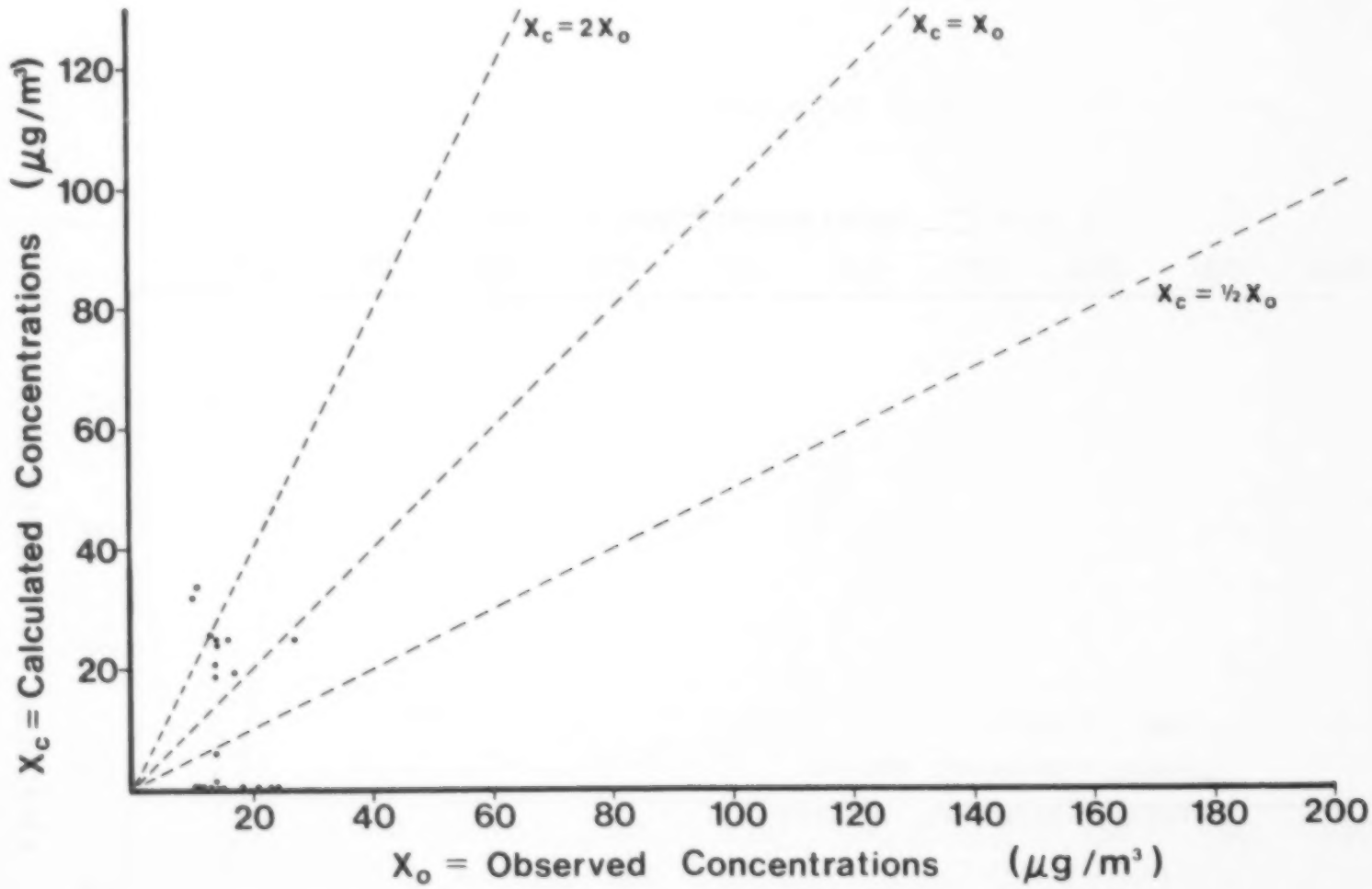

Figure 41. Scatter plot of hourly data points of calculated and observed SO_2 concentrations for occurrences at the Bernander site (site 009).

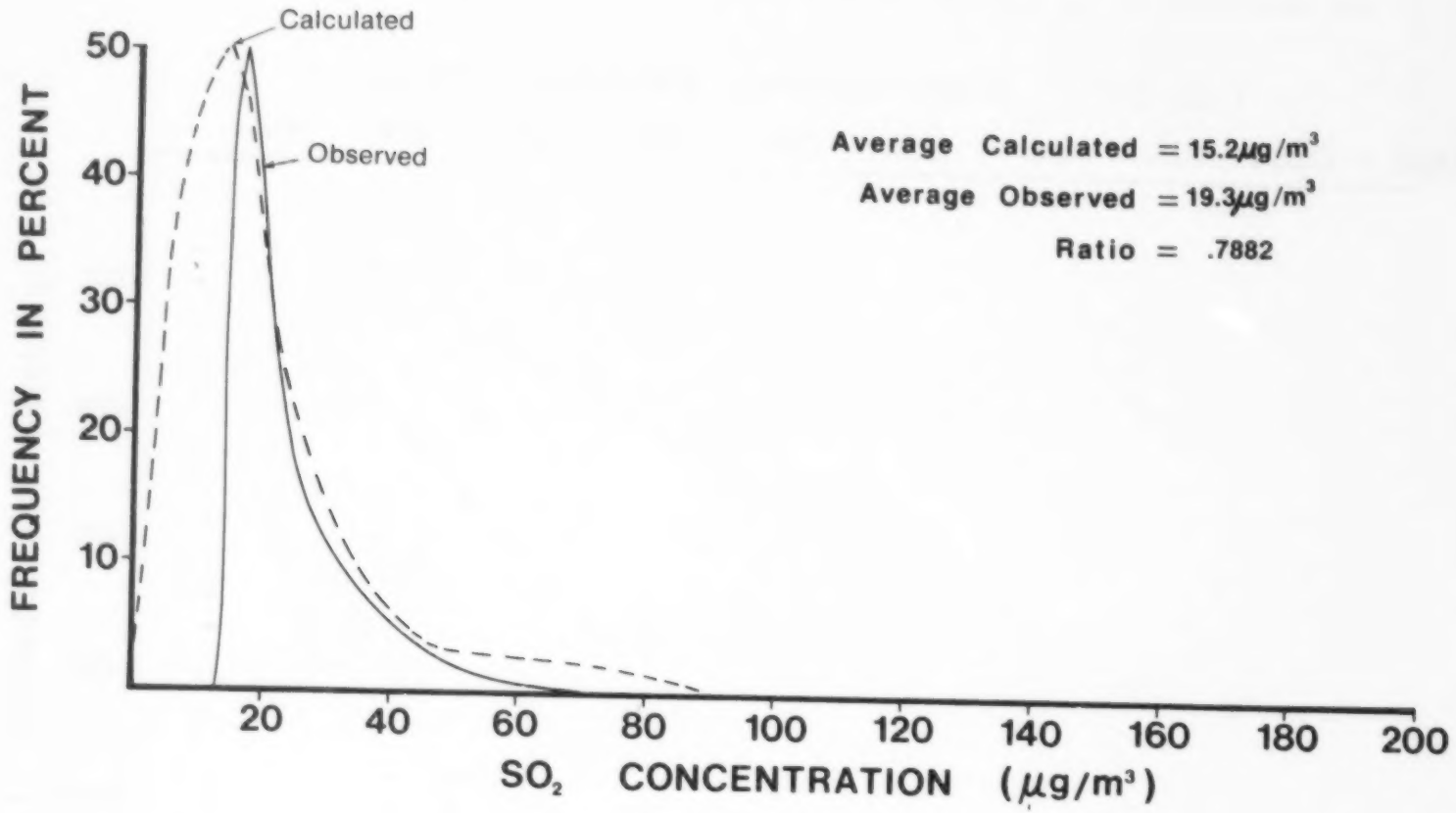

Figure 42. Frequency distributions of calculated and observed SO_2 concentrations for occurrences at the Russell site (site 010).

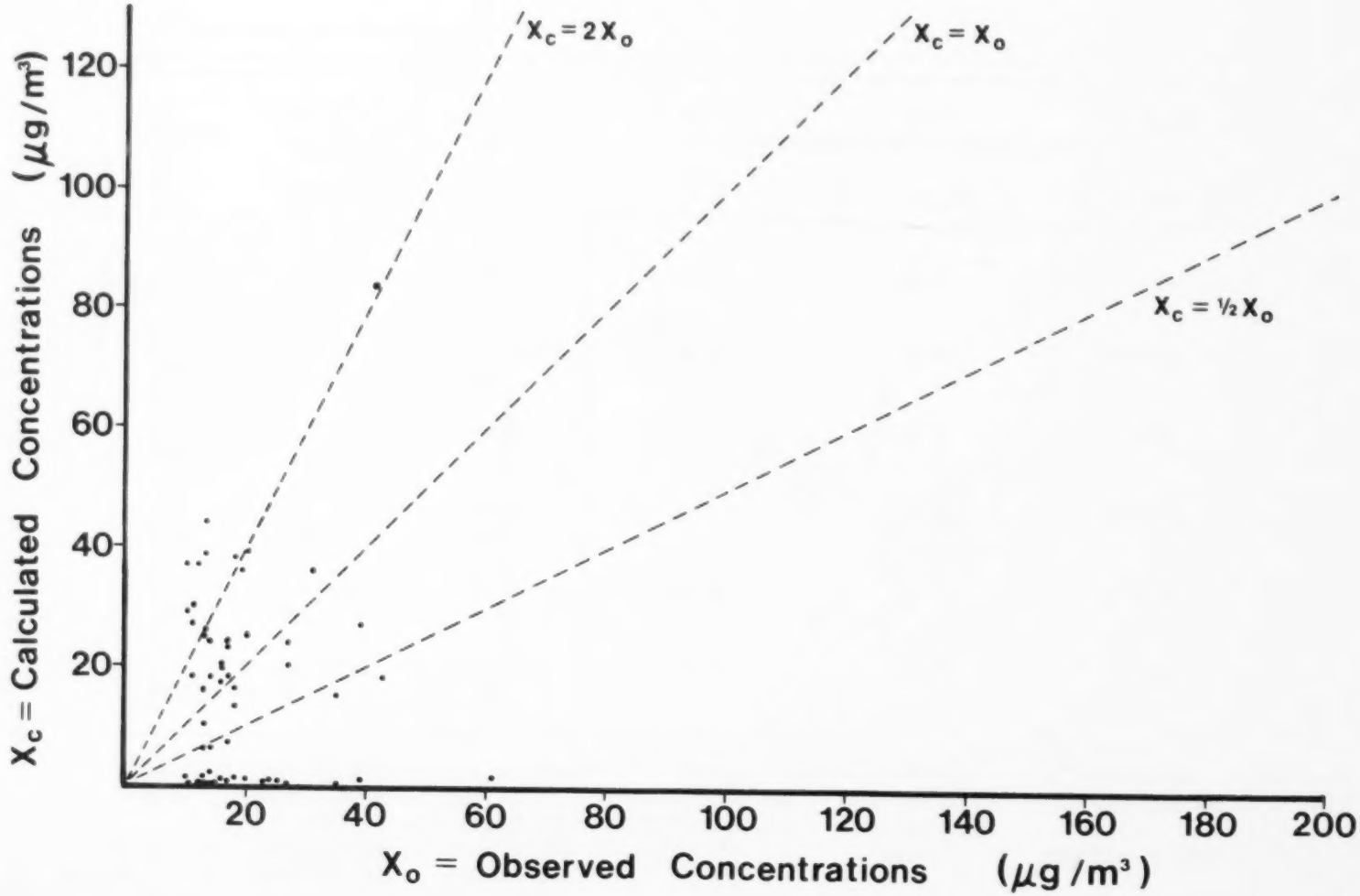

Figure 43. Scatter plot of hourly data points of calculated and observed SO_2 concentrations for occurrences at the Russell site (site 010).

TABLE 13. ANALYSIS OF CALCULATED AND OBSERVED SO_2 AT EACH MONITORING SITE

Site number	Number and percentage of occurrences out of 492	Number and percentage within a factor of 2	Average calculated SO_2 concentration ($\mu g/m^3$)	Average observed SO_2 concentration ($\mu g/m^3$)	Concentration ratio (calculated to observed)
002	54 (11.0)[a]	25 (46.3)	35.2	35.2	1.000
003	104 (21.1)	40 (38.5)	56.8	47.1	1.205
004	102 '20.7)	65 (63.7)	74.7	79.8	0.9358
005	30 (6.1)	12 (46.0)	46.1	37.3	1.237
008	122 (24.8)	65 (53.3)	28.2	35.0	0.8037
009	23 (4.7)	7 (30.4)	11.4	15.4	0.7409
010	57 (11.6)	22 (38.6)	15.2	19.3	0.7882
Overall	492 (100.0)	236 (48.0)	43.5	44.2	0.9846

[a]Percentages in parentheses.

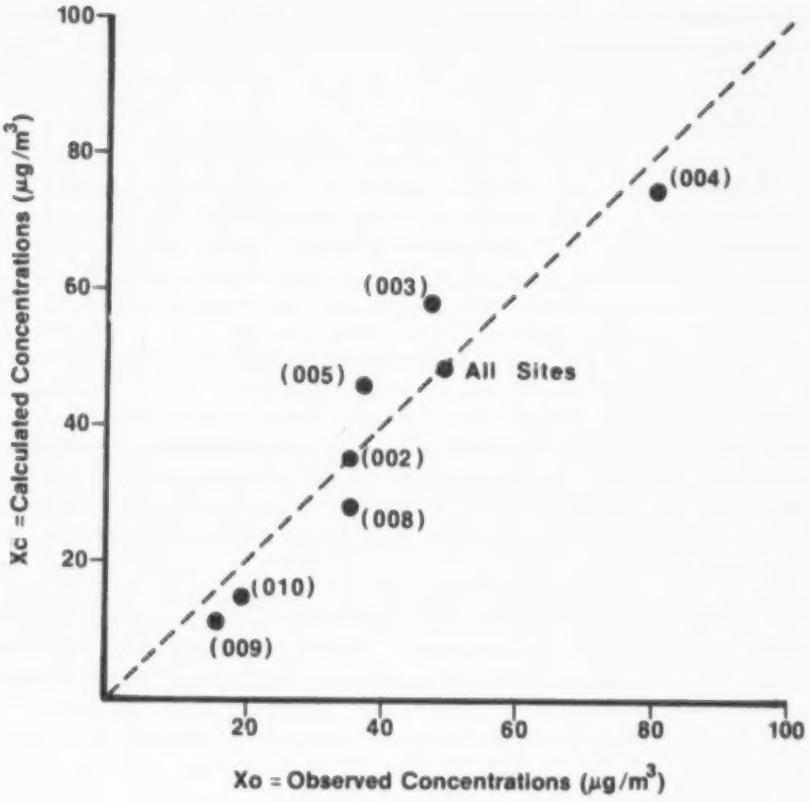

Figure 44. Annual averages of calculated and observed SO_2 concentrations for all seven sites. The correlation coefficient based on these averages is r=0.954.

TABLE 14. CALCULATED AND OBSERVED AVERAGE SO_2 CONCENTRATIONS ($\mu g/m^3$) AT THE SEVEN SO_2 MONITORING SITES ARRANGED IN ORDER OF DECREASING VALUE

Site number	Distance from stack (km)	Calculated value	Observed value
004	4.4	74.4	79.8
003	5.9	56.8	47.1
005	7.3	46.1	37.3
002	9.9	35.2	35.2
008	8.3	28.2	35.0
010	15.5	15.2	19.3
009	14.6	11.4	15.4

Although the highest calculated concentrations did not correspond to the highest measured concentrations on an hour-by-hour basis, the Gaussian model is indeed capable of predicting the highest concentrations. Ragland (1976) has developed analytical equations for the prediction of worst-case concentration for a plume. The worst-case concentrations for a trapping plume are twice as large as those for a coning plume. For distances beyond the position of the maximum concentration the ratio between trapping and coning may be larger than 2.

By means of Ragland's (1976) equations the highest possible concentration at each stability class was calculated. Table 15 shows the worst-case concentrations for coning and trapping plumes and the highest calculated and observed concentrations for each stability class. When the worst observed concentration is compared with the worst concentration for a trapping plume, it can be seen that the model is capable of predicting the worst-case concentrations for most of the stability classes.

TABLE 15. WORST-CASE OR HIGHEST SO_2 CONCENTRATIONS ($\mu g/m^3$) AT THE COLUMBIA GENERATING STATION--1976

Stability class	Coning plume	Trapping plume	Calculated	Observed
A	282	564	191	247
AB	211	422	245	243
B	139	278	134	203
BC	124	248	124	178
C	109	218	252	178
CD	69	138	152	102
D	28	56	53	157

MOBILE MEASUREMENTS OF AIR POLLUTANTS DOWNWIND OF THE STACK

Because of the transient nature of the plume, the use of portable monitoring equipment is important in establishing the highest ground-level concentrations and provides a means of getting more data directly under the plume. Plume traverses yield the concentration as well as the width of the plume. These data were used to supplement the fixed-site data for the purpose of model verification.

A Meloy flame photometric SO_2 analyzer and an Analytical Instrument Development Corp. chemiluminescent ozone meter were operated from an automobile. Once the plume was located, the plume was traversed along available roads at several distances downwind. Each traverse was run at constant vehicle speed until the SO_2 concentration could no longer be detected above ambient levels. Since the ozone levels dropped to zero within the plume, this was a sensitive way to track the plume. The SO_2 analyzer was calibrated weekly with a Metronix permeation tube system. The ozone analyzer was calibrated regularly at the Wisconsin State Hygiene Laboratory with a standard source.

The ground-level concentrations downwind of the stack were highly transient. With strong winds the plume is broken up into blobs. With unstable conditions the plume touches down at varying spots and frequently the wind veers.

Data for which we have good strip-chart recordings of SO_2 concentration are summarized in Table 16. The maximum concentrations based on a 1-min average are all less than 300 $\mu g/m^3$. The mobile monitoring data generally confirm the predictions of the Gaussian plume model.

PREDICTED ANNUAL CONCENTRATIONS OF SO_2, NITROGEN OXIDES, AND PARTICULATE MATTER

In spite of all the scatter in the 492 hourly data points, the annual average predicted by the model is very close to the annual observed value. Not only are the overall averages close, but so are the annual averages for each of the seven sites, as borne out by the correlation coefficient of 0.954, based on the seven pairs of averages. Since the agreement between model values and observed values was good, the model, including the sector averaging, was used to predict the spatial distribution of the annual averages of SO_2, nitrogen oxides, and particulate matter. The emission equations used were those previously given in this section. The plume calculations were performed for all 5,929 data hours of the year at each point of a rectanglar grid and were averaged over the year. The results are given in Figures 45-47. The black dot in the middle of the isopleth represents the generating station stack, and the seven x's show the locations of the SO_2 monitoring sites. The drawings cover an area of 64 km^2 around the generating station. As can be seen from these figures, the annual increase of SO_2 concentrations was 1-3 $\mu g/m^3$ within 10-16 km of the generating station. About the same annual incremental increase is noted in Table 7 between the pre-operational monitoring data and the 1976 data. Predicted annual increases near the

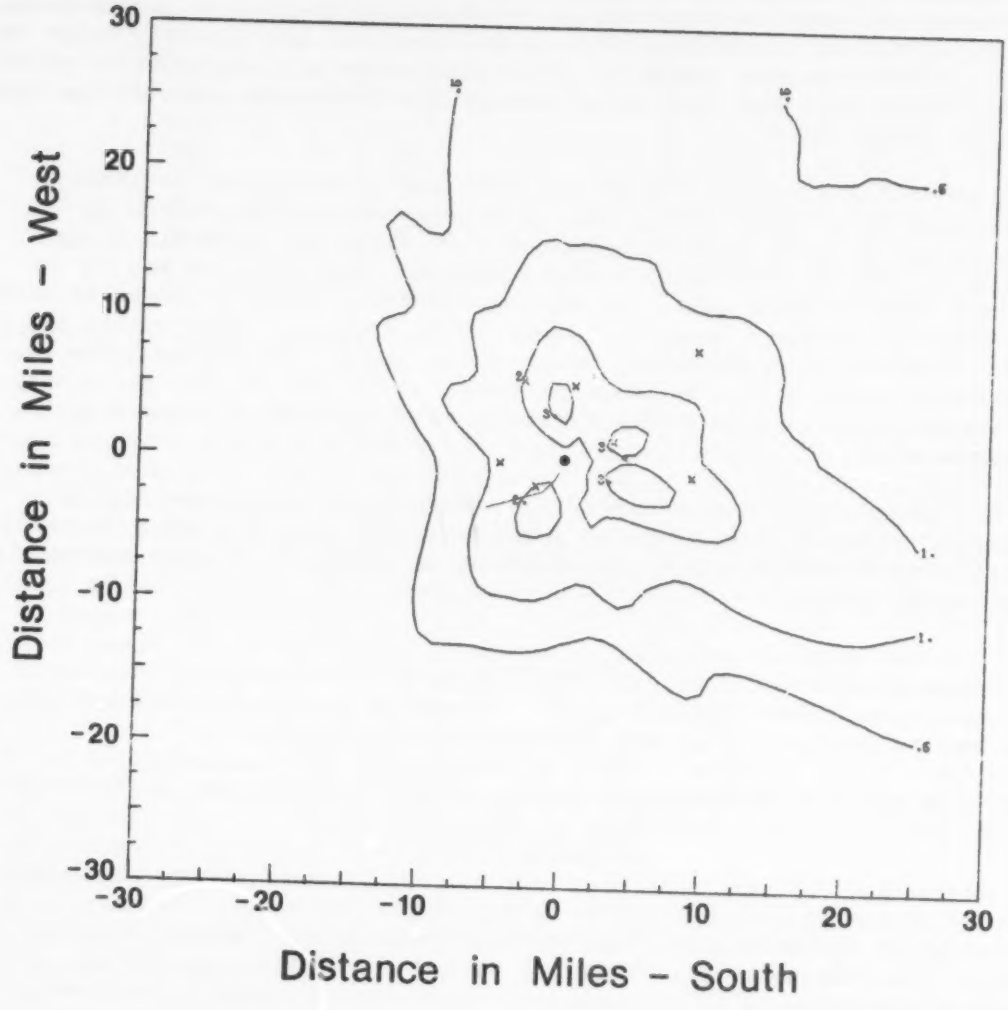

Figure 45. Calculated 1976 average concentrations of SO_2 ($\mu g/m^3$) near the Columbia Generating Station.

● indicates Columbia Generating Station
x indicates monitoring site.

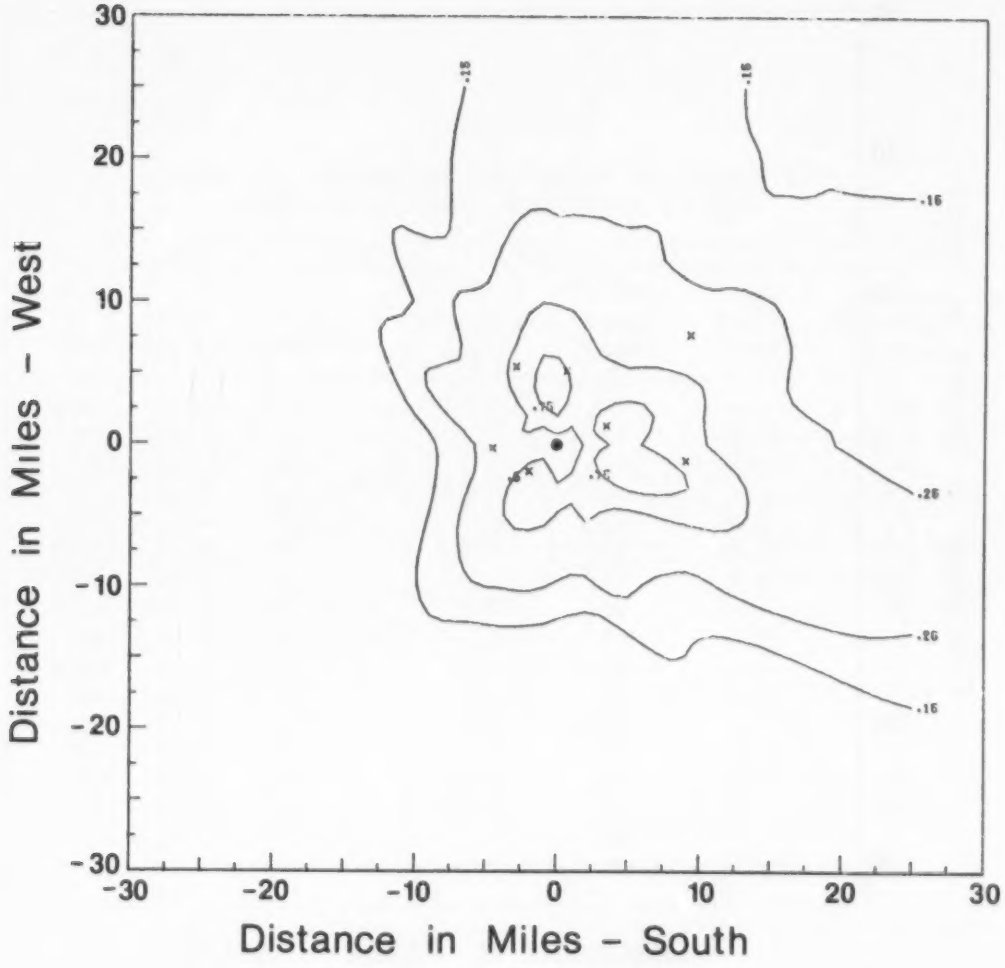

Figure 46. Calculated 1976 average concentrations of NO_X ($\mu g/m^3$) near the Columbia Generating Station.

● indicates Columbia Generating Station
x indicates monitoring site.

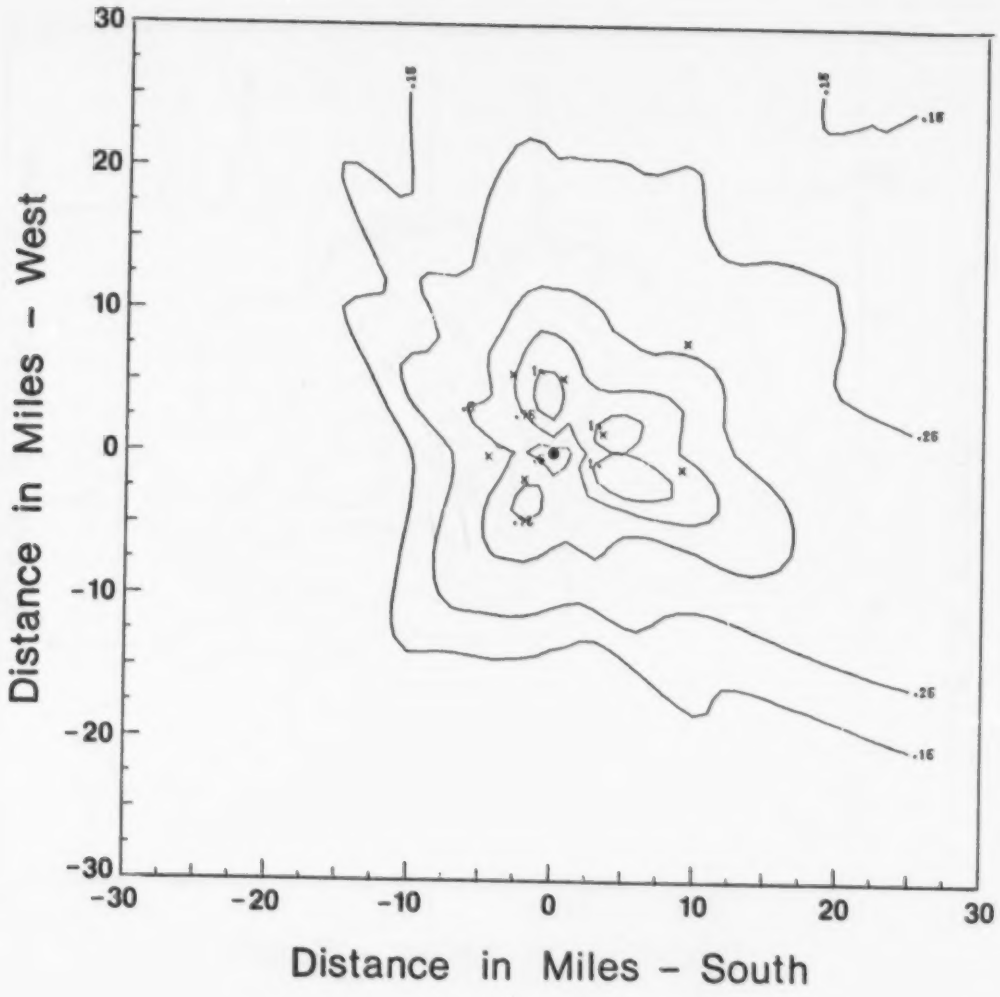

Figure 47. Calculated 1976 average concentrations of particulate matter ($\mu g/m^3$) near the Columbia Generating Station.

• indicates Columbia Generating Station
x indicates monitoring site.

TABLE 16. SUMMARY OF SO_2 MOBILE MONITORING DATA NEAR THE COLUMBIA GENERATING STATION

Date (1976)	Time	Cloud cover	Wind direction	Distance downwind (km)	Vehicle speed (mph)	Plume width (km)	Maximum SO_2 concentration ($\mu g/m^3$)
6/25	1340	10/10	152	10.9	30	---	170
6/25	1350	10/10	152	8.8	40	3.8	78
6/25	1440	10/10	152	7.6	40	---	120
6/25	1550	10/10	152	6.2	40	---	73
6/25	1530	10/10	152	6.2	40	6.8	74
8/2	1045	0/10	0	3.9	30	3.5	288
8/5	1040	8/10	355	4.0	25	2.1	113
8/5	1130	10/10	355	3-12	40	---	65
8/5	1100	8/10	355	4.0	25	2.5	131
8/11	1300	4/10	140	5.0	0	---	170
8/11	1320	4/10	140	5.0	20	1.0	144
8/11	1330	4/10	140	5.0	25	1.1	79
8/11	1400	4/10	140	7.7	20	0.70	100
8/11	1410	4/10	140	7.7	20	0.75	136
8/21	1100	3/10	130	5.1	30	0.70	141
8/21	1105	3/10	130	5.4	30	2.9	63
9/28	1300	0/10	0	5.5	30	1.3	107

generating station are 0.75 $\mu g/m^3$ for nitrogen oxides and 1 $\mu g/m^3$ for particulate matter.

SECTION 4

DRY DEPOSITION OF SULFUR DIOXIDE FROM THE COLUMBIA PLUME

Gaseous and particulate air pollutants emitted into the ambient air by a large coal-fired electric generating station are removed by dry deposition, precipitation scavenging, and chemical transformation. In the case of particulates gravitational settling is not significant because the large particles are removed by emission-control equipment, and the small particles do not grow large enough to settle out. For most emissions dry deposition is the principal removal mechanism from the ambient air. This section concerns dry deposition of sulfur dioxide; the same principles apply to other pollutants including small particles or aerosols.

Dry deposition of air pollutants is caused by impaction of the gaseous molecules or the particles with the surface, which may be vegetation, soil, water, or snow, for example. The rate at which pollutants are removed by impaction depends on the pollutant type, surface material, surface roughness, wind speed, and atmospheric turbulence. The deposition rate is important to determine because it represents an input to the ecosystem and can be an important factor in estimating the ambient air concentration further downwind.

The dry deposition flux of a particular pollutant is assumed to be linearly proportional to the ground-level ambient air concentration of that pollutant for a given surface and set of meteorological conditions. The proportionality constant is referred to as the deposition velocity. Deposition velocities have been measured in the field and in the laboratory for a variety of situations to establish the range of likely values. Sulfur dioxide has one of the highest deposition velocities of any air pollutant and is an order of magnitude greater than small particulates.

Laboratory studies of dry deposition are useful for determining the influence of various surface types, but cannot simulate representative impaction conditions. Field studies, on the other hand, must be done with very low ambient background concentrations of pollutant and have usually required averaging times of hours. Representative recent dry deposition studies may be found in Engelmann and Schmel 1976.

No measurements of SO_2 dry deposition have been reported directly in the plume. Conceivably, transient deposition rates associated with a single plume could be significantly larger than steady-state deposition associated with more widespread background pollutant concentrations. Hence the objective of this study was to measure the dry deposition flux of SO_2 directly in the plume

with an averaging time of minutes. These results would then be more appropriate to plume modeling work.

At least two methods are available for determining the dry deposition rate in the field: the eddy correlation method and the gradient transfer method. The gradient transfer method was chosen for this study because it is more closely related to the modeling approach used for the plume dispersion and deposition predictions.

During 1976 and early 1977 field experiments to determine the deposition velocity of sulfur dioxide were conducted near the Columbia Generating Station. The study area consisted primarily of flat agricultural fields with some wetlands and woods. The area to the southwest of the stack just across the Wisconsin River is the eastern terminus of the Baraboo Bluffs, which are rolling 500-ft hills.

THEORY OF GRADIENT-TRANSFER METHOD

When no deposition occurs the concentration near the surface is essentially constant with height near the ground when dealing with elevated point sources. However, when removal at the surface occurs, a concentration gradient with height is established which depends on the removal rate and the atmospheric turbulence. By simultaneously measuring the concentration, wind, and temperature near the ground, the deposition flux can be deduced. The chief limitation of the method is the need for uniform terrain. Thus, it is not effective near hedges or small woods, but is ideally suited for use over extensive agricultural fields or marshes. The theory of the gradient-transfer method may be found in Businger (1971) and Moneith (1971) and is summarized below.

From Fick's law of diffusion applied to turbulent flow the deposition flux F is given by

$$F(0) = K_z \left(\frac{dC}{dz}\right)_{z=0}, \tag{16}$$

where K_z is the vertical eddy diffusivity. If the deposition velocity concept is used,

$$F(0) = v_d C(0) \tag{17}$$

Combining equations (16) and (17) we have a convenient method for determining the deposition velocity

$$v_d = \frac{K_z}{C(0)} \left(\frac{dC}{dz}\right)_{z=0} \tag{18}$$

Hence the concentration and concentration gradient near the ground must be measured. The eddy diffusivity cannot be measured directly, but is determined from the wind-speed gradient and temperature gradient. The assumption must be made that the eddy diffusivity for momentum is equal to the eddy diffusivity for mass according to Reynolds analogy. The method for determining the eddy diffusivity is described below.

The eddy diffusivity for momentum is defined in relationship to the shear stress τ by

$$\tau = \rho K_M \frac{\partial u}{\partial z} \quad . \tag{19}$$

If we introduce the friction velocity $u_* = \sqrt{\tau_o/\rho}$, where τ_o is the shear stress at the surface, and use the fact that the shear stress is constant near the surface, it follows that

$$K_M = \frac{u_*^2}{\partial u / \partial z} \quad . \tag{20}$$

For neutral atmospheric conditions the wind speed follows a logarithmic profile,

$$u = 2.5 u_* \ln \left(\frac{z-d}{z_o}\right) \quad , \tag{21}$$

where d is the displacement height and z_o is the surface roughness. The friction velocity, u_*, may be determined by a curve fit of the measured wind data. The velocity gradient in Eq. (20) may also be determined by a curve fit of the data. When Eq. (21) is substituted in Eq. (20),

$$K_M = 0.4\, u_*(z-d) \tag{22}$$

If $K_M = K_z$, the deposition velocity may be determined from Eq. (18).

For non-neutral atmospheric conditions the wind-speed profile is more complex than Eq. (21), and the friction velocity, u_*, will take on somewhat different values. However, in practice we were only able to locate the plume on the ground for a 15- to 20-min period during near-neutral conditions. With unstable conditions the plume was shifting too rapidly, and for stable conditions the ground-level concentrations were too low. Hence, further discussion of non-neutral meteorological parameters is not needed here.

The deposition process may be split into an aerodynamic component and a surface component. The aerodynamic component is related to the turbulent mixing near the ground; the surface component depends on how readily the pollutant species is absorbed. To distinguish between these two processes, it is convenient to introduce a transport resistance, r, as

$$r = 1/v_d \tag{23}$$

and note that r is the sum of the aerodynamic resistance, r_a, and the surface resistance, r_s:

$$r = r_a + r_s \tag{24}$$

From Eq. (17) it follows that

$$r = \frac{C(0)}{F(0)} \quad . \tag{25}$$

By analogy with turbulent transport of momentum (Chamberlain 1966) it may be postulated that:

$$r_M = \frac{\rho u}{\tau} = \frac{u}{u_*^2} \cdot \tag{26}$$

If we equate the transport of momentum and the transport of mass in the turbulent boundary layer, then:

$$r_M = r_a \tag{27}$$

In this case the difference between the measured total resistance and the aerodynamic resistance can be interpreted as the surface resistance. Some people have attempted to account for an extra resistance arising from the difference between mass and momentum transport, but this was not considered necessary for our near-neutral conditions.

EXPERIMENTAL TECHNIQUE

The objective was to take deposition measurements in the plume on the ground. The procedure was to locate the plume by means of the sulfur dioxide analyzer and ozone analyzer, which were operated from an automobile. When in the plume the SO_2 would increase and the O_3 decrease (because of NO scavenging the O_3 to form NO_2). The area was traversed until the plume position was established and shown to be near the maximum ground-level position, or at least greater than 30 $\mu g/m^3$. Also, a location with a large uniform surface canopy had to be chosen. Since time was not available to request permission to enter the land, an area where trespassing was not a serious problem had to be selected.

Because of the transient nature of the plume and the desireability to set up in many types of terrain, the equipment needed to have self-contained power and be portable, light, compact, and easy to assemble. The following equipment was used:

(1) A Meloy Inc. SO_2 analyzer Model SA165 with a sample flow rate of 200ml/min.

(2) Rimco cup anemometers with a built-in light system to count the number of revolutions of each anemometer.

(3) Esterline Angus stripchart recorder (portable).

(4) Iron-constantan thermocouples (radiation shielded) ice bath, stepping switch, and Wheatstone bridge.

(5) Bendix air sampling pump, Model BDX-44.

(6) Teflon air sampling bags fitted with teflon tubing and mounted in a plexiglas chamber.

(7) An aluminum mast, 2.2-m high, with five brackets each of which could position a cup anemometer, teflon tube, and thermocouple.

At each site, measurements of wind speed, temperature, and SO_2 concentration were made simultaneously at heights of 0.125, 0.25, 0.50, 1.0, and 2.0 m above the vegetation canopy. The mast had the capability of small height adjustments, but in the case of tall canopies only three measuring heights were used: 0.50, 1.0, and 2.0 m. Care was taken in setting up the instruments not to disturb the upwind and downwind canopy.

Sulfur dioxide profiles were determined by sampling at the five heights simultaneously through small teflon tubes. The ambient air was drawn through the tubes into teflon bags by pumping a slight vacuum in the plexiglas box. After a sampling period of 15 min the ends of the sampling tubes were sealed, and then each bag was connected to the SO_2 analyzer. The SO_2 analyzer and the bags were calibrated regularly with a Metronics Dynocalibrator which used a SO_2 permeation tube.

DATA COLLECTION AND ANALYSIS

In eight cases satisfactory data were obtained. Approximately 35 trips were made to the site to collect data over a period of 1 yr, but locating the plume for any length of time proved very difficult. With intense summer sun, which results in relatively high instantaneous ground-level concentrations, the plume fluctuations were too large to allow sufficient sampling time. Cloudy conditions or time when the sun was not too high provided the best opportunity to obtain data, although even then the wind might veer away from the selected site before the test could be completed. Of course, if the temperature (including chill factor) was too low, the tests were too difficult to run.

The data for the eight completed cases are given in Table 17. The time, site features (including height of the vegetation canopy), cloud cover, wind speed, temperature, and concentration data are recorded for each test. The wind and concentration data are plotted versus the log of the height above the aerodynamic displacement height. For some of the tests one or more measuring heights was below the canopy height; these data are noted with an asterisk and are not plotted.

To analyze the data, the displacement height, d, is first determined by relating the measured winds at three heights with the log profile relationship (Eq. (21)):

$$\frac{u_1-u_2}{u_1-u_3} = \frac{\ln(z_1-d)-\ln(z_2-d)}{\ln(z_1-d)-\ln(z_3-d)} \quad . \tag{28}$$

Once d is determined, the wind, concentration, and temperature are plotted versus $\ln(z-d)$. The next step is to determine the friction velocity, u_*, and the surface roughness, z_o, from the plots. By rewriting Eq. (21) in the form

$$u = 2.5u_* \ln(z-d) \quad -2.5u_* \ln_o z \quad , \tag{29}$$

it is apparent from the plots that

$$u_* = 2.5/\text{slope of velocity} \tag{30}$$

TABLE 17. DATA FROM EIGHT FIELD TESTS IN WHICH SO_2 DEPOSITION WAS MEASURED NEAR THE COLUMBIA GENERATING STATION

Test 1

Site: Pasture, County P & G

Time: 5:00 p.m.

Date: 8-11-76

Canopy Height: 16 cm

Richardson Number at 1 m: -.053

Location	*Height (M)*	*Wind Speed (m/s)*	*Temperature (°C)*	*Concentration ($\mu g/m^3$)*
1	2.00	2.50	32.3	49
2	1.00	2.15	32.8	47
3	0.50	1.58	33.3	50
4	0.25	1.28	34.0	43
5	0.125	0.36	36.4	31

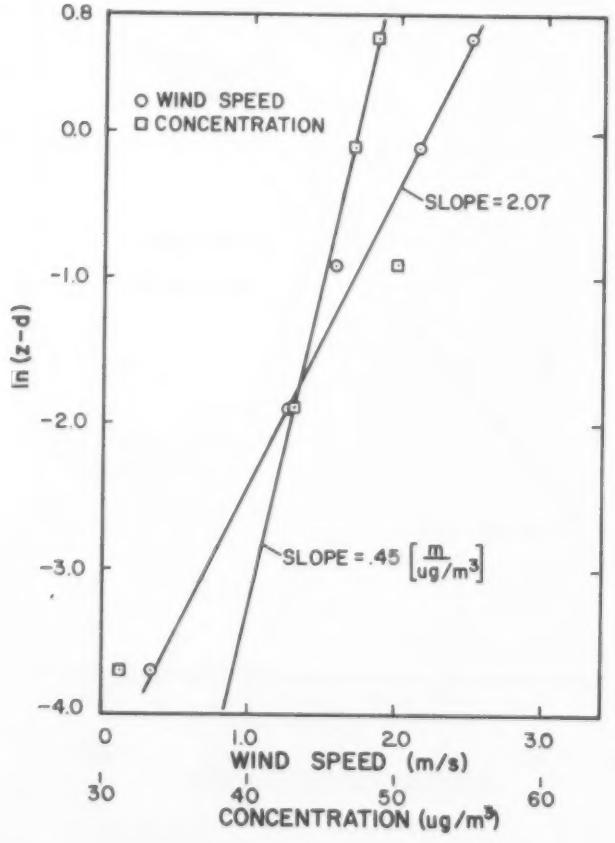

best copy available

Table 17 (continued)

Test 2

Site: Marsh, County G

Time: 1:20 p.m.

Date: 9-22-76

Observations: soil-wet, slightly unstable, 1/10 cloud cover

Canopy height = 81 cm

Richardson Number at 1 m: -.035

Location	*Heigth (m)*	*Wind Speed (m/s)*	*Temperature (°C)*	*Concentration ($\mu g/m^3$)*
1	2.31	2.41	20.7	87
2	1.31	1.75	23.6	80
3	0.81	0.90	25.8	69
4*	0.56	0.74	25.0	60
5*	0.43	0.36	24.1	51

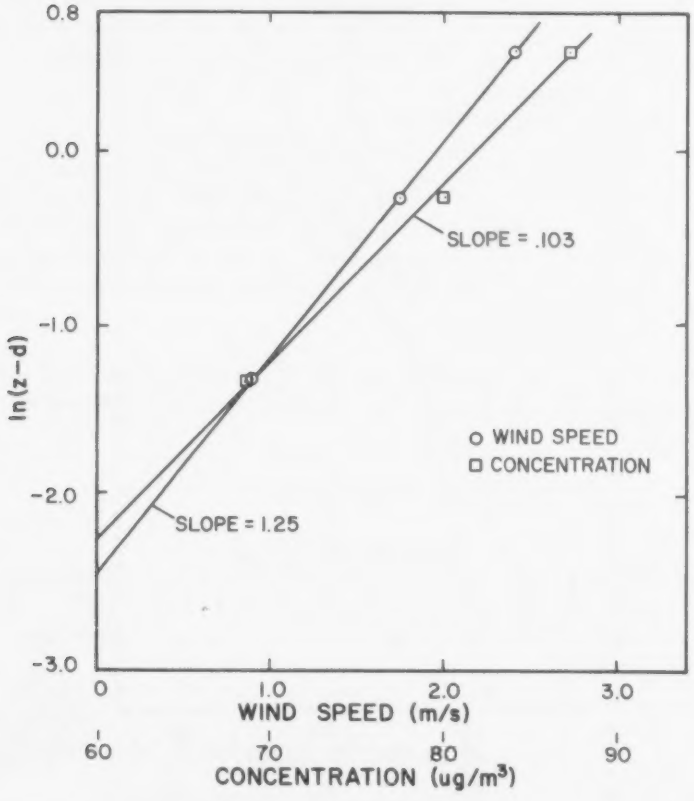

TABLE 17 (continued)

Test 3

Site: Cut alfalfa, Dunnings Road

Time: 2:00 p.m.

Date: 9-29-76

Observations: Very dry sandy soil, patchy alfalfa, 0/10 cloud cover, windy.

Canopy height = 15.5 cm

Richardson Number at 1 m: -.058

Location	*Height (m)*	*Wind Speed (m/s)*	*Temperature (°C)*	*Concentration ($\mu g/m^3$)*
1	2.00	3.87	17.1	149
2	1.00	3.33	17.7	147
3	0.50	2.80	18.5	142
4	0.25	2.18	19.9	139
5	0.125	1.01	21.2	127

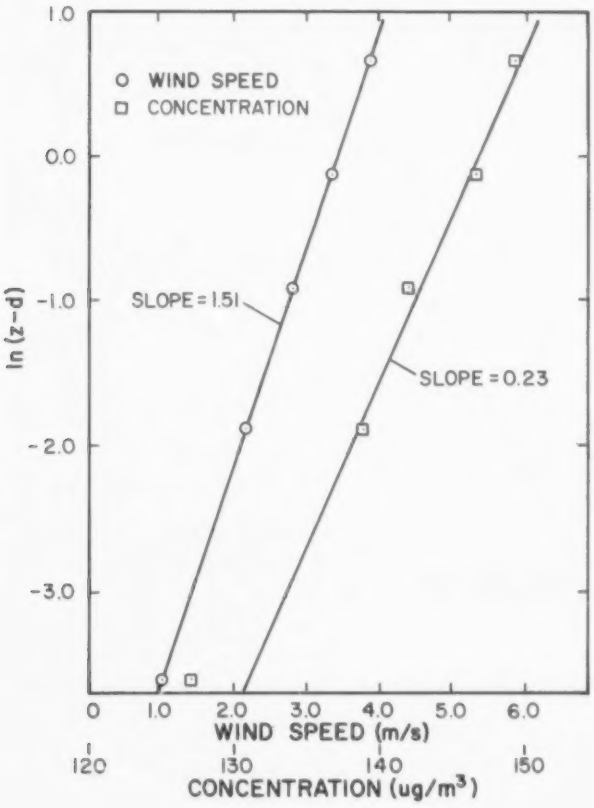

TABLE 17 (continued)

Test 4

Site: Tall prairie

Time: 2:25 p.m.

Date: 10-7-76

Observations: Grass damp, rain day before, 3/10 cloud cover.

Canopy height: 66 cm

Richardson No. at 1 m: -.19

Location	*Height (m)*	*Wind Speed (m/s)*	*Temperature (°C)*	*Concentration ($\mu g/m^3$)*
1	2.00	1.72	12.2	50
2	1.00	1.20	13.6	37
3*	0.50	1.15	14.8	36
4*	0.25	0.66	16.8	39
5*	0.125	0.22	19.3	37

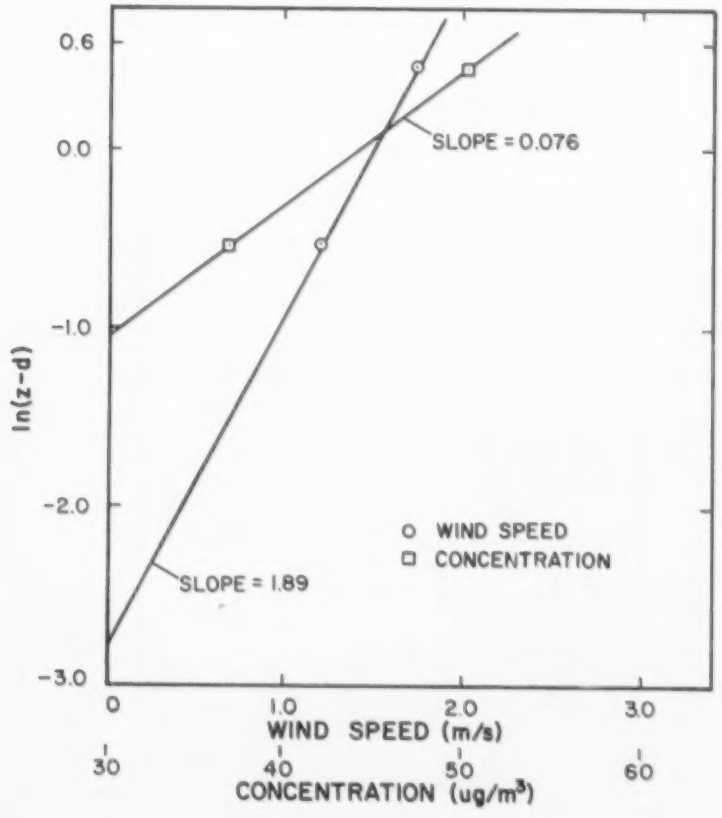

TABLE 17 (continued)

Test 5

Site: Pasture

Time: 4:30 p.m.

Date: 10-7-76

Observations: Moist soil, 3/10 cloud cover.

Canopy Height: 6 cm

Richardson Number at 1 m: 0.0 (assumed)

Location	*Height (m)*	*Wind Speed (m/s)*	*Temperature (°C)*	*Concentration ($\mu g/m^3$)*
1	2.00	2.44	---	65
2	1.00	2.02	---	64
3	0.50	1.74	---	60
4	0.25	1.43	---	43
5	0.125	0.92	---	57

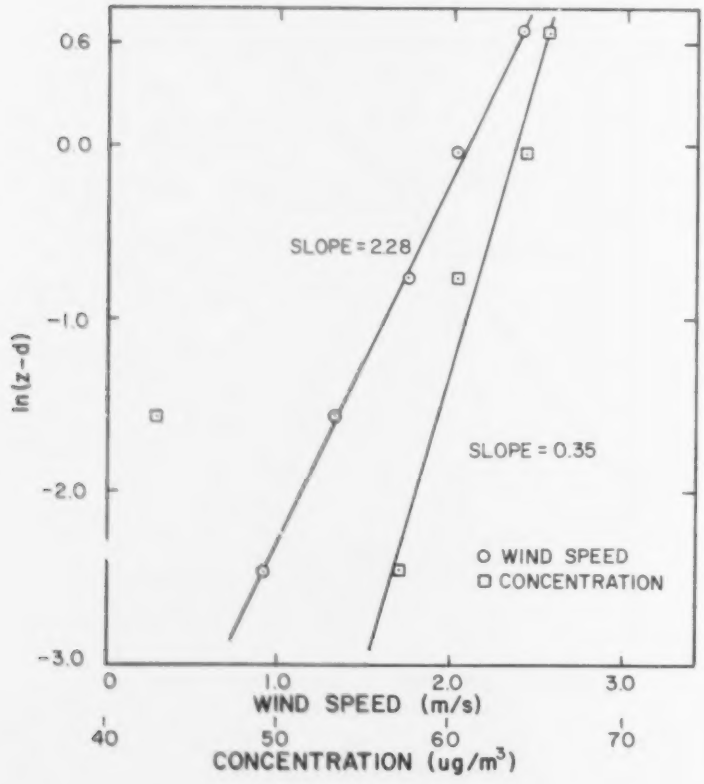

TABLE 17 (continued)

Test 6

Site: Marsh

Time: 3:20 p.m.

Date: 12-10-76

Observations: Soil-dry, slightly unstable atmosphere, 3/10 cloud cover.

Canopy height: 80 cm

Richardson Number at 1 m: -.016

Location	*Height (m)*	*Wind Speed (m/s)*	*Temperature (°C)*	*Concentration ($\mu g/m^3$)*
1	2.50	4.39	6.4	58
2	1.50	3.13	6.7	52
3	1.25	2.82	7.1	56
4	1.00	2.22	8.2	54
5	.75	1.05	9.6	52

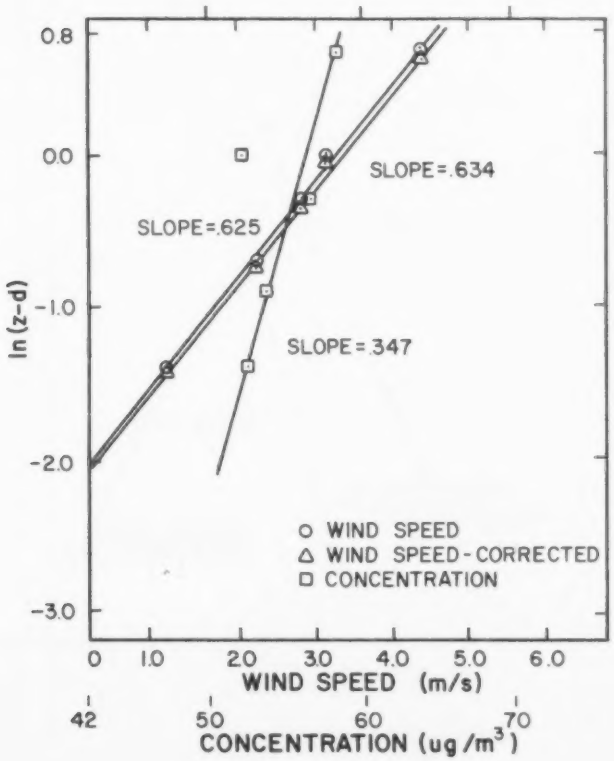

TABLE 17 (continued)

Test 7

Site: Snow covered field

Time: 12:45 p.m.

Date: 2-15-77

Observations: Old-melting snow, 0/10 cloud cover.

Canopy height = 0.0 (m)

Richardson Number at 1 m:

Location	*Height (m)*	*Wind Speed (m/s)*	*Temperature (°C)*	*Concentration ($\mu g/m^3$)*
1	2.00	4.72	1.0	130
2	1.00	4.21	---	126
3	0.50	3.67	---	123
4	0.25	2.94	---	118
5	0.125	2.54	1.0	115

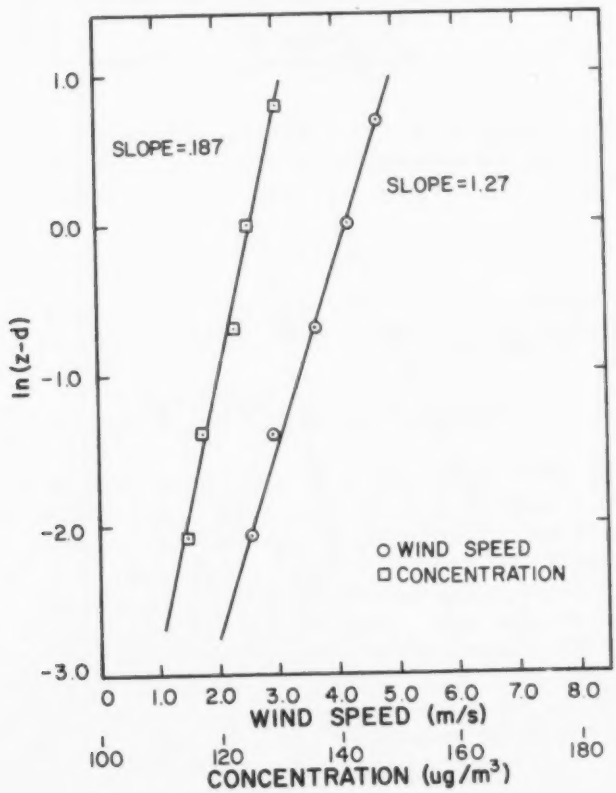

TABLE 17 (continued)

Test 8

Site: Wet land prairie

Time: 1:00 p.m.

Date: 3-8-76

Observations: Soil wet, 0/10 cloud cover, gusty wind.

Canopy height =

Richardson Number at 1 m: -.011

Location	*Height (m)*	*Wind Speed (m/s)*	*Temperature (°C)*	*Concentration (μg/m³)*
1	2.00	3.85	16.8	63
2	1.50	3.50	---	61
3	1.00	2.76	17.4	61
4	0.75	1.96	18.0	59
5*	0.50	1.75	18.0	53

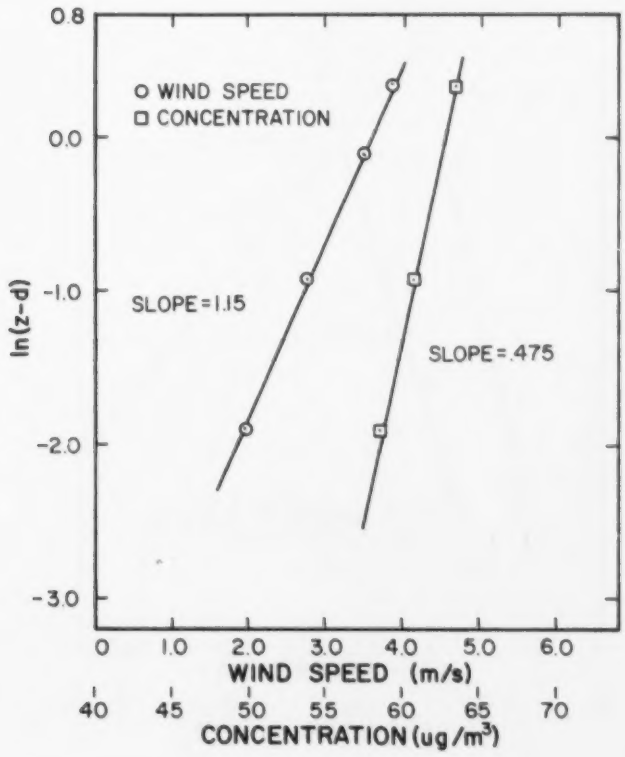

and

$$\ln z_o = \text{y intercept} \tag{31}$$

The information needed to calculate the eddy diffusivity, K_M, is now available for Eq. (22). However, at this point we must choose a reference height for K_M and v_d since experimentally z = 0 cannot be used. A 1-m reference height was chosen so that:

$$K_M(1) = 0.4u_*(1-d) \tag{32}$$

The concentration gradient at the reference height is determined from the slope of the concentration plot as:

$$\frac{dC}{dz} = \frac{1}{(\text{slope of concentration plot})(1-d)} \, . \tag{33}$$

Finally, the deposition velocity at the reference height of 1 m is determined from Eq. (18) as:

$$v_d = \frac{0.4\ u_*}{C(1)(\text{slope of concentration plot})} \, . \tag{34}$$

The temperature was measured at each height to indicate the stability of the atmosphere, which may be characterized by the Richardson Number,

$$Ri = \frac{g}{T} \frac{\partial T/\partial z + \Gamma}{(\partial u/\partial z)^2} \, , \tag{35}$$

where τ is the adiabatic lapse rate. For a neutral condition Ri = 0, for unstable conditions Ri < 0, and for stable conditions Ri > 0. The above theory can be modified for non-neutral conditions. For example,

$$K_M = 0.4\ u_*(z-d)(1-\alpha Ri) \, , \tag{36}$$

where $\alpha = 2.5$ in stable conditions and $\alpha = 9$ in unstable conditions. For our experiments we did not feel that these corrections for atmospheric stability were justified.

RESULTS AND DISCUSSION OF DEPOSITION MEASUREMENTS

The results of the field test data are summarized in Table 18. The deposition velocities range from 0.21 to 1.8 cm/sec. The two tests in pasture showed similar results of 0.35 and 0.32 cm/sec. The two tests over marsh land gave results of 0.75 cm/sec, although one test was done in fall and one in early winter. The cut alfalfa site gave a value of 0.30 cm/sec, which is reasonable in view of the dry conditions. The tall prairie site (run 4), which was still damp after an October rain, showed the highest deposition velocity of 1.8 cm/sec. However, another prairie site (run 8), measured in March when the soil was wet but the vegetation dry, registered the lowest value of 0.21 cm/sec. One test was completed over old wet snow, and a deposition velocity of 0.55 cm/sec was determined.

TABLE 18. SUMMARY OF SO_2 DEPOSITION MEASUREMENTS--REDUCED DATA

Run	C(1) ($\mu g/m^3$)	z_o (----m----)	d	Ri(1)	u_* (--m/sec--)	u(1)	$K_m(1)$ (m^2/sec)	$v_d(1)$ (cm/sec)	Canopy
1	47.0	0.0076	0.10	-0.053	0.20	2.15	0.074	0.35	pasture
2	80.0	0.086	0.54	-0.040	0.44	1.75	0.062	0.75	marsh
3	146.7	0.006	0.098	-0.058	0.27	3.33	0.100	0.30	cut alfalfa
4	36.7	0.060	0.42	-0.19	0.22	1.19	0.050	1.8	tall prairie
5	64.2	0.008	0.036	0.0	0.18	2.02	0.071	0.32	pasture
6	53.7	0.130	0.50	-0.070	0.66	2.22	0.140	0.75	marsh
7	125.8	0.0047	0.00	0.0	0.32	4.21	0.130	0.55	wet snow
8	60.8	0.016	0.60	-0.011	0.37	2.76	0.061	0.21	prairie

The resistance to deposition for each of the tests is shown in Table 19. The surface resistance was always significantly larger than the aerodynamic resistance, indicating that the surface sink is more of a limiting factor than the vertical transport by wind. Aerodynamic resistance was comparable to surface resistance only for tall prairie. Hence, from a plume modeling point of view, accurate knowledge of the surface characteristics is generally more important than the friction velocity when calculating the dry deposition flux.

TABLE 19. SUMMARY OF TOTAL-DEPOSITION-RESISTANCE, AERODYNAMIC-RESISTANCE AND SURFACE-RESISTANCE DATA FOR SULFUR DIOXIDE

Test	r (sec/cm)	r_a	r_s	Canopy
1	2.8	0.5	2.3	pasture
2	1.3	0.1	1.2	marsh
3	3.3	0.5	2.8	alfalfa
4	0.55	0.25	0.30	tall prairie
5	3.1	0.6	2.5	pasture
6	1.3	0.05	1.3	marsh
7	1.8	0.4	1.4	wet snow
8	4.7	0.2	4.5	prairie

In general, test results for the deposition velocity were similar to other values (Chamberlain 1966), which were obtained under steady-state ambient conditions as opposed to our tests in the plume. No evidence was found to suggest that transient conditions result in higher deposition rates.

The results reported here should be regarded as tentative because of the limited amount of data obtained and the impossibility of repeating the experiments under the same conditions. As mentioned, these difficulties were caused by the rapid shifting of the plume.

SECTION 5

CALCULATION OF DRY DEPOSITION OF SULFUR DIOXIDE FROM THE COLUMBIA PLUME

In this section the dry deposition of SO_2 from the plume is calculated by means of ambient air monitoring data and deposition velocity. Deposition due to the plume is distinguished from deposition due to background SO_2. The SO_2 deposition is an indicator of sulfate loading to the soil or water, if SO_2 may be converted to sulfate ions at the surface. Other sulfate loading can occur from wet deposition of sulfates and SO_2. The SO_2 dry deposition flux was calculated at the monitoring sites (Figure 5). The hours when the plume from the station were striking a monitoring site were determined from wind direction and the increase in concentration at the site in the wind sector as compared to other sites at that hour. This incremental concentration value was multiplied by deposition velocity and summed for each hour of plume strike during the year. A deposition velocity of 1 cm/sec was used during April-November, and a value of 0.3 cm/sec was used during of December-March.

Monitoring sites 3 and 4 recorded the most plume strikes during the year and hence had the highest deposition flux (Table 20). When corrected for missing data, the deposition flux was 0.508 and 0.437 kg/ha/yr at sites 3 and 4. The other sites had lower deposition because they were farther away or in a less frequent wind sector. With the same method the SO_2 dry deposition flux due to background concentrations at the monitoring sites is estimated to be 15 kg/ha/yr. Hence, the plume from the generating station contributes 3% of the regional dry deposition of SO_2 annually.

TABLE 20. DEPOSITION OF SO_2 FROM THE PLUME AT THE MONITORING SITES

Monitoring site	Hours sampled	Hours of plume strike	SO_2 deposition (kg/ha/yr)
2	2,329	21	0.158
3	7,952	194	0.508
4	7,952	198	0.437
5	6,869	127	0.115
8	5,623	61	0.067
9	5,623	42	0.037
10	5,623	98	0.090

REFERENCES

Bacci, P., G. Elisei, and A. Longhetto. Lidar Measurement of Plume Rise and Dispersion at Ostiglia Power Station. Atmos. Environ., 8:1177-1186, 1974.

Barber, F.R., and A. Martin. Further Measurements Around Modern Power Stations--I-III. Atmos. Environ., 7:17-37, 1973.

Bowers, J.F., Jr., and M.E. Cramer. West Virginia Power Plant Evaluation. EPA-903/9-75-002, U.S. Environmental Protection Agency, Philadelphia, Pennsylvania, 1975. 57 pp.

Briggs, G.A. Plume Rise: A Recent Critical Review. Nuclear Safety, 12(1):15-24, 1971.

Briggs, G.A. Chimney Plumes in Neutral and Stable Surroundings. Atmos. Environ., 6:507-510, 1972.

Businger, J.A. Flux-Profile Relationships in the Atmospheric Surface Layer, J. Atmos. Sci., 28:181-187, 1971.

Casanady, G.T. Turbulent Diffusion in the Environment. D. Reidel Publishing Co., Boston, Massachusetts, 1973. 238 pp.

Chamberlain, A.C. Transport of Gases to and from Grass and Grass-like Surfaces. Proc. Roy. Soc., A 290: 236-65, 1966.

Conference on atmosphere-suface exchange of particulate and gaseous pollutants, Engelmann, R.J., and Schmel, G.H., ERDA Symposium Series 38 (CONF 740921), 1976. 224 pp.

Gifford, F.A. Turbulent Diffusion-Typing Schemes: A Review. Nuclear Safety, 17(1):25-43, 1976.

Hino, M. Maximum Ground Level Concentration and Sampling Time. Atmos. Environ., 2:149-165, 1968.

Klug, W. Dispersion from Tall Stacks. EPA-600/4-75-006, U.S. Environmental Protection Agency, Washington, D.C. 83 pp.

Lee, R.F., M.T. Mills, and R.W. Stern. Validation of a Single Source Dispersion Model. In: Sixth NATO/CCMS International Technical Meeting on Air Pollution Modeling, Washington, D.C., 1975. pp. 463-511.

Mills, M.T., and F.A. Record. Comprehensive Analysis of Time-Concentration Relationships and Validation of a Single Source Disperison Model. EPA-450/3-75-083, U.S. Environmental Protection Agency. Research Triangle Park, North Carolina, 1975. 143 pp.

Mills, M.T., and R.W. Stern. Model Validation and Time Concentration Analysis of Three Power Plants. EPA-450/3-76-002, U.S. Environmental Protection Agency, Research Triangle Park, North Carolina, 1975. 161 pp.

Moneith, J.L. Principles of Environmental Physics. American Elsevier, New York, New York, 1973. 403 pp.

Pasquill, F. Atmospheric Diffusion. Ellis Horwood Limited, Chichester, England. 429 pp.

Ragland, K.W. Worst-Case Ambient Air Concentrations from Point Sources Using the Gaussian Plume Model. Atmos. Environ., 10:371-374, 1976.

Sauter, G.D. A Generic Survey of Air Quality Simulation Models. Laurence Livermore Laboratory, University of California, Livermore, California, 1975. 110 pp.

Sutton, O.G. Micrometeorology. McGraw-Hill Book Company, Inc. New York, New York, 1953. 333 pp.

Turner, B. Workbook of Atmospheric Dispersion Estimates. AP-26, U.S. Environmental Protection Agency, Washington, D.C., 1970. 52 pp.

U.S. Atomic Energy Commission. Safety Guide: 23 Onsite Meteorological Programs. U.S. Atomic Energy Commission, Washington, D.C., 1972. 102 pp.

Weidner, G. Topographical Influence on Surface Winds near Portage, Wisconsin. M.S. Thesis, University of Wisconsin-Madison, Madison, Wisconsin, 1976. 212 p.

Wisconsin Power and Light Company. Stack Test Results. Wisconsin Power and Light Company, Madison, Wisconsin, 1976.

APPENDIX

Printout of Program GAUSPLM

```
3 @ASG,T METDATA.,U,1234MD
4 @ASG,T COALDATA.,U,2055AL
5 @ASG,T SO2DATA.,U,BG2854
6 @USE 15.,COALDATA.
7 @USE 20.,METDATA.
8 @USE 25.,SO2DATA.
9 @MOVE 15.,6
10 @FOR,SIZ GAUSPLM
11        DIMENSION SO2(7,31,24),R(7),ANG(7)
12        DIMENSION AL(9),AZ(9),BZ(9),CZ(9),DZ(9),AY(9),BY(9),CY(9),DY(9)
13        DIMENSION STAB(15),WD(2)
14        DIMENSION PANG(9)
15        DIMENSION GMW(24)
16        DIMENSION L(21),K(11,21),KOUNTR(11),FREQ(21)
17        DATA AL/.4,.3475,.295,.2475,.2,.165,.13,1.,.098/
18        DATA AZ/.000452,.000226,.1158,.0579,.222,.111,.784,1.,.746/
19        DATA BZ/2.1,2.1,1.09,1.09,.911,.911,.636,1.,.587/
20        DATA CZ/0.,.0579,0.,.111,0.,.392,0.,1.,0./
21        DATA DZ/1.,1.09,1.,.911,1.,.636,1.,1.,1./
22        DATA AY/.000452,.000226,.1158,.0579,.222,.111,1.896,1.,5.7/
23        DATA BY/2.1,2.1,1.09,1.09,.911,.911,.54,1.,.366/
24        DATA CY/0.,.0579,0.,.111,0.,.948,0.,1.,0./
25        DATA DY/1.,1.09,1.,.911,1.,.54,1.,1.,1./
26        DATA STAB/1.,1.5,2.,3.,3.,1.5,2.,2.5,3.5,4.,2.,3.,3.,4.,4./
27        DATA HS/152.4/
28        DATA PANG/.6864,.6020,.5154,.4352,.3536,.2921,.2313,1.0,.1747/
29        DATA R/9.9,5.9,4.4,7.3,8.3,14.6,15.5/
30        DATA ANG/332.,69.,227.,267.,1.,97.,37./
31        DATA L/0,10,15,20,25,30,35,40,45,50,60,70,80,90,100,120,140,160,18
32       C0,200,250/
33 C      Y IS YEAR, M IS MONTH, D IS DAY, H IS HOUR, GMW IS GROSS MEGAWATT LOAD,
34 C      TCH IS THE TONS OF COAL PER HOUR, US IS THE WIND VELOCITY AT STACK HEIGHT
35 C      IN METERS PER SECOND
36 C      DIR REPRESENTS THE WIND DIRECTION, GIVEN IN DEGREES
37 C      ZM IS THE MIXING HEIGHT, ISTAB IS A STABILITY NUMBER,
38 C       STABILITY CLASSES AS DETERMINED BY TEMPERATURE STRATIFICATION
39 C       1=A, 2=B, 3=C, 4=D, 5=E
40        DO 9999 LZAHL=1,7
41         DO 4919 IMOUMB=1,6
42        CALL TOTPSF(15)
43  4919 CONTINUE
44        DO 5002 I=1,11
45        DO 5002 J=1,21
46        K(I,J)=0
47        FREQ(J)=0.
48        KOUNTR(I)=0
49  5002 CONTINUE
50        SUM1=0.
51        SUM2=0.
52        SUM3=0.
53        SUM4=0.
54        SUM3P=0.
```

```
      SUM2P=0.
      SUM2S=0.
      NMONTH=12
      DO 3000 MONTH=1,NMONTH
      MAC=0
      READ(25,26) NDIM,NORP
   26 FORMAT(I2,I1)
      IBOD=1
       IBID=NORP
       IF(NORP.GE.6) IBOD=2
       IF(NORP.GE.6) IBID=7
       DO 505 I=IBOD,IBID
       DO 510 J=1,NDIM
  510 READ(25,515,END=111) (SO2(I,J,KTT),KTT=1,24)
  515 FORMAT(32X,12F4.0/32X,12F4.0)
  505 CONTINUE
  111 DO 4000 I=1,7
       DO 4000 J=1,31
       KANT=0
       DO 4000 K1=1,23
       IF(SO2(I,J,K1).LT.10..OR.SO2(I,J,K1).GT.9000.) GO TO 3995
       KP1=K1+1
       IF(SO2(I,J,KP1).GT.9000.) GO TO 3995
       DIF=ABS(SO2(I,J,K1)-SO2(I,J,KP1))
       IF(DIF-2.) 3900,3900,3950
 3900 KANT=KANT+1
       IF(KANT.EQ.1) K2=K1
       IF(K1.EQ.23) GO TO 3950
       GO TO 4000
 3950 IF(KANT.LT.4) GO TO 3990
       K3=K2+KANT
       DO 3980 ID=K2,K3
       SO2(I,J,ID)=0.
 3980 CONTINUE
 3990 KANT=0
       GO TO 4000
 3995 IF(KANT.GE.4) GO TO 3950
 4000 CONTINUE
    1 READ(15,5,END=500) IY,M,ID,(GMW(I),I=1,24)
    5 FORMAT(3(I2),24'F3.0))
      DO 1000 IH=1,24
      READ(20,6,END=500) SR,C4,WD(1),WD(2),C32,C34,SWS
    6 FORMAT(12X,F5.2,20X,F5.1,5X,2(F5.0),3(F5.1))
      IF(M.EQ.1) GO TO 198
      READ(20,7)
    7 FORMAT(1X)
  198 IBOY=IFIX((WD(1)-WD(2))/180.)
      IF(IBOY) 201,205,203
  201 IF(IBOY.LE.-2) GO TO 202
      WD(1)=WD(1)+360.
      GO TO 205
  202 DIR=WD(1)
      GO TO 30
  203 IF(IBOY.GE.2) GO TO 204
      WD(2)=WD(2)+360.
      GO TO 205
  204 DIR=WD(2)
      GO TO 30
  205 FUD=ABS(WD(1)-WD(2))
      IF(FUD.GT.45.) GO TO 1000
```

```
115       DIR=(WD(1)+WD(2))/2.
116       IF(DIR-777.) 206,1000,1000
117   206 IF(DIR-360.) 30,30,207
118   207 DIR=DIR-360.
119    30 DO 200 J=IBOD,IBID
120       IF(J.NE.LZAHL) GO TO 200
121       IF(J.GT.4) GO TO 31
122       ISITE=J+1
123       GO TO 32
124    31 ISITE=J+3
125    32 THETA1=ABS(DIR+180.-ANG(J))
126       THETA2=ABS(DIR-180.-ANG(J))
127       IF(THETA1.GT.22.5.AND.THETA2.GT.22.5) GO TO 200
128       IF(SO2(J,ID,IH).LT.10..OR.SO2(J,ID,IH).GT.9000.) GO TO 199
129       IF(THETA1-THETA2) 8005,8010,8010
130  8005 THETA=DIR+180.-ANG(J)
131       GO TO 8015
132  8010 THETA=DIR-180.-ANG(J)
133  8015 SO2B=SO2(J,ID,IH)
134       SO2(J,ID,IH)=0.
135       NAB=NORP-1
136       AVE=0.
137       SO2MAX=0.
138       DO 520 I=IBOD,IBID
139       IF(SO2(I,ID,IH)-9999.) 525,530,530
140    530 SO2(I,ID,IH)=0.
141       NAB=NAB-1
142    525 IF(SO2(I,ID,IH).LT.10.) SO2(I,ID,IH)=0.
143       AVE=AVE+SO2(I,ID,IH)
144       IF(SO2(I,ID,IH)-SO2MAX) 520,535,535
145    535 SO2MAX=SO2(I,ID,IH)
146    520 CONTINUE
147       IF(NAB.EQ.0) GO TO 200
148       AVE=AVE/NAB
149       DO 5201 I=1,21
150       IF(AVE.GT.L(I)) K(9,I)=K(9,I)+1
151  5201 CONTINUE
152       KOUNTR(9)=KOUNTR(9)+1
153       SUM1=SUM1+AVE
154       SO2(J,ID,IH)=SO2B
155       SO2BB=SO2B-AVE
156       IF(SO2BB-10.) 1000,1000,521
157    521 IF(ABS(C32).GT.50.) GO TO 800
158       IF(ABS(C34).GT.50.) GO TO 810
159       US=(ABS(C32)+ABS(C34))/2.
160       GO TO 825
161    800 IF(ABS(C34).GT.50.) GO TO 1000
162       US=ABS(C34)
163       GO TO 825
164    810 US=ABS(C32)
165    825 IF(US.LT.1.) GO TO 1000
166       USI=2.237*US
167       IF(GMW(IH).GT.100.) GO TO 1000
168       IF(GMW(IH).LT.175.) GO TO 400
169       IF(GMW(IH).LT.400.) GO TO 405
170       TCH=.5426*GMW(IH)+1.15
171       GO TO 410
172    400 TCH=.3394*GMW(IH)+42.74
173       GO TO 410
174    405 TCH=.5137*GMW(IH)+12.4
175    410 IF(SR.GT.4..OR.SWS.GT.50.) GO TO 1000
```

```
      IF(IH.LT.7.OR.IH.GT.17) GO TO 139
      IF(SWS.GT.0.) II=1
      IF(SWS.GT.1.99) II=2
      IF(SWS.GT.2.99) II=3
      IF(SWS.GT.3.99) II=4
      IF(SWS.GT.6.) II=5
      JJ=10
      IF(SR.GT..4) JJ=5
      IF(SR.GT..817) JJ=0
      KK=II+JJ
      SN=STAB(KK)
      IF(SR.LT..015) SN=4.
      GO TO 141
  139 SN=5.
      IF(SWS.GT.4.) SN=4.
  141 ISTAB=IFIX(2*(SN-.5))
      IF(C4.GT.40.) C4=20.
      TAK=C4+273.
      ZM=1500.
C     CMS IS THE STACK FLOW RATE IN CUBIC METERS PER SECOND
      CMS=1.7*GMW(IH)+103.9
C     TS IS THE STACK GAS EXIT TEMPERATURE IN DEGREES FAHRENHEIT
C     TA IS THE AMBIENT AIR TEMPERATURE IN DEGREES FAHRENHEIT
C     THE FOLLOWING STEPS CHANGE TS AND TA TO ABSOLUTE TEMPERATURE SCALE IN
C     DEGREES KELVIN
      TSK=.064*GMW(IH)+370.8
C     QH IS THE GAS EXIT HEAT FLUX IN KCAL PER SECOND
      QH=84.88*CMS*(TSK-TAK)/TSK
      IF(ISTAB.GT.4) GO TO 20
C     DH IS THE PLUME RISE IN METERS
C     THE FOLLOWING EQUATION GIVES DH IN UNSTABLE AND NEUTRAL ATMOSPHERES
      DH=2.47*CBRT(QH)*(HS**.6667)/US
      GO TO 25
C     STATEMENT 20 GIVES DH IN STABLE ATMOSPHERES
   20 DH=2.45*CBRT(QH/(.0064*US))
   25 H=HS+DH
      IF(H-1500.) 50,50,301
   50 X=1000.*R(J)
      Y=0.
   60 SIGMAY=AL(ISTAB)*(X**.903)
      IF(X.GT.10000.) GO TO 315
  305 SIGMAZ=(AZ(ISTAB)*(X**BZ(ISTAB))+CZ(ISTAB)*(X**DZ(ISTAB)))/2.
      GO TO 320
  315 SIGMAZ=(AY(ISTAB)*(X**BY(ISTAB))+CY(ISTAB)*(X**DY(ISTAB)))/2.
  320 ZZ=SIGMAZ*SIGMAZ
      AA=.318/SIGMAY/SIGMAZ/US
      E=0.
      DO 100 N=1,10
      S=(2.*ZM*H*N-2.*N*N*ZM*ZM)/ZZ
      SS=(-2.*ZM*H*N-2.*N*N*ZM*ZM)/ZZ
      IF(ABS(S).GT.10.) GO TO 105
      IF(ABS(SS).GT.10.) GO TO 90
      ET=EXP(S)+EXP(SS)
      GO TO 95
   90 ET=EXP(S)
   95 E=E+ET
  100 CONTINUE
  105 SSS=-H*H/2./ZZ
      IF(SSS.LT.-10.) GO TO 200
      EN=EXP(SSS)*(1.+E)
C     1000000 ALLOWS FOR CONVERSION FROM GRAMS TO MICROGRAMS, ALSO FOR ACCURACY
      CC=1000000.*AA*EN
C     CALCULATE EMISSIONS
C     QSO2 IS THE SO2 EMISSION RATE IN GRAMS/SEC
      QSO2=3.8*ICH
```

```
C     THE FOLLOWING CONCENTRATIONS ARE IN MICROGRAMS/CUBIC METER
      CCSO2=CC*QSO2
      CBAR=2.5066*SIGMAY*CCSO2/X/PANG(ISTAB)
      IF(CBAR.GT.CCSO2) CBAR=CCSO2
      GO TO 302
  301 CCSO2=0.
      CBAR=0.
      GO TO 302
  302 DO 304 I=1,21
      IF(CBAR.GT.L(I)) K(J,I)=K(J,I)+1
      IF(CBAR.GT.L(I)) K(8,I)=K(8,I)+1
      IF(SO2BB.GT.L(I)) K(10,I)=K(10,I)+1
      IF(CCSO2.GT.L(I)) K(11,I)=K(11,I)+1
  304 CONTINUE
      KOUNTR(J)=KOUNTR(J)+1
      KOUNTR(8)=KOUNTR(8)+1
      KOUNTR(10)=KOUNTR(10)+1
      KOUNTR(11)=KOUNTR(11)+1
      SUM2=SUM2+SO2BB
      SUM3=SUM3+CBAR
      SUM4=SUM4+CCSO2
      SUM3P=SUM3P+CBAR*CBAR
      SUM2P=SUM2P+SO2BB*SO2BB
      SUM23=SUM23+CBAR*SO2BB
      WRITE(6,303) IY,M,ID,IH,ISITE,SN,THETA,DIR,USI,AVE,SO2MAX,SO2B,CCS
     CO2,CBAR,SO2BB
  303 FORMAT(1X,5(I2,3X),F3.1,3X,F5.1,3X,8(F5.1,5X))
      GO TO 200
  199 MAC=MAC+1
      AVE=0.
      NAB=NORP
      DO 1999 I=IBOD,IBID
      IF(SO2(I,ID,IH)-9999.) 1991,1992,1992
 1992 SO2(I,ID,IH)=0.
      NAB=NAB-1
 1991 IF(SO2(I,ID,IH).LT.10.) SO2(I,ID,IH)=0.
      AVE=AVE+SO2(I,ID,IH)
 1999 CONTINUE
      IF(NAB.EQ.0) GO TO 200
      AVE=AVE/NAB
      SUM1=SUM1+AVE
      KOUNTR(9)=KOUNTR(9)+1
      DO 1993 I=1,21
      IF(AVE.GT.L(I)) K(9,I)=K(9,I)+1
 1993 CONTINUE
  200 CONTINUE
 1000 CONTINUE
      GO TO 1
  500 CALL CLOSE(15,0)
      CALL CLOSE(20,0)
      CALL CLOSE(25,0)
 2550 CALL IOTPSP(15,$2600)
      GO TO 2550
 2600 CALL IOTPSP(20,$2650)
      GO TO 2600
 2650 CALL IOTPSP(25,$3000)
      GO TO 2650
 3000 CONTINUE
      WRITE(-,-) ((K(I,J),J=1,21),I=1,10)
      DO 3600 J=1,11
```

```
      DO 3500 I=1,21
      IF(KOUNTR(J).EQ.0) GO TO 3510
      FREQ(I)=100.*FLOAT(K(J,I))/FLOAT(KOUNTR(J))
3500  CONTINUE
      GO TO 3540
3510  DO 3525 I=1,21
      FREQ(I)=0.
3525  CONTINUE
3540  WRITE(6,3550) (FREQ(I),I=1,21)
3550  FORMAT(1X,21(F5.1,1X))
3600  CONTINUE
      AVE1=SUM1/KOUNTR(9)
      AVE2=SUM2/KOUNTR(10)
      AVE3=SUM3/KOUNTR(8)
      AVE4=SUM4/KOUNTR(11)
      WRITE(-,-) AVE1,AVE2,AVE3,AVE4,(KOUNTR(I),I=1,11)
      TOP=FLOAT(KOUNTR(10))*SUM23-SUM3*SUM2
      BOTTOM=(FLOAT(KOUNTR(10))*SUM3P-SUM3*SUM3)*(FLOAT(KOUNTR(10))*SUM2
     CP-SUM2*SUM2)
      RCOR=TOP/SQRT(BOTTOM)
      WRITE(-,-) RCOR
      REWIND 15
      REWIND 20
      REWIND 25
 9999 CONTINUE
      STOP
      END
@XQT
@FIN
EOF..
```

TECHNICAL REPORT DATA
(Please read Instructions on the reverse before completing)

1. REPORT NO.	2.	3. RECIPIENT'S ACCESSION NO.
EPA-600/3-80-048		

4. TITLE AND SUBTITLE
AIR POLLUTION STUDIES NEAR A COAL-FIRED POWER PLANT
Wisconsin Power Plant Impact Study

5. REPORT DATE
May 1980 issuing date

6. PERFORMING ORGANIZATION CODE

7. AUTHOR(S)
Kenneth W. Ragland, Bradley D. Goodell, and Terry L. Coughlin

8. PERFORMING ORGANIZATION REPORT NO.

9. PERFORMING ORGANIZATION NAME AND ADDRESS
Department of Mechanical Engineering
University of Wisconsin-Madison
Madison, Wisconsin 53706

10. PROGRAM ELEMENT NO.
1NE831

11. CONTRACT/GRANT NO.
Grant R803971

12. SPONSORING AGENCY NAME AND ADDRESS
Environmental Research Laboratory
Office of Research and Development
U.S. Environmental Protection Agency
Duluth, Minnesota 55804

13. TYPE OF REPORT AND PERIOD COVERED
Final; 7/75-7/78

14. SPONSORING AGENCY CODE
EPA/600/03

15. SUPPLEMENTARY NOTES

16. ABSTRACT

Concentrations of dry deposition of sulfur dioxide were investigated near a new 540-MW coal-fired generating station located in a rural area 25 miles north of Madison, Wisconsin. Monitoring data for 2 yr before the start-up in July 1975 and for the year 1976 were used to assess the impact of the plume and to investigate the hourly performance of the Gaussian plume model. The Gaussian plume model was successful in predicting annual average concentrations ($r = 0.95$), but inadequate for simulating hourly averages ($r = 0.36$). The incremental annual average increase in ambient SO_2 concentrations within 15 km of the plant was 1-3 $\mu g/m^3$.

Dry deposition of SO_2 was measured within the plume using the gradient transfer method. An annual SO_2 dry deposition flux of 0.5 kg/hectare-year or less within 10 km of the plant was inferred, which is about 3% of the regional background deposition.

17. KEY WORDS AND DOCUMENT ANALYSIS

a. DESCRIPTORS	b. IDENTIFIERS/OPEN ENDED TERMS	c. COSATI Field/Group
Air pollution	Coal-fired power plants	13/B
Atmospheric	Dispersion	04/A
Deposition	Exhaust gases	06/F
Gaussian Plume Model	Plumes	07/B
Meteorology	Portage, Wisconsin	
Models	Sulfur dioxide	
Sulfur dioxide		

18. DISTRIBUTION STATEMENT	19. SECURITY CLASS *(This Report)*	21. NO. OF PAGES
RELEASE TO PUBLIC	UNCLASSIFIED	114
	20. SECURITY CLASS *(This page)*	22. PRICE
	UNCLASSIFIED	

EPA Form 2220-1 (Rev. 4-77) PREVIOUS EDITION IS OBSOLETE

U.S. GOVERNMENT PRINTING OFFICE: 1980-657-146/5686

best copy available

United States
Environmental Protection
Agency

Center for Environmental Research
Information
Cincinnati OH 45268

Postage and
Fees Paid
Environmental
Protection
Agency
EPA-335

Official Business
Penalty for Private Use, $300

Special Fourth-Class Rate
Book

Please make all necessary changes on the above label, detach or copy, and return to the address in the upper left-hand corner.

If you do not wish to receive these reports CHECK HERE □, detach, or copy this cover, and return to the address in the upper left-hand corner.

EPA-600/3-80-048